

Centralized and Auction-based Approaches for Dynamic Spectrum Allocation in Cellular Network

A thesis submitted in partial fulfillment of
the requirements for the degree of

Doctor of Philosophy

by

Indu Yadav
(Roll No. 154070005)

Under the guidance of:
Prof. Abhay Karandikar
and
Prof. Prasanna Chaporkar



Department of Electrical Engineering
Indian Institute of Technology Bombay
Powai, Mumbai 400076

2021

To my Parents and Brother

Thesis Approval

The Thesis entitled

Centralized and Auction-based Approaches for Dynamic Spectrum Allocation in Cellular Network

by

Indu Yadav

(Roll No. 154070005)

is approved for the degree of

Doctor of Philosophy



Prof. P. Rajalakshmi (Examiner)



Prof. S. Vijayakumaran (Examiner)



Prof. Abhay Karandikar (Advisor)



Prof. Prasanna Chaporkar (Co-Advisor)



Prof. Rushikesh K. Joshi (Chairperson)

Date: (14/06/2021)

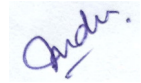
Place: IIT Bombay, Mumbai

Declaration

I, Indu Yadav, declare that this written submission represents my ideas in my own words and wherever others' ideas or words have been included, I have adequately cited and referenced the original sources. I also declare that I have adhered to all principles of academic honesty and integrity and have not misrepresented or fabricated or falsified any idea/ data/ fact/ source in my submission. I understand that any violation of the above will be cause for disciplinary action by IIT Bombay and can also evoke penal action from the sources which have thus not been properly cited or from whom proper permission has not been taken when needed.

Date : 14 June, 2021

Place: IIT Bombay, Mumbai



Indu Yadav

Abstract

The unprecedented growth of data traffic drives academia and standardization organizations towards the dynamic spectrum allocation, which can circumvent the problem of under-utilization of the spectrum. Despite being supported by current standards, dynamic spectrum sharing has not been widely adopted due to concerns over performance degradation. This thesis addresses dynamic spectrum allocation problems for various scenarios appropriate in the existing and next-generation cellular network. For efficient utilization of radio resources, we need to appropriately utilize the scarce resources by considering the spatio-temporal traffic variations in the network.

In practice, auctions are commonly preferred for spectrum allocation in the network. The spectrum auctions differ from conventional auctions due to frequency reuse; spectrum (frequency band) can be reused or reallocated after a certain fixed distance depending on the coverage area of base stations. In this work, we formulate the dynamic spectrum allocation problem within the sealed-bid auction framework with the aim of maximizing social welfare subject to interference constraints. First, we investigate the problem of dynamic spectrum allocation across base stations in the network. In literature, the problem is proved to be NP-Hard in nature. We propose a computationally efficient strategy-proof dynamic spectrum allocation mechanism, which achieves near-optimal social welfare, spectrum utilization, and fairness. Using simulations, we demonstrate that the proposed mechanism is suitable for implementation in large networks (with number of base stations > 500).

Next, we consider dynamic spectrum allocation across multiple operators, where multiple base stations are associated with an operator. We analyze the problem for the single-channel as well as the multiple channel allocation scenarios. Besides, we also consider flexible bidding at the base stations of an operator. Flexible bidding refers

to the pattern of non-increasing marginal bid with the demand at a base station. We propose a strategy-proof mechanism for the single-channel scenario. In the multiple-channel scenario, we introduce the notion of weak strategy-proofness. Using simulations, we establish that the proposed mechanisms outperform existing mechanisms.

To support the data requirements of exponentially increasing number of cellular users, wireless cellular networks are undergoing significant architectural enhancements. The heterogeneous network architecture is one such advancement, which can augment the capacity of cellular networks through the addition of femto/pico (small) cells. However, fiber connectivity to each small cell is not feasible. In such scenarios, wireless backhaul enables connectivity between small cells and core network (CN). Integrated Access and Backhaul (IAB) has emerged as a solution in Fifth Generation (5G) network, where wireless backhauling is supported. In IAB networks, IAB-donors are connected to the CN through fiber connectivity, and the multiple IAB-nodes are associated with IAB-donors through wireless backhaul. IAB-nodes can support small cells and provide last-mile connectivity to users, and IAB-donors act as wireless backhaul providers. For efficient utilization of the spectrum in wireless backhaul, we design an auction-based mechanism to allocate resources dynamically across IAB-nodes considering the spatial and temporal variations of the network traffic.

Finally, we propose a novel Software Defined Network (SDN) based architecture which enables the convergence of unicast and multicast services in the next-generation mobile network. The architecture provides flexible switching of the traffic between unicast and multicast transmission modes for efficient utilization of resources in the wireless network. For the unified architecture, we propose an efficient radio resource allocation algorithm for unicast and multicast transmission for guaranteed minimum Quality of Service (QoS) to every user in the system. Our scheme considers dynamic traffic variation in the network. We formally prove the optimality of the proposed algorithm. Although the simulations are performed on a Long Term Evolution (LTE) network, the results, and algorithms are also applicable in 5G and beyond networks.

Acknowledgments

The work presented in this thesis would not have been possible without the support of many people who have helped me through my journey as a doctoral student at IIT Bombay. I take this opportunity to express my sincere gratitude and appreciation to all who have made this Ph.D. thesis possible.

I am deeply grateful to my advisor Prof. Abhay Karandikar for his invaluable guidance and encouragement. He has guided me to carry on through these years and has contributed to this thesis with a major impact. His mentoring through the subtleties of scientific writing has been tremendously useful. His enthusiasm, positive outlook and unparalleled energy have always been a source of inspiration. Each discussion with him has provided me new insights and learnings which will always remain valuable to me. He has been extremely supportive whenever I needed any help. This thesis reflects the trust and support that he has lent me over the years.

I am immensely grateful to my co-advisor Prof. Prasanna Chaporkar for his continuous support, guidance, encouragement and inspiration. From him, I have learned how to handle tough situations patiently. I owe a lot of gratitude for him for always being so warm, friendly and extremely understanding throughout this journey. Innumerable discussions with Prof. Prasanna Chaporkar has been insightful for me.

I am grateful to Prof. Ankur A. Kulkarni for many insightful discussions and suggestions during the course of my Ph.D. I have learned a lot through his classes. I consider myself very fortunate to have the opportunity to interact with him.

I would also like to thank Mr. Pranav Jha for his guidance and help during the journey of my Ph.D. Working with him has been an enriching experience. He made every discussion and conversation between us interactive and interesting. I am thankful for his insightful suggestions.

I would like to thank the members Research Progress Committee (RPC), Prof. Gaurav Kasbekar and Prof. Vijayakumaran Saravanan for their valuable suggestions, comments and feedback regarding my work. Their perspectives have brought greater clarity about my work to me. I thank them for their suggestions which have helped me improving the overall quality of the thesis. I thank all the faculty members who I interacted with over the years. I have been fortunate to have attended classes taught by many fantastic IITB professors. I thank all my teachers whose passion for learning and teaching has brought me this far.

My sincere gratitude to Sangeeta Ma'am, Sonal, Margaret, Beena, Aditya Ji and Rajesh Ji for their assistance in all official works. I would also like to acknowledge all the help provided by EE Office staff, in particular Mr. Santosh and Ms. Tanvi. Their prompt responses made the official work smooth.

I would like to thank all my labmates, with whom I have shared moments of deep anxiety but also of big excitement. Their presence was very important in a process that is often felt as tremendously solitaire. It is my pleasure to thank Anushree, Arghyadip, Akshatha, Meghna, Meera, Rashmi Ma'am, Sadaf, Pragnya, and Shashi for their support. Also, I want to thank my friends including Jerin, Prachi, Reshma, Nidhi, Annapurna, who have been major support when things would get discouraging and made my life at IIT Bombay memorable. Many thanks to friends who may not be physically close to me but has always been close to my heart.

The journey would have been impossible without the support of my family. I thank my parents and brother for unconditional support and encouragement.

Indu Yadav

June 2021

Contents

Abstract	vii
Acknowledgments	ix
List of Acronyms	xv
List of Tables	xix
List of Figures	xxi
1 Introduction	1
1.1 Dynamic Spectrum Allocation in 5G Networks	3
1.2 Taxonomy of Spectrum Sharing Techniques	5
1.3 Challenges in Dynamic Spectrum Allocation	6
1.4 Motivation of the Thesis	7
1.5 Contributions and Organization of the Thesis	9
2 Dynamic Spectrum Allocation: Auction-based Approaches	13
2.1 Auction Preliminaries	13
2.1.1 Strategy-Proof Spectrum Auctions	15
2.1.2 Vickrey-Clarke-Groves Mechanism	16
2.2 Spectrum Auctions in Cellular Network	17
2.3 Spectrum Auctions in Hierarchical Settings	19
2.4 Spectrum allocation in unified unicast multicast framework	19
3 Dynamic Spectrum Allocation across Base Stations	23
3.1 System Model and Problem Formulation	24

3.2	Group based Optimal Strategy-proof Allocation Algorithm	28
3.2.1	Channel Allocation Strategy	28
3.2.2	Pricing Scheme	31
3.3	Illustrative Example	34
3.3.1	Allocation in Proposed Algorithm	35
3.4	Applications	36
3.4.1	Spectrum Band Specific Channel Allocation	37
3.4.2	Generalization of the proposed mechanism	37
3.5	Simulation Results	40
3.6	Conclusions	47
4	Dynamic Spectrum Allocation across Operators	49
4.1	System Model	51
4.1.1	Notations and Definitions	53
4.2	Strategy-proof auction for Single Channel demand	54
4.2.1	Complexity Analysis	60
4.3	Non-uniform demand across Operators	61
4.3.1	Example	63
4.4	Weakly Strategy-proof Algorithm for Non-uniform Demand	65
4.4.1	Example	69
4.5	Summary of the Proposed Mechanisms	73
4.6	Simulation Results	73
4.6.1	Performance evaluation for Single Channel	75
4.6.2	Performance evaluation for Multiple Channels	77
4.7	Conclusions	80
5	Dynamic Spectrum Allocation for Wireless Backhaul in Heterogeneous Networks	83
5.1	System Model	85
5.1.1	Mechanism Design Framework	87
5.1.2	Problem Statement	89
5.2	Hierarchical Allocation Preliminaries	89

5.3	Proposed Mechanism	90
5.3.1	Tier 2 Auction Mechanism (π_2)	91
5.3.2	Tier 1 Auction Mechanism (π_1)	93
5.3.3	Pricing Scheme for π	94
5.4	Simulation Results	96
5.5	Conclusions	97
6	Dynamic Spectrum Allocation in Unicast Multicast Convergence in 5G Network	99
6.1	Proposed System Architecture	102
6.1.1	Call Flow Description	105
6.2	System Model	107
6.2.1	Problem Formulation	111
6.3	Resource Allocation Algorithm	112
6.3.1	User (UE) Arrival	112
6.3.2	User (UE) Departure	117
6.3.3	Optimal Resource Allocation Algorithm	120
6.4	Resource Allocation : Limited Resource Scenario	121
6.4.1	Proposed Algorithm	123
6.5	Simulation Results	126
6.5.1	Simulation Settings	126
6.5.2	Performance Comparison	128
6.5.3	Limited Resource Scenario	131
6.6	Conclusions	133
7	Summary of the Contributions and Future Research Directions	135
7.1	Summary of the Contributions	135
7.2	Future Research Directions	138

List of Acronyms

2G	Second Generation
3G	Third Generation
4G	Fourth Generation
5G	Fifth Generation
3GPP	Third Generation Partnership Project
AA	Auction Algorithm
BMSC	Broadcast Multicast Switching Center
BS	Base Station
BSS	Basic Service Set
CBR	Constant Bit Rate
CDN	Content Delivery Network
CQI	Channel Quality Indicator
CSMA/CA	Carrier Sense Multiple Access/ Collision Avoidance
CTS	Clear to Send
CSI	Channel State Information
CU	Control Unit
DC	Dual Connectivity
DHCP	Dynamic Host Configuration Protocol
DIFS	Distributed Coordination Function Inter-Frame Space
DNS	Domain Name System
DSA	Dynamic Spectrum Allocation
DSL	Digital Subscriber Line
DU	Data Unit
EB	ExaByte

eNodeB	Evolved NodeB
EPC	Evolved Packet Core
FDD	Frequency Division Duplex
FDMA	Frequency Division Multiple Access
GBR	Guaranteed Bit Rate
gNB	Next Generation Node B
GSM	Global System for Mobile Communications
HetNet	Heterogeneous Network
IFOM	Internet Protocol Flow Mobility
IMSI	International Mobile Subscriber Identity
IP	Internet Protocol
I-WLAN	Interworking-Wireless Local Area Network
LTE	Long Term Evolution
ILP	Integer Linear Programming
MAC	Medium Access Control
MBS	Multicast Base Station
MCC	Mission Critical Communications
MME	Mobility Management Entity
MNC	Mobile Network Controller
OFDM	Orthogonal Frequency Division Multiplexing
OFDMA	Orthogonal Frequency Division Multiple Access
PDCP	Packet Data Convergence Protocol
PDN	Packet Data Network
PDU	Protocol Data Unit
PLMN	Public Land Mobile Network
PRB	Physical Resource Block
QoS	Quality of Service
RB	Resource Block
RAT	Radio Access Technology
RE	Resource Element
R.H.S.	Right Hand Side

RRC	Radio Resource Control
RRM	Radio Resource Management
SDN	Software Define Networking
SIFS	Short Inter-Frame Space
SNR	Signal to Noise Ratio
STA	Wireless Station
TCP	Transmission Control Protocol
TTI	Transmission Time Interval
UDP	User Datagram Protocol
UE	User Equipment
UMTS	Universal Mobile Telecommunications System
UPF	User Plane Function
VCG	Vickrey Clarke Groves
VoIP	Voice over Internet Protocol
WBA	Wireless Broadband Alliance
WiFi	Wireless Fidelity
WLAN	Wireless Local Area Network
WPA2	Wireless Fidelity Protected Access 2

List of Tables

1.1	5G frequency spectrum [1]	4
4.1	Summary	74
6.1	Notations and their significance	110
6.2	Simulation parameters	127

List of Figures

1.1	Number of Subscribers growth over the years [2].	1
1.2	Illustration of spatial and temporal variation of traffic in the cellular network.	2
1.3	Illustration of Spectrum Sharing Techniques.	5
2.1	Auction mechanism design steps.	14
2.2	Auction mechanism requirements.	16
3.1	System model	24
3.2	Illustration of auction duration $[T_1, T_2]$ and demand time intervals t_1, t_2 and t_3 corresponding to base stations 1, 2 and 3, respectively.	25
3.3	(a) Interference graph (b) Channel demand time slots	35
3.4	Re-constructed interference graph considering demand time intervals for each base station.	36
3.5	(a) Interference graph (b) Channel demand time slots	38
3.6	Re-constructed interference graph considering demand time intervals for each base station.	38
3.7	(a) Demand time slots (b)Augmented Interference graph	40
3.8	Re-constructed interference graph considering demand time intervals for each base station.	41
3.9	Performance comparison for different algorithms in small network.	42
3.10	Performance comparison for different algorithms in large network.	43
3.11	Performance comparison for different algorithms with degree distribution $p(x = k) = \frac{k}{10}$ where $k = \{1, 2, 3, 4\}$	45
3.12	Performance comparison for different algorithms with degree distribution $p(x = k) = \frac{5-k}{10}$ where $k = \{1, 2, 3, 4\}$	46

3.13	Comparison of fairness index for different algorithms in large networks. . .	47
4.1	Illustration of system model.	51
4.2	Network of 3 operators (a) Conflict Graph (b) Bid vector table corresponding to operator \tilde{A} , \tilde{B} and \tilde{C}	58
4.3	Conflict graph of the 3 operators.	63
4.4	Updated conflict graph after the first iteration.	64
4.5	Updated conflict graph after the first iteration.	65
4.6	Updated conflict graph after channel allocation phase is complete.	70
4.7	Performance comparison of the VCG, SC-SPAM, SPECIAL and SMALL in three operator scenario.	76
4.8	Comparison of execution times of various algorithms.	77
4.9	Performance comparison for uniform demand $d = 2$ across the base stations of multiple operators, with linearly increasing bid with demand at each base station.	78
4.10	Comparison of percentage of base stations allocated channel in wireless networks.	79
4.11	Comparison of spectrum utilization and number of channels for NUD-WSPAM in large networks.	80
5.1	Illustration of IAB network	84
5.2	Illustration of system model	86
5.3	Illustration of mechanism design framework	87
5.4	Performance comparison of social welfare vs. number of IAB-nodes	96
6.1	Illustration of existing 3GPP architecture for MBMS services (courtesy 3GPP).	101
6.2	SDN based converged mobile network architecture for 5G and beyond.	103
6.3	Call flow for resource allocation on UE arrival in the network.	106
6.4	System Model.	108
6.5	Illustration of UE structure.	109
6.6	Illustration of simulation settings.	126
6.7	Resource Utilization (RBs required) vs. number of UEs [$R = 3.5$ Mbps].	129

6.8	Resource Utilization (RBs required) vs. number of UEs [For $t = [0, 10]$: $\lambda_b = 5$; and $t = [10, 40]$: $\lambda_a = 1$, $R = 3.5$ Mbps].	129
6.9	Comparison of the number of RBs saved in Algorithm 10 against multicast scheme at different UE data rates [Data rates $R = \{2.0, 2.5, 3.0\}$ Mbps]. . .	130
6.10	Resource Utilization (RBs required) vs. time [For $t = [0, 10]$: $\lambda_a = 4$ and $t = [10, 45]$: $\mu_d = 1/10$, $R = 3.5$ Mbps].	131
6.11	Percentage of UEs served vs. RBs in limited resource scenario.	132
6.12	System throughput vs RBs in limited resource scenario.	132

Chapter 1

Introduction

With recent advancements in wireless communication technologies, the telecom market has witnessed exponential growth in end-user traffic in the past few decades. As per the Ericsson report estimates, globally we have 7.9 billion mobile subscriptions [2]. Moreover, the figure is expected to reach 8.8 billion by the end of 2026, wherein 91% of the total mobile subscriptions is estimated to be for mobile broadband. With the continuous rise in smartphone penetration, 75 percent of the global mobile subscriptions are associated with smartphones.

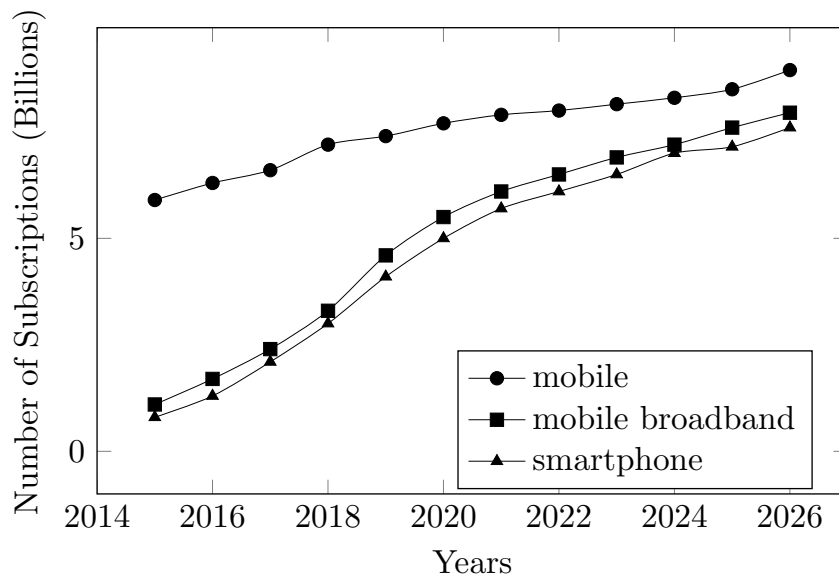


Figure 1.1: Number of Subscribers growth over the years [2].

Figure 1.1 illustrates that the mobile subscriptions are expected to increase steadily across the globe over the years. This continuous increase in mobile data traffic is one of

the most critical challenges to be handled in the next-generation wireless networks.

Recently, the tremendous growth of multimedia traffic in the mobile network has been observed, which has transitioned from the age of downloads to an age of streaming. The paradigm shift is driven by the popularity of the Over The Top (OTT) platforms such as Netflix, Hotstar, Amazon Prime among the users. Besides, users prefer streaming content over the cellular network on their mobile devices like smart-phones and tablets, as it is convenient and can be carried anywhere. This requires transmitting the same content to a large set of users simultaneously. Traditionally, the users are delivered content via unicast transmission mode, where each user requires a dedicated (orthogonal) set of resources for the duration of content delivery. Consequently, to deliver the same content across a set of users simultaneously, we allocate a separate set of resources individually to each user. However, in such scenarios, multicasting the content across the users simultaneously on common resources optimizes resource utilization in the network.

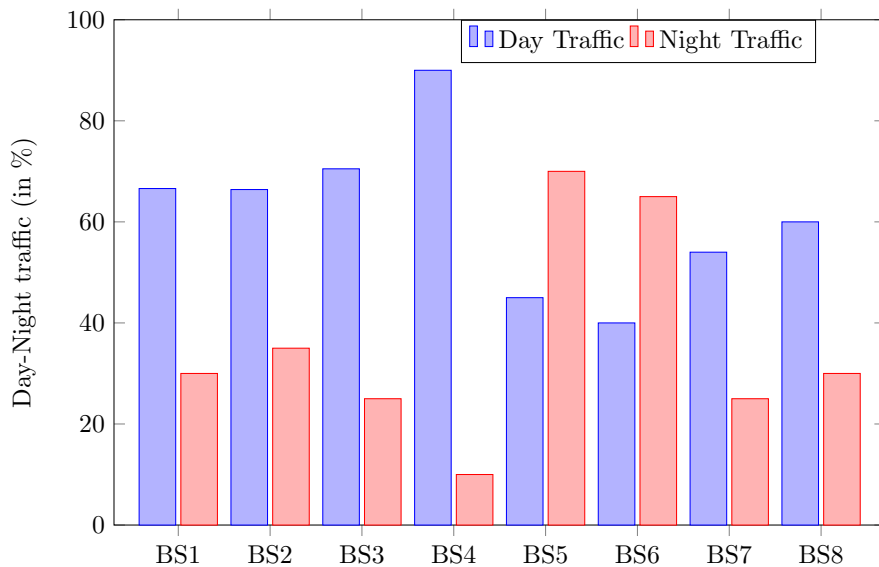


Figure 1.2: Illustration of spatial and temporal variation of traffic in the cellular network.

The collected traffic statistics suggest that the mobile data traffic varies temporally as well as spatially across the network [3,4]. According to the U.S. Federal Communications Commission (FCC) [5], the temporal and spatial variations results in under-utilization of the allocated spectrum in the range of 15% to 85% as illustrated in Figure 1.2.

In general, a network has diverse Quality of Services (QoS) requirements depending on the type of traffic, which can be classified as elastic (real-time) or inelastic (non real-

time). The traffic with strict latency and data requirements such as Voice over Internet Protocol (VoIP) is inelastic, whereas file downloads with no strict latency or data requirements are elastic. Satisfying the increasing number of end-users with the desired QoS has further contributed to the crisis of limited, scarce, and expensive spectrum. Therefore, efficient utilization of spectrum is a requirement that cannot be ignored. Hence, the main focus of the next-generation wireless network is to meet the diverse QoS requirements of the end-users by efficiently utilizing the spectrum.

The prominent solution to address spectrum scarcity is efficient utilization of the available radio resources by employing Dynamic Spectrum Allocation (DSA) mechanisms. The pertinence of DSA is motivated by the fact that a significant amount of licensed spectrum remains under-utilized in the spatial and temporal domains, and thus it aims to address the anomaly between the spectrum shortage and under-utilization [6]. Moreover, the recent advances such as Software Defined Networks (SDN) [7–9] have led to the feasibility of this solution by enhancing the utilization of spectrum in a very flexible and adaptive manner.

1.1 Dynamic Spectrum Allocation in 5G Networks

Dynamic spectrum allocation (DSA) is one of the most prominent solutions that need to be considered in addressing the spectrum scarcity by efficiently utilizing the spectrum in Fifth Generation (5G) and beyond network [10, 11]. DSA provides flexibility to share a frequency band among multiple users (primary or secondary or both) of same/different priorities without obstructing one another to optimize the usage of spectrum.

In 5G, spectrum allocation is categorized into three disjoint frequency bands, namely, low, high and very high, as summarized in Table 1.1. Typically, the spectrum band having frequencies below 2 GHz [1, 12] have excellent penetration characteristics and therefore enables coverage in large areas along with deep indoor coverage. However, the spectrum band between 2 – 6 GHz has relatively high frequencies with large bandwidths. The frequency band around 3.4 GHz to 3.8 GHz [12] provides the capacity to support connection to several devices simultaneously. Typically, this spectrum provides the best trade-off between the coverage and the capacity requirements.

Table 1.1: 5G frequency spectrum [1]

Category	Spectrum	Coverage
Low Frequencies	< 2 GHz	<ul style="list-style-type: none"> • Large areas • Deep indoor coverage
High Frequencies	2 to 6 GHz	<ul style="list-style-type: none"> • Focused areas • Relatively large bandwidths • Very high number of connected devices • High speed of concurrent connected devices
Very high Frequencies	> 24 GHz	<ul style="list-style-type: none"> • Small coverage areas (50 to 200 m) • Very large bandwidths • Ultra-high capacity • Peak data rates (Gbps) • Very low latency

Typically, frequencies greater than 24 GHz, have large bandwidths and best suited for the line of sight applications. This spectrum provides high capacity and works well for the applications demanding low latency [12]. As we move towards the higher end of the spectrum band, the frequencies suffer attenuation, and therefore, the cell coverage at these frequencies reduces considerably (from 50 m to 200 m).

Furthermore, existing and the next-generation mobile networks can have various types of spectrum sharing licenses depending on the use case, such as Exclusive license, License-Exempt (unlicensed), Licensed Shared Access (LSA) and Authorized Shared Access, Pluralistic licensing, and License Assisted Access (LAA) co-primary shared access. The detailed overview of the above mentioned license schemes is presented in [13]. The authors also discuss the spectrum sharing characteristics for inter-operator and virtualized network architecture.

1.2 Taxonomy of Spectrum Sharing Techniques

Spectrum Sharing Techniques can be categorized into three approaches : Network architecture, Spectrum Allocation Behavior, Spectrum Access Method as illustrated in Figure 1.3.

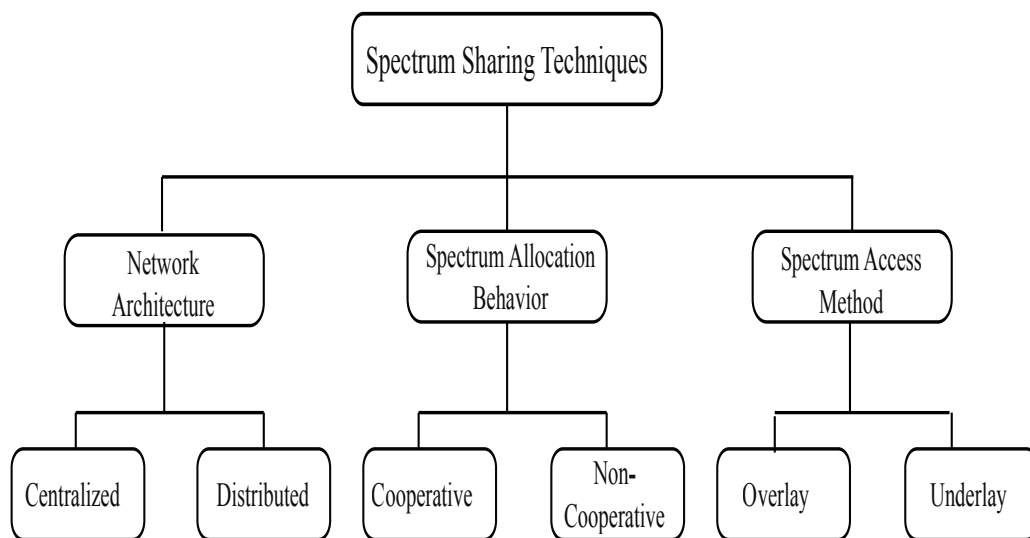


Figure 1.3: Illustration of Spectrum Sharing Techniques.

As a network architecture can be either centralized or distributed, spectrum sharing techniques may have network dependency. A study of centralized and distributed approaches with considering various performance parameters is presented in [14].

- *Centralized Spectrum Sharing*: The network architecture has a centralized entity, which is responsible to control the spectrum assignment and access methods [15–17]. The measurement reports related to the spectrum allocation method are forwarded to the central entity, which prepares the spectrum mapping for the network entities.
- *Distributed Spectrum Sharing*: Distributed spectrum sharing solutions are suited for the cases where the construction of an infrastructure (infrastructure-less) is not preferable [14, 18–23]. In these approaches, each entity is involved in spectrum allocation, and spectrum access is based on local (or possibly global) policies.

Another, approach is spectrum allocation behavior, which can either be cooperative or non-cooperative. The authors in [18], have discussed both behaviors, particularly in Licensed Shared Access (LSA) (non-cooperative) and Television White Space (TVWS) (cooperative).

- *Cooperative Spectrum Allocation* : Cooperative Spectrum Allocation can occur not only between incumbent users and secondary (cognitive) users but also between secondary users to enhance the throughput of the system. Efficient sharing of the spectrum is achieved through information exchange; thus, it mitigates interference and increases the spectrum utilization in the network.
- *Non-cooperative spectrum sharing* : Contrary to the cooperative solutions, non-cooperative (or non-collaborative) spectrum allocation considers individual entities [19–21], without any information exchange between the entities. While the communication overhead and signaling across the network entities reduces, the resource utilization may suffer.

The basic idea behind the third approach is to allow the access of licensed spectrum to secondary users by restricting the interference experienced by incumbent users (licensees). The underlay and overlay spectrum sharing approaches are used to share spectrum between incumbent and secondary users.

- *Underlay Spectrum Sharing*: The spread spectrum techniques developed for cellular networks are utilized for underlay spectrum sharing [22]. This approach enforces the constraints on the transmission power of non-incumbent users such that they do not degrade the QoS of incumbent users. With extremely low transmission power, secondary users can achieve high data rate for short distance communications.
- *Overlay Spectrum Sharing*: In overlay spectrum sharing approach, spectrum sensing is performed to locate the the portion of the spectrum that has not used by the incumbent users [15, 19–21, 23]. Consequently, no interference is caused to the incumbent users in the network. Thus, the approach identifies the spectrum holes (white spaces) that arise due to spatial and temporal traffic variations in the network and exploit the instantaneous spectrum available locally in a non-intrusive manner.

1.3 Challenges in Dynamic Spectrum Allocation

The current developments in 5G and beyond mobile networks focus on achieving high spectral efficiency, better coverage, and low latency. The densification of the network by overlay deployment of small cells resulting in Heterogeneous Networks (HetNet), seems to be the most promising solution to address the data rate requirement of the next-

generation network. The densification of network results in high spectral efficiency, low power consumption and significantly improves network coverage. In general, one of the most critical challenges is interference management in the cellular network. Although HetNet seems to be very attractive with all the benefits stated above, resource allocation becomes much more complicated.

Third Generation Partnership Project (3GPP) [24] advocates the convergence of backhaul and access in next-generation networks. One of the key advancement in this direction is “Integrated Access and Backhaul” (IAB) introduced in Release 15. IAB enabled 5G networks comprises IAB-donor and IAB-node. Typically, IAB-donors are connected to the core network (CN) through fiber, and IAB nodes are connected to IAB-donors via a wireless backhaul. The IAB node supports small cells in HetNet settings and appears as a base station to UEs connecting to it. IAB-enabled 5G HetNet seems to be a good alternative to fiber connectivity. Thus, the IAB feature can further simplify the deployment of small cells as well as cost-efficient. Additionally, IAB nodes can support multi-hop wireless backhauling, by connecting one IAB-node via another IAB-node. In such settings, the problem of dynamic spectrum allocation becomes all the more challenging, as it requires dynamic spectrum allocation across all the multi-hop links.

While employing the dynamic spectrum allocation in the network, the computational complexity of the mechanism plays a vital role. In order to consider the spatial and temporal variations, the algorithm needs to be computationally efficient. In practical scenarios, dynamic spectrum allocation among the service providers is not common due to interference issues, which may significantly degrade the user experience. Spectrum problem can be formulated as an optimization problem in general Non-deterministic Polynomial-time hard (NP-Hard) [25] in nature. Hence, achieving an optimal solution is computationally intractable. Due to the intractability of the optimal solution, it is hard to implement in real scenarios.

1.4 Motivation of the Thesis

Having introduced the importance of dynamic spectrum allocation for efficient utilization of limited spectrum (radio resources) in the cellular networks, we now explore the various

scenarios of the dynamic resource allocation pertaining to the existing as well as the next-generation cellular network. Typically, auction-based mechanisms are prominently used for spectrum allocation across the service providers. As stated above, traditionally, the spectrum is allocated for a long duration, wherein the spatio-temporal variations in the traffic are not taken into account. Hence, the spectrum remains under-utilized in the long run.

In general, resource allocation mechanisms are designed as per the goals of the system, which may include maximization of social welfare, efficient and fair utilization of limited resources, and maximization of revenue. We aim at maximizing the social welfare of the auction subject to the interference constraints in the cellular network. Maximization of social welfare ensures that the radio resources (spectrum) are allocated to those who value it the most. Most of the existing literature is focused on dynamic spectrum allocation between incumbent and secondary users in TV White Spaces (TVWS), unlicensed spectrum or licensed spectrum. However, with the advent of 5G, there can be many other potential scenarios of dynamic spectrum allocation, which have not been addressed. In our work, we attempt to explore the dynamic spectrum allocation mechanisms appropriate for 4G, 5G, and beyond cellular networks.

One of the most critical requirements of any dynamic spectrum allocation mechanism is computational efficiency (polynomial-time complexity). The polynomial-time complexity of the mechanism can be implemented in real-time scenarios; thus, the traffic variations in the network can be taken into account by frequently repeated allocations. Typically, maximizing social welfare subject to interference constraint in a cellular network is NP-Hard. To address the trade-off between complexity and optimal solution, we sacrifice the optimality of the solution. We focus on achieving the near-optimal solution with low computational complexity.

The dynamic spectrum allocation solutions proposed in this thesis are suitable for implementation within a centralized framework. Note that although the solutions in this thesis are developed for an Long Term Evolution (LTE) network, the framework considered by us, is generic and can be implemented easily in 5G and beyond cellular networks.

1.5 Contributions and Organization of the Thesis

In this section, we outline some of the salient contributions of the thesis. The thesis is organized into seven chapters. Chapter 2 presents a review of relevant literature and open challenges. Chapters 3 – 6 present our contributions. The chapter wise contributions are outlined below.

In Chapter 3, we study the dynamic spectrum allocation across base stations using a sealed-bid auction framework. The framework considers centralized dynamic spectrum approach assuming non-cooperative base stations in the network. Although vast literature is present on the dynamic spectrum allocation, none of the works focus on achieving a certain degree of fairness while allocating spectrum along with maximizing social welfare. We propose an auction-based algorithm (GOSPAL), not only achieves near-optimal social welfare but also ensures fairness in allocation across base stations. Fairness in resource allocation plays a vital role in avoiding the monopoly of specific service providers in the region. With the low computational complexity, the proposed algorithm efficiently considers the spatial and temporal traffic variations in the wireless network. Using Monte Carlo simulations, we observe that the proposed dynamic spectrum allocation scheme achieves near-optimal social welfare, spectrum utilization, and fairness simultaneously while allocating spectrum dynamically across the base stations. We also analyze the effects of the degree distribution of interfering base stations in the wireless network over the performance parameters. Moreover, we observe that the proposed algorithm performs well even in large networks (number of base stations > 500).

In Chapter 4, we discuss the system model for multi-operator co-existence and formulate the dynamic spectrum allocation across operators in the multi-parameter environment using a sealed-bid auction framework. While there is abundant literature on the dynamic spectrum allocation considering individual base stations as the participants in the auction, the specific problem of the dynamic spectrum allocation across operators has not been addressed so far. When we consider the operators (service providers) as the participants in spectrum auctions, the dynamic spectrum problem becomes much more challenging due to the interference constraints across the base stations deployed in the region. Furthermore, dynamic spectrum allocation at operator level has a vector of bids (corresponding to each base station), unlike at base station. Therefore, an algorithm

needs to ensure that operator does not have an incentive to mis-report bid at any of the associated base stations. We outset the analysis with a simple scenario considering only a single channel available for auction across operators. As the problem is NP-Hard in nature, we propose a strategy-proof mechanism that achieves near-optimal social welfare. The complexity analysis of the proposed algorithm is done, which shows considerable improvement compared to the classical algorithm Vickrey Clarke Groves (VCG). Next, we extend the analysis for multiple channel scenarios with uniform as well as for non-uniform demand across the base stations of the operators. In addition to the flexibility of the demand (channel requirement) at the base station of an operator, we also allow the operators to have flexible bids at their base stations. For the generic setting of the dynamic spectrum allocation across operators, we introduce a new concept of weakly strategy-proofness. Our simulations indicate that the proposed mechanisms outperform the existing mechanisms in various performance parameters considered.

In Chapter 5, we consider dynamic spectrum allocation in Heterogeneous Networks (HetNet), a significant enhancement to efficiently utilize the limited and expensive radio resources. HetNet deployment is a way to achieve higher spectral efficiency in regions with high user density when the available radio resources are limited. With an overlay deployment of small cells in HetNets, the dynamic spectrum allocation becomes much more complex, due to the hierarchical settings. In such scenarios, wireless backhaul enables connectivity between small cells and core network (CN). Integrated Access and Backhaul (IAB) has emerged as a solution in the 5G network, where wireless backhauling is supported. In IAB networks, IAB-donors are connected to the CN through fiber connectivity, and the multiple IAB-nodes are associated with IAB-donors through wireless backhaul. IAB Nodes can support small cells and provide last-mile connectivity to users, and IAB-donors act as wireless backhaul providers. For efficient utilization of the spectrum in wireless backhaul, we design an auction-based mechanism to allocate resources dynamically across IAB-nodes considering the spatial and temporal variation of the network traffic. Moreover, using Monte Carlo simulations, we show that the proposed mechanism achieves optimal social welfare.

In Chapter 6, our focus is on the efficient utilization of the spectrum or radio resources by multicasting the content requested by multiple users in the wireless network simulta-

neously. However, the existing network lacks a unified architecture that can enable the convergence of unicast and multicast services. Therefore, we propose a novel SDN based architecture for unified control and management of unicast and multicast transmissions in the Fifth Generation (5G) and beyond mobile networks. The proposed architecture brings significant flexibility to selecting transmission modes (unicast or multicast) for individual users. We also propose an integrated scheme for radio resource allocation for unicast and multicast transmissions. The proposed scheme enables efficient utilization of radio resources in the network while ensuring the required Quality of Service (QoS) to users.

Finally, Chapter 7 summarizes the contributions of the Thesis and points out some aspects that could be investigated in future.

Chapter 2

Dynamic Spectrum Allocation: Auction-based Approaches

As pointed out in the previous chapter, the traditional exclusive licensing spectrum allocation scheme results in the under-utilization of resources. Therefore, one requires to carefully investigate how the spatial and temporal variations in the network can be exploited to devise mechanisms for efficient utilization of spectrum (resources). In this chapter, we present some existing efforts in the literature towards dynamic spectrum allocation in the cellular network. As discussed in the previous chapter, dynamic spectrum allocation considering the traffic variations may play a significant role in improving the network performance and cost-efficient from service providers' perspective. Accordingly, we review various dynamic spectrum allocation solutions proposed in the literature. In this thesis, we focus on auction-based approaches in the centralized architecture framework, which provides system-wide optimization due to the global view of the network. Hence, in this chapter, we present state-of-the-art techniques in dynamic spectrum allocation, which form the motivation for our investigation in the rest of the thesis.

2.1 Auction Preliminaries

Optimal use of resources has always been a concern. In today's world with increasing demand, efficient use of limited and scarce resource has become a challenge. A resource allocation mechanism must be designed to meet the strategic goals of the system. The

desired strategic goals may include maximization of social welfare, efficient and fair utilization of limited resource and maximization of revenue [26]. Auction based mechanism is a popular way of distributing the available resource among users [27]. Here, it is assumed that each user (participants) has some quantitative valuation of the usefulness of the resource for them. Based on the valuation, users bid for the resource and the auctioneer or centralized controller arbitrates resource distribution based on the received bid values.

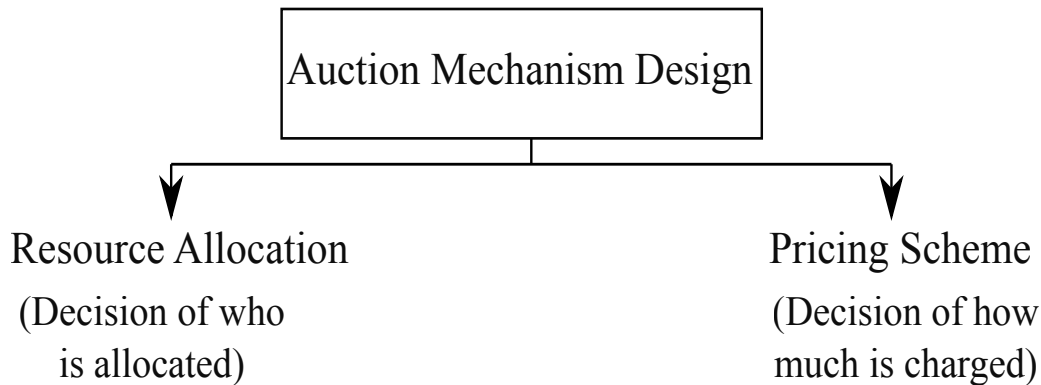


Figure 2.1: Auction mechanism design steps.

As illustrated in Figure 2.1, an auction-based mechanism design involves two steps: 1) resource allocation strategy 2) pricing scheme. Resource allocation strategy is responsible for decision making which player(s) should be allocated resources based on the objective of allocation. Pricing scheme determines the price that is charged from the users in return. Pricing scheme also enforces users to reveal their true value for the resource.

In general, the resource is allocated among the users (participants) using sealed-bid auction format. In sealed bid auctions, interested buyers send their valuations for the object in a closed envelope along with the demand, to the auctioneer (centralized entity responsible for resource allocation). Thus, the privacy of the valuation and demand for the object are ensured for each user. For instance, in spectrum auctions, spectrum valuation for a service provider depends on the desired bandwidth and on other factors such as the number of subscribers and the services desired by the subscribers. Hence, the spectrum valuation is a private information of a service provider which is not known to the auctioneer. Generally, the participants in any auction are selfish and are likely to misreport the actual valuation to the auctioneer if there is incentive to do so. Hence, ensuring the strategy-proofness of auctions is of significant importance [26]. An auction

is said to be strategy-proof if any participant does not gain on deviating from the true or actual value of their demands of the resource.

Strategy-proof auctions not only compel the participants to reveal their true valuations but also makes the process of spectrum allocation easier for the auctioneer and the operators. The operators are neither required to perform complex computations nor they have to invest time to determine the optimal bidding strategy to maximize their utility gains. Hence, it makes the process of resource allocation faster by removing the time and computational overhead. Moreover, strategy-proofness also increases the number of participants in an auction.

2.1.1 Strategy-Proof Spectrum Auctions

In conventional auctions, once an object is allocated to a buyer, it cannot be allocated to other buyers. However, in spectrum auctions, the same spectrum (frequency band) can be reused or reallocated after a certain fixed distance depending on the coverage area of BSs. This implies that any two BSs can be assigned the same frequency band if they do not interfere with each other. This feature provides an advantage in terms of spectrum utilization, but it is more challenging to achieve strategy-proof spectrum auction. Second price auction mechanism [26] ensures strategy-proof behavior in conventional auctions. However, the same is not guaranteed in the spectrum auctions [28]. In second-price auctions, the object goes to the highest bidder and is charged the price of the second highest bidder in the auction. Moreover, not every base station of an operator interferes with each base station of other operators. Therefore, achieving strategy-proof spectrum allocation across the multiple BSs in cellular network using second price auction is not possible. Moreover, it fails to exploit the re-usability of the spectrum which again results in inefficient usage of the spectrum.

In spectrum auctions, three properties are of utmost importance: strategy-proofness, low computational complexity, and optimality of allocation to maximize the social welfare Figure 2.2. Unfortunately, achieving all three properties simultaneously in spectrum auction subject to re-usability constraint is provably NP-Hard.

VCG mechanism is the first strategy-proof mechanism that always chooses the optimal allocation strategy. VCG mechanism selects the set of participants that maximizes



Figure 2.2: Auction mechanism requirements.

the overall sum of valuation in the auction [29–31]. But, determining the optimal allocation and pricing strategy is burdened with the high computational complexity of the auctions. Due to high computational cost, VCG mechanism is not suitable for dynamic spectrum allocation auctions even in wireless networks of moderate size [27]. In general, VCG mechanism is applicable in combinatorial auctions for sealed bid format, where each player submits a bid for the channel without the knowledge of other players' bids in the auction. Unlike second price auctions, VCG is applicable for single parameter environment as well as multi-parameter environment. Next, we describe the VCG mechanism for spectrum allocation.

2.1.2 Vickrey-Clarke-Groves Mechanism

We assume that there are n BSs to participate in spectrum auction which leads to 2^n possibilities. Due to the interference across the BSs, all 2^n combinations may not be feasible for spectrum allocation. The BSs which are sufficiently far can be allocated channels simultaneously. Let the binary vector $x = \{x_1, x_2, \dots, x_n\}$ denote a feasible allocation satisfying all the interference constraints, where $x_i = 1$ if a channel is assigned to the BS i , otherwise $x_i = 0$. Let \mathcal{X} denote the set of feasible allocations. BS i submits a bid b_i based on its valuation. Let $b = \{b_1, b_2, \dots, b_n\}$. The optimal allocation is given

as

$$x^* = \arg \max_{x \in \mathcal{X}} b \cdot x. \quad (2.1)$$

Now, a pricing scheme is defined to make the auction strategy-proof. Using a pricing scheme, the players are enforced to submit true valuation of the object to the auctioneer. VCG pricing scheme charges the BSs with the welfare loss inflicted due to the presence of BS i .

Let ρ_i denote the price charged to BS i .

$$\rho_i = \max_{x \in \mathcal{X}} \sum_{j \neq i} x_j \cdot b_j - \sum_{j \neq i} x_j^* \cdot b_j, \quad (2.2)$$

where x^* is the optimal allocation obtained from Equation (2.1). The price charged using Equation (2.2) also ensures individual rationality i.e., $0 \leq \rho_i \leq b_i$. In other words, any BS would never be charged more than its submitted bid. The individual rationality reflects that the utility gain at a BS can never be negative if a BS bids at its true value.

Though VCG mechanism achieves the optimal channel allocation for social welfare maximization, it becomes intractable for a large set of BSs. Hence, it is not feasible for practical implementation. Next, we propose strategy-proof mechanisms to maximize the social welfare of the spectrum for various scenarios. The proposed algorithms are also computationally efficient in comparison to VCG. VCG is implemented in two steps: Channel Allocation ($\mathcal{O}(2^n)$) and Price Charging scheme ($\mathcal{O}(2^n)$).

2.2 Spectrum Auctions in Cellular Network

In this section, we review some related work on Dynamic Spectrum Access (DSA). Auction-based spectrum allocation approaches have been extensively studied in the literature [32–38]. As stated above, achieving strategy-proof optimal allocation and computational feasibility in a mechanism is NP-Hard. In [37], the authors present a DSA mechanism in cellular networks which achieves near-optimal allocation for revenue maximization using greedy graph coloring approach. The authors in [32] study real-time spectrum allocation mechanism. Though, the mechanisms proposed in [37], [32] are computationally feasible in terms of implementation, they are not guaranteed to be strategy-proof. In [38], the authors propose a mechanism which ensures a certain fair chance of spectrum allocation along with the maximization of social welfare. In [39], the authors propose a revenue

maximization mechanism for spectrum allocation. For revenue maximization, the combination of well known Vickrey-Clarke-Groves (VCG) [29–31] mechanism and Myerson’s Lemma [40] are studied. In [28], the authors proposed VERITAS, a sealed bid strategy-proof auction mechanism which follows a certain monotonicity behavior. The authors in [41] propose another strategy-proof mechanism SMALL which groups non-conflicting base stations and sacrifices the base station(s) corresponding to the lowest bid in the winner group. SMALL has better allocation efficiency than that of the algorithm proposed in [28]. In [32], the authors propose an auction-based approach for fine grained (i.e., a channel is sliced into smaller frequencies) channel allocation. However, it does not satisfy the strategy-proofness property. As interference is one of the major concerns in wireless, the authors in [34], propose an auction based power allocation mechanism. However, it fails to be strategy-proof.

Both VERITAS [28] and SMALL [41] assume that the channel valuation increases linearly with the demand. In [42–44], strategy-proof double auction mechanisms are studied. The authors in [45, 46] studies auction-based approaches for DSA in cognitive networks. In [33], the game-theoretic aspect of the DSA in cognitive networks is explored.

The authors in [47] consider adaptive-width spectrum allocation problem where the channel valuation is a non-increasing function of the demand. To take the decrease in valuation with the demand into account, strategy-proof mechanism SPECIAL is proposed. Here, it is assumed that all the base stations bid for all the channels available for auction. To improve the social welfare and revenue of VERITAS, the concept of reserve price in valuation is incorporated in [48].

Most of the existing works is centered on designing a computationally feasible strategy-proof spectrum auction mechanism for non-cooperative base station participation in auctions. Moreover, [28, 37, 38, 41–44, 46, 47] consider base stations with uniform channel demand. However, only few works [28, 41, 47] consider multiple channel demand across the BSs. Except [47], all the works assume that the channel valuation scales linearly with the demand, which may not be true in general as throughput may not increase linearly as a function of bandwidth.

To the best of our knowledge, none of the previous works has considered the operators as the players in the spectrum auction. In comparison, in our work, we consider that non-

cooperative and rational operators participate in spectrum auctions and each operator has multiple BSs. Our work also considers non-uniform channel requirement at the BSs.

2.3 Spectrum Auctions in Hierarchical Settings

Most of the work in resource allocation using auctions is focused on the single stage auction with direct interaction between the resource owner and the users. Moreover, these works consider only one-sided auctions. However, in our work we consider multiple stage hierarchical auction in wireless. Authors in [49] have presented the first ever analyses of resource allocation in hierarchical settings. But, the work does not consider application and lacks focus on mechanism design. In [50], authors have investigated the Nash implementation of a combinatorial auction for indivisible resources.

Authors in [51], have studied how the transit and customer prices affect Quality of Service (QoS) in 3-Tier settings. The main focus is on pricing equilibrium, instead of the mechanism design. For wireless virtualization an opportunistic sharing based approach has been proposed by authors in [52]. Authors in [53], have proposed a scheme for spectrum sharing across multiple operators dynamically using bankruptcy game. However, works in [52] and [53] do not consider user involvement. Another work [54] has proposed a combinatorial auction for virtualization of network in hierarchical settings.

Authors in [55], have proposed three-stage spectrum allocation framework. However, middlemen is restricted to get atmost one unit of resource. In contrast, our work considers multiple unit resource demand at every stage with no restrict on the number of units that can be allocated. In [56], have studied the spectrum allocation in hierarchical settings. Authors have proposed an auction for upper level resource allocation and in lower level price demand method is considered.

2.4 Spectrum allocation in unified unicast multicast framework

The authors in [57], emphasize on the necessity of integration of unicast and multicast services under one framework in 5G networks. However, no specific framework has been

discussed in the paper. The authors in [58], analyze the use case where multicast, broadcast and unicast transmission share resources in 5G New Radio (NR) [59]. The authors claim that 5G NR results in better coverage to cell-edge UEs as compared to eMBMS.

In [60], the authors propose and analyze architectures for 5G mobile core network to provision multicast and broadcast services. The proposed architectures are applicable for Digital Terrestrial Television, Public Warning, Internet of Things, V2X (vehicle to everything) and Mission Critical Communications (MCC).

The authors in [61], propose a multicast resource allocation scheme where the transmission rate is limited by the worst channel condition experienced by the UE requesting the content in the network. A detailed survey on multicasting in wireless access networks has been presented by the authors in [62]. The authors in [63], present the requirement of handling the hybrid unicast-multicast approaches for efficient utilization of radio resources in the network. An approach that considers the channel conditions experienced by the UEs has been proposed by the authors in [64]. Here, UEs with good channel conditions receive content via unicast transmission, whereas UEs experiencing poor channel conditions are delivered content via multicast transmission. However, the selection of the transmission mode is made by individual UEs and may not be efficient due to the unavailability of network wide resource utilization information with the UEs.

In [65], a resource allocation algorithm has been proposed to maximize the Quality of Experience (QoE) of all UEs in an LTE MOOD system. The authors consider physical resource block allocation to each live stream individually, based on the UE demand. The authors in [66], discuss the enhancements made to LTE eMBMS for TV services and MOOD. Furthermore, use cases for each of the enhancements are also described.

The authors in [67], have proposed a mechanism to address the trade-off between fairness and efficiency in resource allocation. The game-theoretic bargaining approach has been used in modeling the fairness and efficiency of the system.

The authors in [68], have proposed joint content delivery of unicast and e-MBMS services to UEs in LTE networks. In [69], the authors jointly optimize the content delivery of unicast and multicast in the network for the given set of UEs in the system. They focus on maximizing the sum-rate of the best effort UEs by adaptive power and subcarrier allocation across UEs.

Various algorithms have been proposed for determining optimal grouping of UEs into different multicast groups in [70], [71]. The authors in [72], have proposed a scheme for grouping UEs into different multicast groups, considering the time varying channel conditions. An efficient and optimal grouping mechanism is proposed by the authors such that the UEs with good channel conditions are not grouped with the UEs experiencing poor channel conditions [73]. However, dynamic traffic in the wireless network has not been considered.

To the best of our knowledge, none of the available works propose a unified framework for the management of unicast and multicast delivery with the help of dual connectivity and SDN, which enables utilization of network-wide information for decision making as has been proposed in this work.

Additionally, most of the existing literature, while focusing on objectives, such as efficient resource utilization, maximization of throughput or achievement of fairness across UEs in multicast delivery, consider a fixed number of UEs. This may be particularly limiting as network traffic is typically dynamic in practice. In order to address this limitation, we have considered the dynamic arrival and departure of UEs in the network.

Chapter 3

Dynamic Spectrum Allocation across Base Stations

To support the exponentially increasing data requirements of users, efficient use of scarce and limited spectrum is paramount. As described in Chapter 1, the static spectrum allocation results in under-utilization of resources due to spatial and temporal traffic variations in the network. In this chapter, we investigate the issue of inefficient utilization of spectrum across multiple base stations, where their resource requirements are time-varying in nature. We address the problem by allocating the spectrum dynamically for shorter durations considering temporal variations in the network traffic. Resource allocation across neighboring base stations also needs to satisfy the spectrum reuse constraints for guaranteed Quality of Service (QoS) requirements in the network. However, the optimal resource allocation is known to be NP-hard and hence, computationally infeasible even for the modest network sizes [28].

We formulate the dynamic spectrum allocation problem within the sealed-bid auction framework with the aim of maximizing social welfare. Due to the NP-hard nature of the problem, we propose an efficient strategy-proof spectrum allocation mechanism with near-optimal social welfare. Moreover, the proposed algorithm exploits the limited constraint set property of the wireless access network. In other words, a base station receives interference from a limited number of base stations (usually 6 in a hexagonal cell deployment) present in the network. Using Monte Carlo simulations, we show that the proposed algorithm can be implemented in large networks. It not only has near-optimal

social welfare but also provides fair allocation in spite of some base stations bidding much higher values than others in the system.

The rest of the chapter is organized as follows. In Section 3.1, we describe the system model and the problem formulation. The proposed mechanism is presented in Section 3.2. In Section 3.3, the proposed mechanism is illustrated using an example. We discuss the other scenarios for time-varying traffic in which the proposed mechanism is applicable in Section 3.4. In Section 3.5, we compare the performance of the proposed mechanism with that of the other mechanisms using Monte Carlo simulations. In Section 3.6, we conclude the chapter.

3.1 System Model and Problem Formulation

We consider a spectrum allocation framework comprising an auctioneer, a spectrum database, and a set of base stations illustrated in Figure 3.1. The auctioneer is responsible for spectrum allocation across the base stations. The spectrum database contains the information about the spectrum available for allocation. In general, the spectrum is divided into multiple channels. For the sake of simplicity, we assume that only one channel is available in the spectrum database. As traffic in a network possess time-varying nature, the base stations are allocated spectrum for average traffic requirements for a longer duration. For peak traffic requirements, base stations are allocated spectrum using auctions in every short duration.

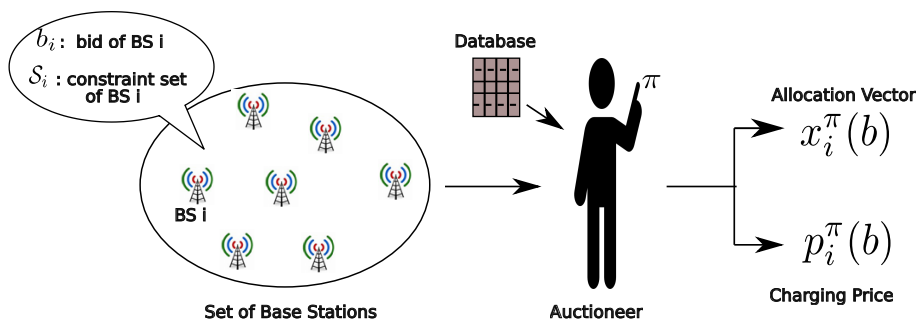


Figure 3.1: System model

Let $\mathcal{N} = \{1, 2, \dots, n\}$ denotes the set of base stations. We assume that the base stations are selfish, rational and do not collude. To communicate its valuation for the

resource, the base station projects a bid to the auctioneer. The bids may not be equal to their respective actual valuations. Let b_i denote the bid of base station i for the resource.

We consider a spectrum allocation problem where the spectrum is allocated dynamically based on the demands of the base stations. In general, the base station deployment is common knowledge in a wireless network. Therefore, we assume that the conflict graph is known to everyone, including the auctioneer, which is true to the practical setup of the wireless network. We assume that the sealed-bid spectrum auction is performed for a specific duration. The auction duration is adjusted depending on the spatio-temporal variations in the traffic of the network.

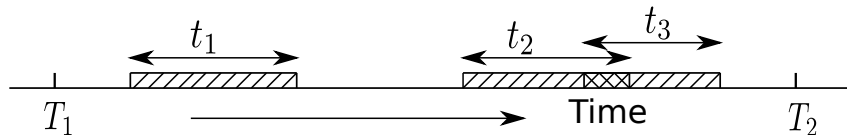


Figure 3.2: Illustration of auction duration $[T_1, T_2]$ and demand time intervals t_1 , t_2 and t_3 corresponding to base stations 1, 2 and 3, respectively.

We consider that the auctioneer broadcasts the duration $[T_1, T_2]$ for spectrum auction to the base stations. To exploit the re-usability aspect of the spectrum, the auctioneer requests the base stations to report time interval t_i and the corresponding bid b_i , where $t_i = [t_{si}, t_{ei}]$ denote the interval in which base station i desires additional resource and b_i denote its bid value. Here, t_{si} and t_{ei} denote the start and the end time of the demand interval for base station i such that $T_1 \leq t_{si} \leq t_{ei} \leq T_2$. Let v_i denote the true valuation for base station i . In sealed-bid auctions, v_i is private information of base station i not known to others.

As we described earlier, base stations are selfish and therefore, base stations may report a bid which is deviated from their respective true valuations if doing so results in utility gain, i.e., b_i may or may not be equal to v_i . We assume that base station i may report any bid $b_i \geq 0$ for the desired spectrum slot. In case a base station reports zero bid, then we consider it does not require spectrum in the interval $[T_1, T_2]$. Therefore, it (base station) is removed from the network topology. Without loss of generality, we denote bid of n base stations in the network as $\mathbf{b} = (b_1, \dots, b_n)$ such that $\mathbf{b} \in \mathbb{R}_+^n$. Further, we define $\mathbf{b}_{-i} = (b_1, \dots, b_{i-1}, b_{i+1}, \dots, b_n) \in \mathbb{R}_+^{n-1}$ as the bids of all the base stations except i . The aim of the auction mechanism is to arbitrate spectrum allocation and pricing based on the

received $\{(t_i, b_i)\}_{i \in \mathcal{N}}$. In wireless networks, spectrum allocation must respect interference constraints, the reason for which we describe next.

If two nearby base stations transmit simultaneously on the same channel, then they cause interference to each other and this may lead to an unacceptable degradation of Quality of Service (QoS). Thus, to meet the QoS requirements, the spectrum must not be allotted to the base stations in close proximity. We model the interference in the network through conflict graph $\mathcal{G}' = (V, \mathcal{E}')$, where nodes denote base stations and edges denote interfering pairs of base stations in the network. The graph \mathcal{G}' is an undirected graph. Note that if $(i, j) \in \mathcal{E}'$, then the same channel cannot be allocated to the base stations i and j at the same time. Let \mathcal{S}'_i denote the set of neighbors (interfering base stations) for base station (node) i in \mathcal{G}' . Observe that if $j \in \mathcal{S}'_i$, then $i \in \mathcal{S}'_j$. The conflict graph \mathcal{G}' captures the constraints on spectrum allocation. Next, we define the set of feasible allocations.

Let a binary vector $\mathbf{x} = (x_1, \dots, x_n)$ denote the allocation vector. Here, $x_i = 1$ signifies base station i is allocated channel in the interval t_i .

Definition 1. A vector \mathbf{x} is a feasible channel allocation if $t_i \cap t_j \neq \phi$ for any $j \in \mathcal{S}'_i$ then $x_i + x_j \leq 1$. Allocation vector $\bar{\mathbf{x}}$ is said to be maximal if for every j such that $x_j = 0$, there exists $i \in \mathcal{S}'_j$ satisfying $t_i \cap t_j \neq \phi$ and $x_i = 1$.

Note that any feasible \mathbf{x} does not allocate spectrum simultaneously to the interfering base stations. Let \mathcal{X} denote the set of all feasible channel allocations. Now, we define auction based spectrum allocation mechanism.

Definition 2. An auction based spectrum allocation mechanism π is a map from \mathbb{R}_+^n to $\mathcal{X} \times [0, \infty)^n$, i.e., for given bid vector \mathbf{b} , π outputs a feasible allocation vector $\mathbf{x}^\pi(\mathbf{b}) = (x_1^\pi(\mathbf{b}), \dots, x_n^\pi(\mathbf{b}))$ and a price vector $\mathbf{p}^\pi(\mathbf{b}) = (p_1^\pi(\mathbf{b}), \dots, p_n^\pi(\mathbf{b}))$.

Thus, a spectrum allocation mechanism π outputs a feasible channel allocation for any given bid vector \mathbf{b} , along with the price that each base station needs to pay for the allocated channel. Let Π denote the set of all auction-based allocation policies.

Definition 3. Social welfare under mechanism π for bid values \mathbf{b} is defined as $W_s^\pi(\mathbf{b}) = \sum_{i=1}^n v_i \cdot x_i^\pi(\mathbf{b})$, where $x_i^\pi(\mathbf{b})$ denote the allocation at base station i . Moreover, the utility for base station i for bids \mathbf{b} under π is given as $U_i^\pi(\mathbf{b}) = (v_i - p_i^\pi(\mathbf{b}))x_i^\pi(\mathbf{b})$.

Note that the social welfare is the sum of true valuations v_i 's, not the bid values b_i 's reported by the base stations to mechanism π . Moreover, the utility for a base station is the difference between its true valuation v_i and price p_i^π charged under the mechanism π . Typically, the aim of the auctioneer is to design a mechanism π that maximizes social welfare, i.e., it needs to evaluate

$$\pi^* \in \arg \max_{\pi \in \Pi} W_s^\pi(\mathbf{b}), \quad (3.1)$$

while each base station wants to bid to maximize its utility. Note that \mathbf{v} is the private information of the base stations, and the spectrum auctioneer does not know it. Therefore, we need to design a mechanism in which rational base stations do not have any incentive to submit a bid other than their true valuation. This implies that the auctioneer has to ensure $\mathbf{b} = \mathbf{v}$.

Definition 4. *A mechanism π is truthful (strategy-proof) if*

$$U_i^\pi(v_i, \mathbf{b}_{-i}) \geq U_i^\pi(b_i, \mathbf{b}_{-i}), \text{ for all } (b_i, \mathbf{b}_{-i}).$$

Note that for a strategy-proof mechanism π , a base station has no incentive to bid anything other than its true valuation. Thus, for a strategy-proof mechanism, social welfare is equal to the sum of bid values of the base stations to whom the spectrum is allocated. The well known VCG auctions are strategy-proof and maximize social welfare. However, for spectrum auctions, computing VCG allocation is NP-hard. Hence, we need a computationally feasible mechanism that achieves near-optimal social welfare. Our proposed scheme is described next.

Remark: In our system model, nodes in the conflict graph represent the base stations in the wireless network. Typically, the base stations are static. Therefore, we have not assumed the mobility of nodes in the conflict graph over the time, which happens to be true in most of the existing wireless network. The dynamic resource allocation approach presented in the chapter is applicable for static nodes scenarios only.

3.2 Group based Optimal Strategy-proof Allocation Algorithm

In this section, we propose a computationally efficient, strategy-proof spectrum auction mechanism for time-varying demand intervals/slots during the auction period. The proposed mechanism consists of a channel assignment strategy and a pricing scheme. Each base station is charged based on the pricing scheme to ensure strategy-proofness.

3.2.1 Channel Allocation Strategy

The resource allocation strategy aims to choose an allocation vector in \mathcal{X} to meet the desired goal. The first step in our approach is to randomly partition the set of all the base stations $i \in \mathcal{N}$ into non-conflicting groups denoted as $\{G_1, \dots, G_\eta\}$, where $\eta = \max_{i \in \mathcal{N}} |\mathcal{S}_i| + 1$. Here, $|\mathcal{A}|$ denote the cardinality of set \mathcal{A} . The partitioning is performed using a randomized iterative greedy algorithm. In the first iteration a base station is selected at random and put in group G_1 . In further iterations, another base station i is chosen at random from $\mathcal{N} \setminus \cup_{k=1}^{\eta} G_k$ and placed in the group $G_{u_{\min}}$ such that $u_{\min} = \min\{u : u \in \{1, \dots, \eta\} \text{ and } G_u \cap \mathcal{S}_i = \phi\}$. We continue this process until $\cup_{k=1}^{\eta} G_k = \mathcal{N}$. The randomized conflict-free grouping is presented in Algorithm 1. Here, bid independent randomized partitioning of the users in each round of resource allocation ensures better resource utilization and fairness when some users consistently bid higher than the others.

Remark: Randomization is used to group the non-conflicting base stations such that all the base stations in a group can be allocated a channel simultaneously. Grouping of base station requires the constraint set of each base station in the wireless network. Moreover, randomized grouping of base stations does not require any information regarding the bid of the base stations. Thus, the claim regarding strategy-proofness of the algorithm holds for any base station grouping mechanism as long as the base stations in a group do not conflict (cause interference to each other).

Lemma 1. *If $\mathbf{x} \in \mathcal{X}$, then $x_i + x_j \leq 1$ for all i and $j \in \mathcal{S}_i$.*

Proof. This follows from Definition 1. □

Algorithm 1 Randomized conflict-free grouping**Input:** \mathcal{N} , \mathcal{S}_i for every $i \in \mathcal{N}$ **Output:** A conflict-free partition $\{G_1, \dots, G_\eta\}$

- 1: Initialize $\mathcal{N}_{\text{temp}} = \mathcal{N}$ and $G_u = \phi$, $\forall u = 1, \dots, \eta$
- 2: **while** $\mathcal{N}_{\text{temp}} \neq \phi$ **do**
- 3: Choose i , from $\mathcal{N}_{\text{temp}}$ uniformly w.p. $\frac{1}{|\mathcal{N}_{\text{temp}}|}$
- 4: Find $u_{\min} = \min\{u : u \in \{1, \dots, \eta\} \text{ and } G_u \cap \mathcal{S}_i = \phi\}$
- 5: $G_{u_{\min}} \leftarrow G_{u_{\min}} \cup \{i\}$
- 6: $\mathcal{N}_{\text{temp}} \leftarrow \mathcal{N}_{\text{temp}} \setminus \{i\}$
- 7: **end while**

The following lemma summarizes key properties of the partitioning step.

Lemma 2. *A conflict-free grouping given in Algorithm 1 outputs a partition $\{G_1, \dots, G_\eta\}$ of \mathcal{N} such that if $i, j \in G_u$, then $j \notin \mathcal{S}_i$.*

Proof. We need to show that the RHS in Step 4 of the algorithm is a non-empty set in each iteration. The rest follows immediately from the set construction. As we know that the maximum number of partitions η is restricted to $\max_i |\mathcal{S}_i| + 1$. This implies that the maximum cardinality of \mathcal{S}_i for every $i \in \mathcal{N}$ is less than or equal to $\eta - 1$. Thus, there exist at least one group index u such that $G_u \cap \mathcal{S}_i = \phi$. \square

Lemma 2 states that the channel can be allocated to all the members of any group G_u without violating the allocation constraint. Moreover, it is important to note that the grouping does not depend on the bid values \mathbf{b} .

Now, let Ω_g denote the set of all possible orderings of the sets $\{G_1, \dots, G_\eta\}$ obtained using conflict-free grouping algorithm. Thus, $|\Omega_g| = \eta!$. Furthermore, let $\omega_j \in \Omega_g$ denote the j^{th} ordering of the groups in the set Ω_g . We denote ω_j by a tuple $(G_{j_1}, \dots, G_{j_\eta})$. For example if $\eta = 3$, then there are $|\Omega_g| = 3! = 6$ different orderings. One of the possible 6 group ordering or tuple is $\omega_j = (G_2, G_1, G_3)$. Thus, $G_{j_1} = G_2$, $G_{j_2} = G_1$ and $G_{j_3} = G_3$. Channel allocation in a given group ordering ω_j is done as follows. We first assign the channel to each base station in G_{j_1} , then to all the base stations in $G_{j_2} \setminus (\cup_{i \in G_{j_1}} \mathcal{S}_i)$, and so on. Pseudo-code to obtain channel allocation corresponding to group ordering ω_j is given in Algorithm 2. Following guarantee can be given about output of the algorithm.

Algorithm 2 Pseudo code for channel allocation for given group ordering ω_j

Input: G_{ju} for every $1 \leq u \leq \eta$, \mathcal{S}_i for every $i \in \mathcal{N}$

Output: A channel allocation $\mathbf{x}(j)$

- 1: Initialize $G_{\text{temp}} = \phi$, $\ell = 1$ and $x_i(j) = 0$ for all $i \in \mathcal{N}$
 - 2: **while** $\ell \leq \eta$ **do**
 - 3: $G_a \leftarrow G_{j\ell} \setminus (\cup_{i \in G_{\text{temp}}} \mathcal{S}_i)$
 - 4: $x_i(j) \leftarrow 1$ for every $i \in G_a$
 - 5: $G_{\text{temp}} \leftarrow G_{\text{temp}} \cup G_a$
 - 6: $\ell \leftarrow \ell + 1$
 - 7: **end while**
-

Lemma 3. *The channel allocation vector $\mathbf{x}(j)$ given by Algorithm 2 corresponding to any group tuple ω_j is feasible, i.e., $\mathbf{x}(j) \in \mathcal{X}$. Moreover, $\mathbf{x}(j)$ is a maximal allocation vector for every j .*

Proof. Let $\mathbf{x}_\ell(j)$ denote the allocation after ℓ iterations of the algorithm. We first show that $\mathbf{x}_\ell(j) \in \mathcal{X}$ for every $1 \leq \ell \leq \eta$. Note that for $\ell = 1$, $x_{\ell i} = 1$ only for $i \in G_{j1}$. From Lemma 2, $\mathbf{x}_1(j) \in \mathcal{X}$ follows. Suppose $\mathbf{x}_\ell(j) \in \mathcal{X}$ holds for every $1 \leq \ell \leq \ell'$. Consider $(\ell' + 1)^{\text{th}}$ iteration of the algorithm. Note that the G_{temp} in every iteration contains base stations to which the channel is allocated until that iteration. Note that in Step 5 of the algorithm the channel is allocated only to base stations in $G_{j(\ell'+1)}$ that do not conflict with the base stations in G_{temp} . Thus, $\mathbf{x}_{\ell'+1}(j) \in \mathcal{X}$ and the required follows using induction. Now, we prove that the channel allocation is maximal. Suppose not, then there exist a base station u such that $x_{\ell u}(j) = 0$ in the output of the algorithm, but \mathbf{x}' such that $x'_i = x_{\ell i}(j)$ for every $i \neq u$ and $x'_u = 1$ is in \mathcal{X} . Since, $(G_{j1}, \dots, G_{j\eta})$ is a partition of \mathcal{N} , u must belong to some $G_{j\ell}$. Also, u must not belong to \mathcal{S}_i for any i which is allocated the channel in first $\ell - 1$ iterations. But, then the algorithm will allocate channel to base station u in ℓ^{th} iteration. Hence, no such base station exists, proving the required. \square

Now define, with a little abuse of notation, the perceived social utility under allocation $\mathbf{x}(j)$ as

$$\tilde{U}_j(\mathbf{b}) = \sum_{i=1}^n b_i x_i(j).$$

Moreover, define $j_{\mathbf{b}}^* = \arg \max_{\{j: \omega_j \in \Omega_g\}} \tilde{U}_j(\mathbf{b})$. Thus, $\omega_{j_{\mathbf{b}}^*}$ is the group permutation for which perceived utility is maximized among all possible group permutations. We choose allocation $\mathbf{x}(j_{\mathbf{b}}^*)$. Note that even though the grouping does not depend on the bids \mathbf{b} , the chosen channel allocation does. Let $\tilde{U}^*(\mathbf{b}) = \tilde{U}_{j_{\mathbf{b}}^*}(\mathbf{b})$. Next, we describe our proposed pricing scheme.

3.2.2 Pricing Scheme

After the channel allocation, we propose the appropriate pricing scheme, which ensures the strategy-proofness. That is, if any base station tries to deviate from its v_i , it is penalized. Let $(\epsilon, \mathbf{b}_{-i})$ denote the bid vector in which the bids of all the base stations except i are same as that in \mathbf{b} , but the bid of base station i is $\epsilon > 0$. Now, the price charged from the base station i is given as:

$$p_i(\mathbf{b}) = \left[\lim_{\epsilon \downarrow 0} \tilde{U}^*(\epsilon, \mathbf{b}_{-i}) - (\tilde{U}^*(\mathbf{b}) - b_i) \right] \times x_i(j_{\mathbf{b}}^*). \quad (3.2)$$

Algorithm 3 Pseudo code for Proposed mechanism

Input: bid vector \mathbf{b} , \mathcal{S}_i for every $i \in \mathcal{N}$

Output: Resource allocation $\mathbf{x}(\mathbf{b})$ and price vector $\mathbf{p}(\mathbf{b})$

- 1: Use Algorithm 1 to obtain conflict free grouping (G_1, \dots, G_η)
 - 2: **for** $\omega_j \in \Omega_g$ **do**
 - 3: Find allocation $\mathbf{x}(j)$ using Algorithm 2
 - 4: Compute $\tilde{U}_j(\mathbf{b}) = \sum_{i=1}^n b_i x_i(j)$
 - 5: **end for**
 - 6: Find $j_{\mathbf{b}}^* = \arg \max_{\{j: \omega_j \in \Omega_g\}} \tilde{U}_j(\mathbf{b})$
 - 7: Choose $\mathbf{x}(\mathbf{b}) = \mathbf{x}(j_{\mathbf{b}}^*)$
 - 8: Compute prices using (3.2)
-

We state the following straightforward result.

Lemma 4. *Under any bid values $\mathbf{b} > 0$, $0 \leq p_i \leq b_i$ for every $i \in \mathcal{N}$.*

Proof. It suffices to consider i such that $x_i(j_{\mathbf{b}}^*) = 1$. For every $\epsilon > 0$, $\tilde{U}^*(\epsilon, \mathbf{b}_{-i}) \geq \tilde{U}^*(\mathbf{b}) - b_i + \epsilon$. Thus, the proof follows by taking limit $\epsilon \downarrow 0$ on both sides of the above inequality. \square

This lemma clearly shows that for any truthful base station i , the utility obtained is non-negative, irrespective of the bids reported by other base stations.

Note that the optimal group permutation under bid vectors \mathbf{b} and $(\epsilon, \mathbf{b}_{-i})$ can be different. Unlike VCG, in our pricing scheme, we do not entirely remove base station i from the network; instead, base station i is always present. Only the bid value of base station i is set to $\epsilon \downarrow 0$. Hence, the interference graph remains the same. Subsequently, the feasible set of allocation remains the same with the negligible bid at the base station for which the price is evaluated. This distinction is essential as removing a base station changes the conflicting base stations in the network. The proposed algorithm is given in Algorithm 3. Next, we prove the key properties of the proposed algorithm.

Lemma 5. *If base station i is allocated channels at bid \mathbf{b} , then it will also be allocated channels at bid $(\epsilon, \mathbf{b}_{-i})$ for every $\epsilon > b_i$. Moreover, optimal group permutation under \mathbf{b} and $(\epsilon, \mathbf{b}_{-i})$ are the same, i.e., $j_{\mathbf{b}}^* = j_{(\epsilon, \mathbf{b}_{-i})}^*$.*

Proof. Without loss of generality, let $\epsilon = b_i + \Delta$ for some $\Delta > 0$. Note that since the bid value of only base station i has changed, we can conclude that

$$\tilde{U}_j(\epsilon, \mathbf{b}_{-i}) - \tilde{U}_j(\mathbf{b}) \leq \Delta, \quad (3.3)$$

for every group permutation ω_j . Moreover,

$$\tilde{U}_{j_{\mathbf{b}}^*}(\mathbf{b}) + \Delta = \tilde{U}_{j_{\mathbf{b}}^*}(\epsilon, \mathbf{b}_{-i}), \quad (3.4)$$

i.e., the perceived social utilities under group permutation $j_{\mathbf{b}}^*$ for bid vectors \mathbf{b} and $(\epsilon, \mathbf{b}_{-i})$ differ by amount Δ with latter having a larger value. Thus, we can conclude from Equation (3.3) and Equation (3.4) that $j_{\mathbf{b}}^*$ is optimal group permutation for $(\epsilon, \mathbf{b}_{-i})$ as well. Now, the required follows from Algorithm 2. \square

Lemma 13 implies that if a base station unilaterally increases its bid, then it is more likely to get the channels. Next, we prove that the proposed algorithm is strategy-proof.

Theorem 1. *Algorithm 3 is strategy-proof.*

Proof. We prove the required by considering two scenarios.

Scenario 1 : Base station i bids more than its true valuation, i.e., $b_i > v_i$. Without loss of generality, $b_i = v_i + \Delta$ for some $\Delta > 0$. Bids of the other base stations can be arbitrary.

Thus, we compare two bid vectors, viz. \mathbf{b} and (v_i, \mathbf{b}_{-i}) , where latter corresponds to base station i bidding truthfully. This scenario is further bifurcated into three cases.

Case (i): Base station i gets channel under both bid vectors \mathbf{b} and (v_i, \mathbf{b}_{-i}) . By Lemma 13, it follows that the optimal group permutation remains same for both the bid vectors. Also, the optimal perceived utility values satisfy $\tilde{U}^*(\mathbf{b}) = \tilde{U}^*(v_i, \mathbf{b}_{-i}) + \Delta$. Now, $p_i(\mathbf{b}) = p_i(v_i, \mathbf{b}_{-i})$ from Equation (3.2). Thus the required holds.

Case (ii): base station i does not get the channel under (v_i, \mathbf{b}_{-i}) , but gets it under \mathbf{b} . Note that utility for base station i under (v_i, \mathbf{b}_{-i}) is zero as it does not get the channel. Now, we bound base station i utility under \mathbf{b} . Since the bid for only base station i is different under two bid vectors, we can conclude that

$$\tilde{U}^*(\mathbf{b}) - \tilde{U}^*(v_i, \mathbf{b}_{-i}) \leq \Delta. \quad (3.5)$$

Now, from Equation (3.2), it follows that

$$\begin{aligned} p_i(\mathbf{b}) &= \lim_{\epsilon \downarrow 0} \tilde{U}^*(\mathbf{b}) - (\tilde{U}^*(\mathbf{b}) - b_i) \\ &= \lim_{\epsilon \downarrow 0} \tilde{U}^*(\mathbf{b}) - (\tilde{U}^*(\mathbf{b}) - v_i) + \Delta \end{aligned} \quad (3.6)$$

$$= (\tilde{U}^*(v_i, \mathbf{b}_{-i}) - \tilde{U}^*(\mathbf{b})) + v_i + \Delta \quad (3.7)$$

$$\geq v_i. \quad (3.8)$$

Equality (3.6) follows as $b_i = v_i + \Delta$. Equality (3.7) follows by Lemma 13. Note that for every ϵ smaller than v_i base station i can not get channel as it can not get it at bid value v_i . Moreover, since only bid for base station i is changing, the optimal perceived social utility remains unchanged. Hence, the limiting value equals maximum perceived social utility for bid (v_i, \mathbf{b}_{-i}) . Finally, Equation (3.8) follows from Equation (3.5). Now, Equation (3.8) implies that the utility for base station i under \mathbf{b} can at most be 0, which is same when it bids true valuation v_i . This proves the required.

Case (iii): Base station i neither gets channel at (v_i, \mathbf{b}_{-i}) , nor at \mathbf{b} . Here, utility for base station i will remain zero.

Scenario 2 : Base station i bids less than its true valuation, i.e., $b_i < v_i$. Without loss of generality, $v_i = b_i + \Delta$ for some $\Delta > 0$. Bids of the other base stations can be arbitrary.

Thus, we compare two bid vectors, viz. \mathbf{b} and (v_i, \mathbf{b}_{-i}) . This scenario is further bifurcated into three cases.

Case (i): The base station i is allocated channel under (v_i, \mathbf{b}_{-i}) and also under \mathbf{b} . Analysis of this case is similar to that in Case (i) of Scenario 1. Again here, it can be shown that the utility for base station remains unchanged, and hence there is no benefit for deviating from true valuation.

Case (ii): The base station i is allocated channel under (v_i, \mathbf{b}_{-i}) , but it does not get it under \mathbf{b} . This implies that the base station i has utility $v_i - p_i(v_i, \mathbf{b}_{-i})$ for bid vector (v_i, \mathbf{b}_{-i}) , but on deviation its utility becomes zero. Now, the required follows from Lemma 4.

Case (iii): The base station i neither gets a channel at (v_i, \mathbf{b}_{-i}) nor at \mathbf{b} . Here, the utility for the base station remains zero. Thus, no incentive on deviation from true value. This completes the proof. \square

3.3 Illustrative Example

Example: As illustrated in Figure 3.3(a), we consider a wireless network consisting of 6 base stations. The wireless network is represented as a graph. The nodes denote base stations and edges denote interfering pairs of base stations in the graph. We consider that the auctioneer collects the spectrum demand from the base stations a priori for $[T_1, T_2] = [0, 1]$, auction duration. We assume that the base stations submit a non-zero bid along with the time slot in the interval $[0, 1]$ for which channel is required to the auctioneer. Let the bid vector be $\mathbf{b} = [9 \ 10 \ 8 \ 7 \ 5 \ 7]$. For simplicity of calculations, we assume each base station needs spectrum for $\tau = 0.1$ time unit in the interval of auction. Let the vector $t_{si} = [0.45 \ 0.50 \ 0.35 \ 0.40 \ 0.55 \ 0.70]$ denote the start of the demand time slot corresponding to each base station. In Figure 3.3(b), t_i represents the time interval for channel demand corresponding to base station i . For instance, the time interval for base station 1 corresponds to $[0.45, 0.55]$.

We know that a channel can be allocated between any pair of interfering base stations in non-overlapping time slots. For efficient spectrum usage, we exploit the temporal variation in the demand across the base stations of the network. In case the channel is

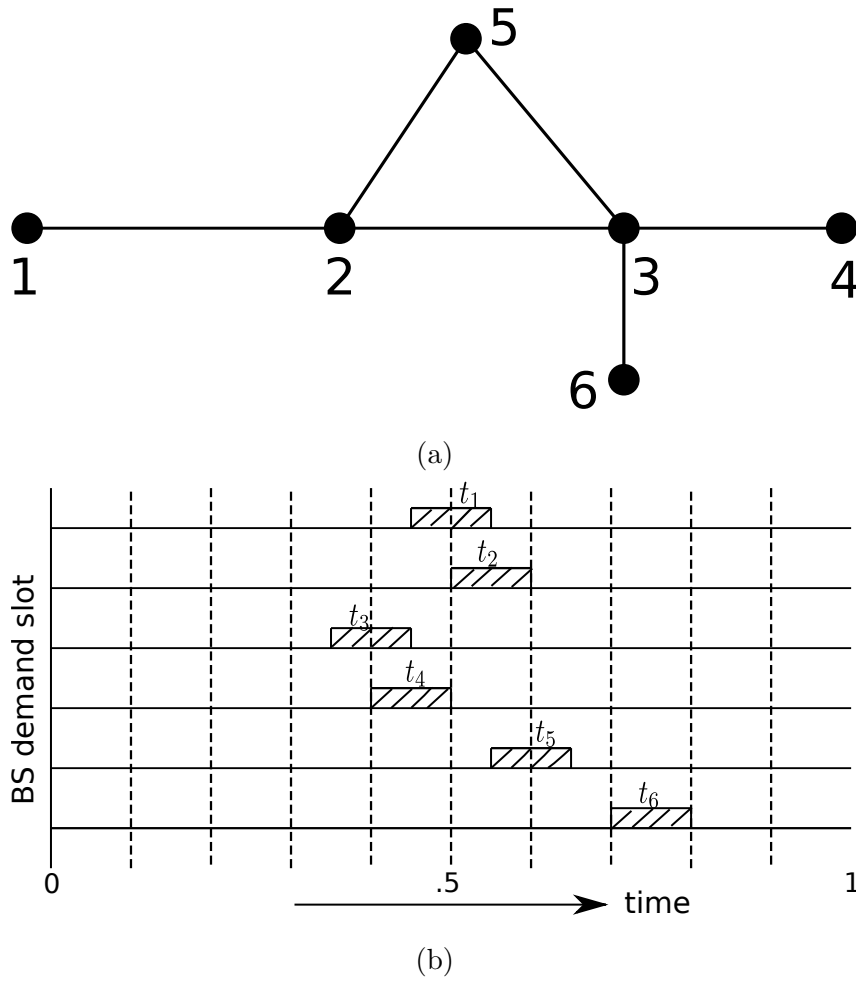


Figure 3.3: (a) Interference graph (b) Channel demand time slots

required in non-overlapping time slots, the edge joining them can be removed. Therefore, on consideration of the demand time slots, the conflict graph in Figure 3.3(a) reduces to the conflict graph illustrated in Figure 3.4. We briefly describe the channel allocation for the proposed strategy-proof mechanism and compare it with the two other strategy-proof mechanisms SMALL [41] and greedy [28].

3.3.1 Allocation in Proposed Algorithm

As discussed in Section 3.2, the proposed algorithm first reconstructs the conflict/interference graph based on the demand time interval of the spectrum for each base station in the network. Then, it performs a grouping of the non-conflicting base stations, irrespective of their bids. Let the base stations in the re-constructed interference graph mentioned in Figure 3.4 be grouped into 2 groups, namely $G_1 = \{1, 4, 5\}$ and $G_2 = \{2, 3, 6\}$. These

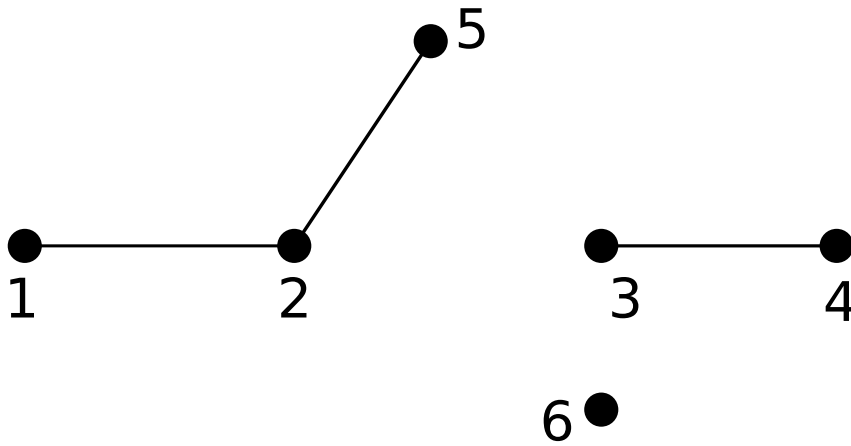


Figure 3.4: Re-constructed interference graph considering demand time intervals for each base station.

two groups result in two arrangements $[G_1, G_2]$ and $[G_2, G_1]$.

Based on the bid vector \mathbf{b} , we determine the social welfare for each arrangement. The social welfare for arrangements $\omega_1 = [G_1, G_2]$ and $\omega_2 = [G_2, G_1]$ are 28 and 26, respectively. Since the arrangement ω_1 has maximum social welfare, the arrangement corresponds to the channel allocation $\mathbf{x}^*(\mathbf{b}) = (1, 0, 0, 1, 1, 1)$ (see Algorithm 2). Using the pricing scheme (see 3.2), the base stations 1, 4, 5 and 6 get channel at the price 6, 4, 2 and 0, respectively. It is important to note that the consideration of demand slots reduces the number of groups to 2, whereas no matter how the base stations are grouped in the network illustrated in Figure 3.3(a) the minimum number of groups required is 3. In the example, the number of groups reduction from 3 to 2 decreases the group arrangements from 6 to 2. Thus, the decrease in the number of groups reduces the possible arrangements significantly. In other words, the fewer number of groups will have a smaller set of possible arrangements.

3.4 Applications

In this section, we describe various dynamic spectrum allocation scenarios where GOSPAL can be applicable. In a wireless network, the requirement of resources can be classified based on the type of service. We discuss some scenarios of spectrum allocation where GOSPAL is applicable.

3.4.1 Spectrum Band Specific Channel Allocation

We consider the scenario where channels are not identical; instead, they are from different spectrum bands. In this scenario, a base station may require a spectrum in the specific band as per the service required by the UEs in the network. Therefore, each base station reports a spectrum band-specific bid to the auctioneer. Due to heterogeneous spectrum, base station valuation may differ for each spectrum band. In this particular case, dynamic spectrum auction can be performed separately for each spectrum band using GOSPAL mechanism.

3.4.2 Generalization of the proposed mechanism

Here, we discuss spectrum allocation scenarios for the proposed mechanism when a base station requests spectrum in multiple slots within an auction duration. The two possible variations of the proposed mechanism are as follows:

- Base station spectrum demand intervals are strict, i.e., a base station accepts a channel only if it is allocated spectrum in all the requested demand slots. As we know that any two base stations can be allotted a channel simultaneously only if (i) base stations are far apart such that do not cause interference to each other or (ii) two interfering base stations request spectrum in non-overlapping intervals. Based on the above mentioned criteria of resource allocation, we re-construct the conflict graph. Then GOSPAL is applied on the updated conflict graph.

To illustrate the above scenario, we revisit the example mentioned in Section 3.3. Here, we consider that the base stations demand spectrum at multiple slots and the demand is the strict type given in Figure 3.5. The re-constructed graph is given in Figure 3.6. Thus, considering strict demand across base stations in the network only changes the re-constructed graph. Note that in the worst case, the re-constructed conflict graph would be the same as the initial conflict graph obtained from the network.

- The base station accepts channel for any subset of the requested demand slots. In other words, base stations request spectrum in multiple slots within the auction duration and willing to accept the spectrum in slots less than or equal to any number

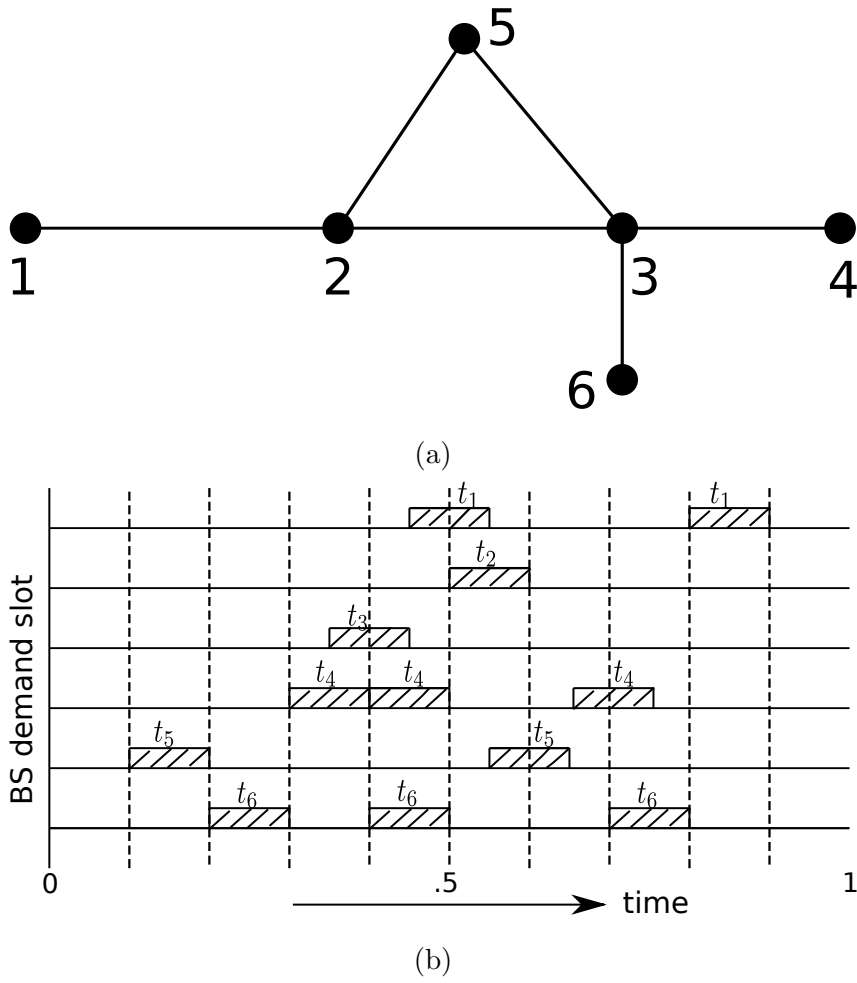


Figure 3.5: (a) Interference graph (b) Channel demand time slots

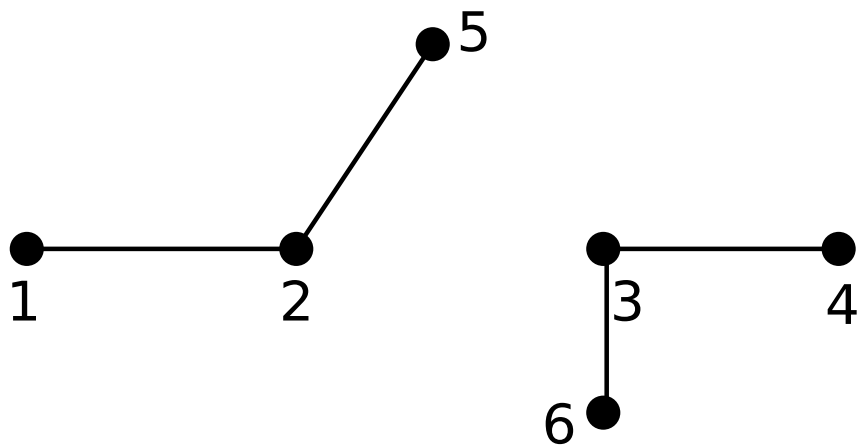


Figure 3.6: Re-constructed interference graph considering demand time intervals for each base station.

of requested slots. In this scenario, we are required to determine the conflicting base stations for each requested slot individually. Therefore, the conflict graph needs to

be augmented with additional nodes (one less than the number of time slots) to account for the requested slots individually by a base station.

To illustrate the application of the proposed algorithm in this particular scenario, we revisit the example given in Figure 3.5(a). As each time slot needs to be considered separately, time slots are numbered as t_i^ℓ , where ℓ denotes the requested time slot number for base station i in Figure 3.7(a). We described earlier that the first step is to obtain an augmented conflict (interference) graph. The conflict graph with augmented additional nodes is shown in Figure 3.7(b). Now, we reconstruct a conflict graph by checking the overlapping time slots of the interfering base stations shown in Figure 3.8. For instance, we can see that although base stations 1 and 2 are interfering pair of base stations, but time slot t_1^2 does not overlap with the t_2^1 . Therefore, the connecting edge (t_1^2, t_2^1) is removed from Figure 3.8.

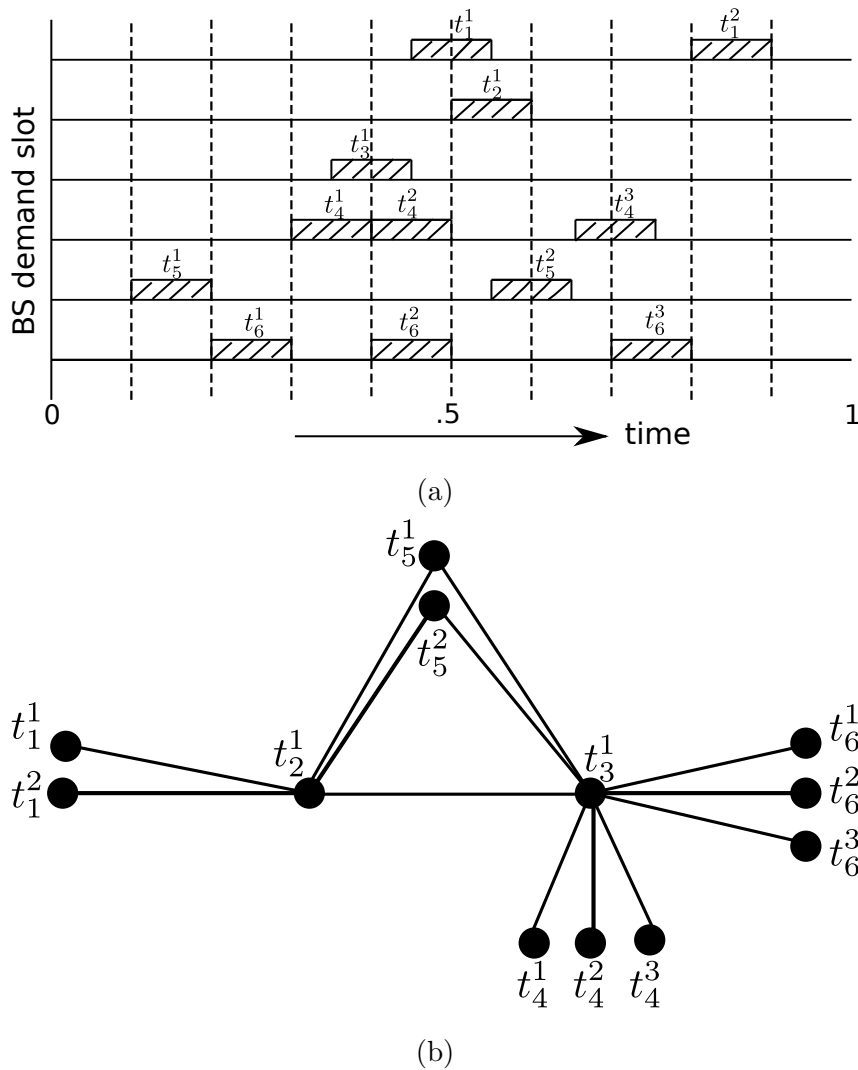


Figure 3.7: (a) Demand time slots (b) Augmented Interference graph

3.5 Simulation Results

In this section, we compare the performance of the proposed algorithm with various other algorithms for spectrum allocation in wireless networks. To model the wireless network, we generate a random undirected graph $\mathcal{G} = (V, \mathcal{E})$ whose nodes represent base stations and the set of interfering base stations (constraint set) for base station i equals the set of connected nodes in \mathcal{G} . The random graphs are generated with the desired degree distribution using the configuration model [74]. In all our simulations, the maximum degree is restricted to 4. The performance of the proposed scheme is compared against VCG, SMALL, and greedy schemes. Simulations are performed in MATLAB [75]. We compare the performances based on three parameters:

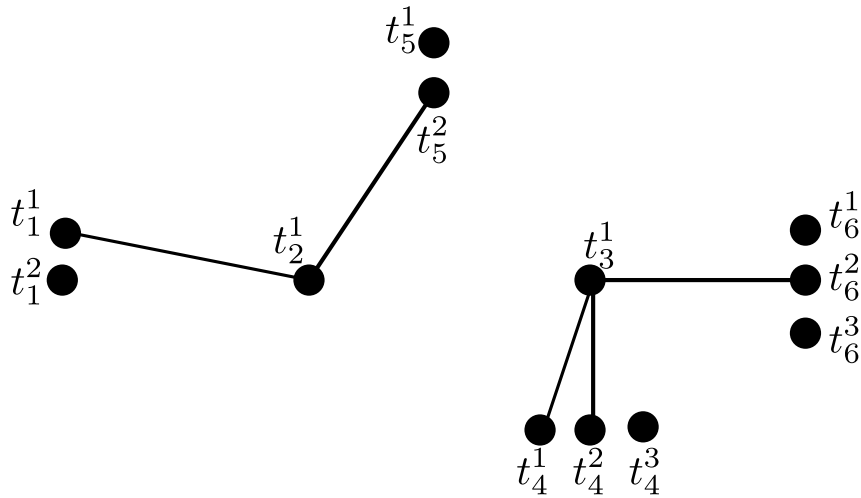


Figure 3.8: Re-constructed interference graph considering demand time intervals for each base station.

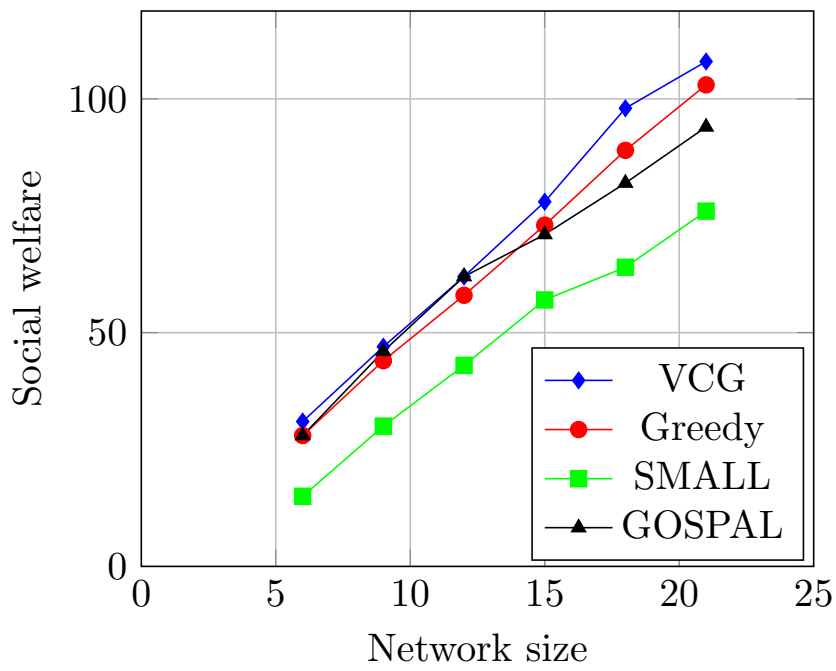
- **Social Welfare:** It is defined as the sum of the valuations of the base stations which are assigned channels.
- **Spectrum Utilization:** It is defined as the total number of base stations which are assigned channels in the allocation phase.
- **Fairness across time:** It quantifies disparity between the average number of times the channel is allocated to various base stations.

To compare the fairness of resource allocation algorithms in repeated auctions across the base stations, we use Jain's Fairness Index [76]. Jain's fairness index is a metric used in networking to determine the share of system resources allocated to a user. Mathematically, fairness is calculated as

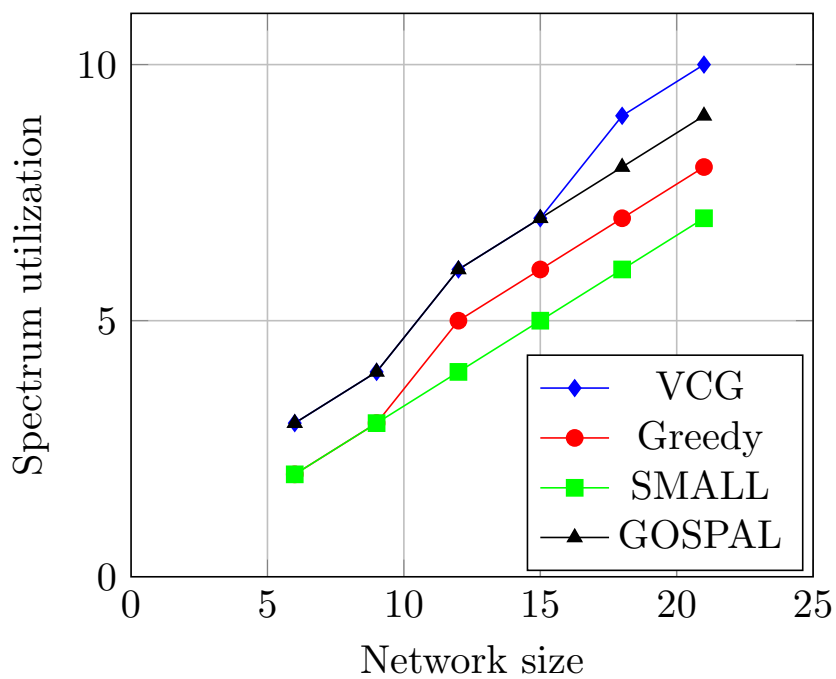
$$f_i(\alpha_1^\pi, \dots, \alpha_n^\pi) = \frac{(\sum_{i=1}^n \alpha_i^\pi)^2}{n \cdot \sum_{i=1}^n (\alpha_i^\pi)^2},$$

where $f_i(\alpha_1^\pi, \dots, \alpha_n^\pi)$ is the Jain's fairness index for base station i , n is the total number of base stations in the wireless network and α_i^π denote the fraction of times base station i is allocated resource under mechanism π .

First, we compare the performance of the proposed mechanism, SMALL and greedy, with VCG for small network sizes (up to 21 nodes). At each node, bids are generated at random, uniformly distributed in the interval [5, 15]. Figure 3.9 shows the social welfare and the spectrum utilization obtained under the four schemes. Note that VCG based



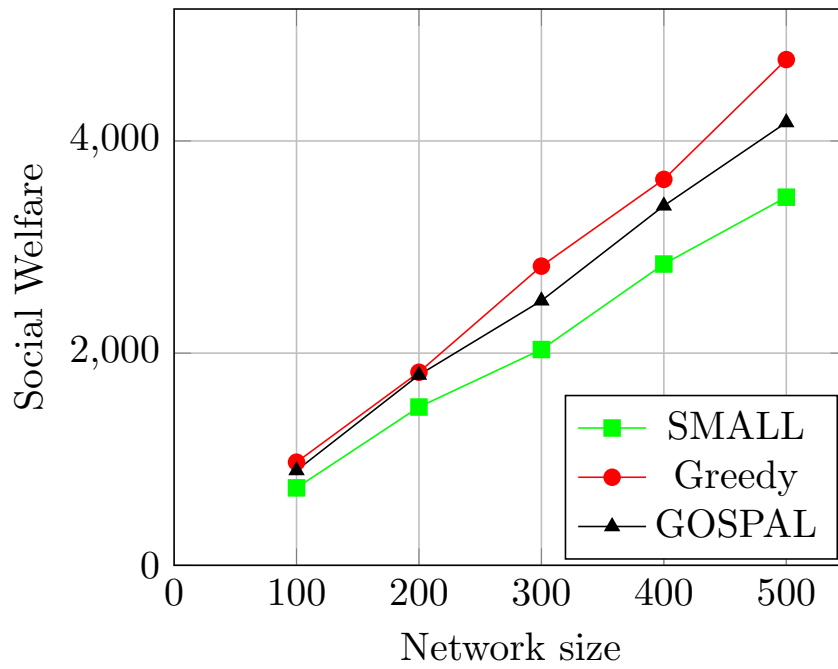
(a) Social Welfare



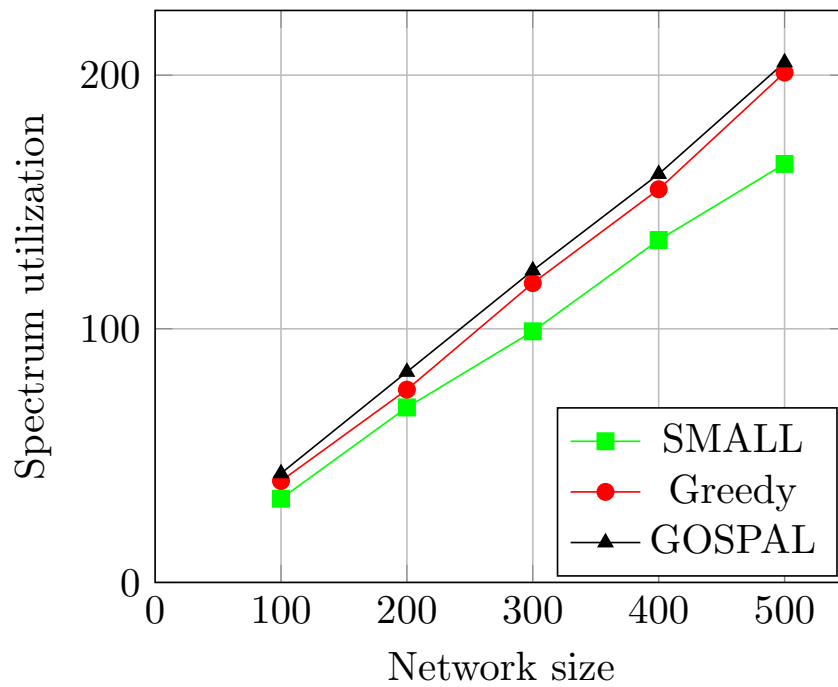
(b) Spectrum utilization

Figure 3.9: Performance comparison for different algorithms in small network.

allocation provides better (optimal) allocation in comparison to GOSPAL, SMALL and greedy. However, VCG allocation is computationally challenging even for a sparse modest size network. On the other hand, GOSPAL, SMALL, and greedy can be used to provide



(a) Social Welfare



(b) Spectrum utilization

Figure 3.10: Performance comparison for different algorithms in large network.

resource allocation for large networks. Note that our proposed algorithm outperforms SMALL in all the cases significantly. More importantly, resource utilization under our scheme is much better than both SMALL and greedy, which is close to that in VCG.

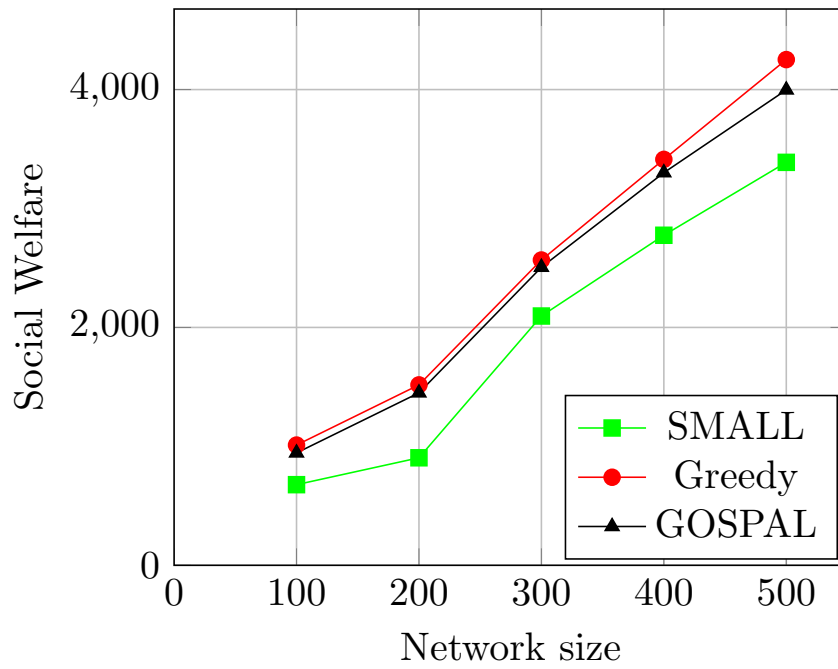
To further understand the performance of the proposed algorithm, we perform simulations on large networks (up to 500 base stations). In this case, because of the computational intractability of VCG allocation, we compare the results of our scheme only with SMALL and greedy resource allocation mechanisms. In Figure 3.10, we consider networks in which degree distribution is uniform over $\{1, 2, 3, 4\}$. The base station bids are uniformly distributed in the interval $[8, 30]$. The results shown are averaged over 100 different topologies with bids chosen independently for each base station. It can be observed that the greedy mechanism provides the highest value of social welfare among all the schemes. However, GOSPAL provides marginally better spectrum utilization. Both these schemes significantly outperform SMALL.

Next to understand the impact of the degree distribution on the performance of various schemes, we repeat the same experiment as above with the following probability mass functions over degree values $k = \{1, 2, 3, 4\}$: (a) $p(x = k) = \frac{k}{10}$ and (b) $p(x = k) = \frac{5-k}{10}$. Note that in case (a), the network will have a large number of nodes (base stations) with degree four, while in case (b) a large number of nodes will have degree 1. Figures 3.11 and 3.12 provide the results in case (a) and (b), respectively. Note that the results follow a similar pattern as that in the uniform degree case. These experiments demonstrate that although the proposed algorithm outperforms SMALL, it only provides comparable performance with respect to greedy.

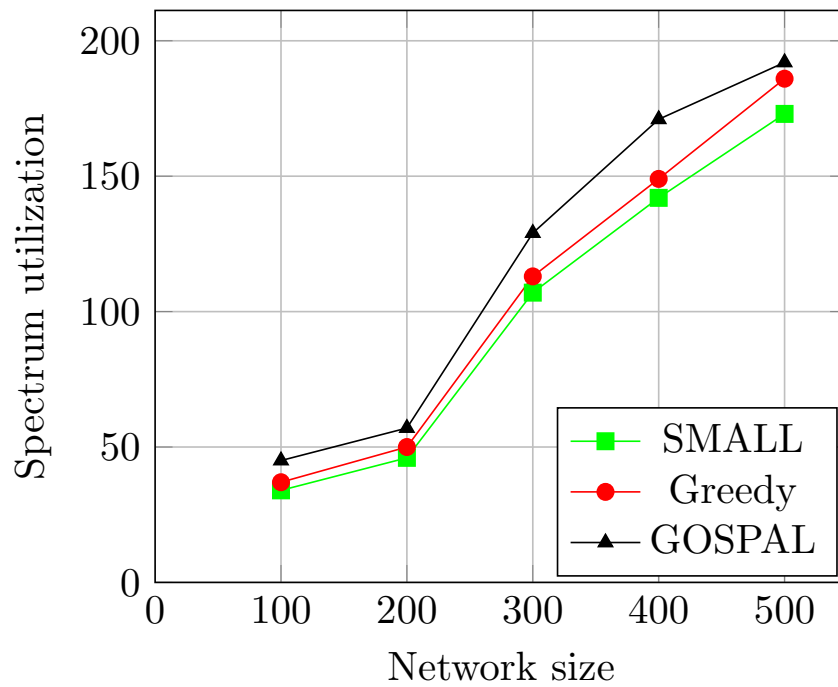
When a large percentage of base stations within the network has a high degree of conflict, both social welfare and resource utilization are reduced. This is illustrated in Figure 3.11. On the other hand, as shown in Figure 3.12, a reduction in the percentage of base stations with a high degree of conflict sets, leads to improvements in the above mentioned parameters. This reflects the fact that lesser number of base stations are allocated channels if the constraint set \mathcal{S}_i is large and vice versa.

Next, we perform simulations to see how various algorithms perform when the resource allocation process is repeated periodically. For this, we generate a random network topology and keep it fixed. For the given topology, we consider 100 different randomly generated bid values and calculate the resource allocation under all the three schemes. Based on the vector α_i^π we calculate Jain's fairness index.

We consider a scenario in which bid values are independent and identically dis-



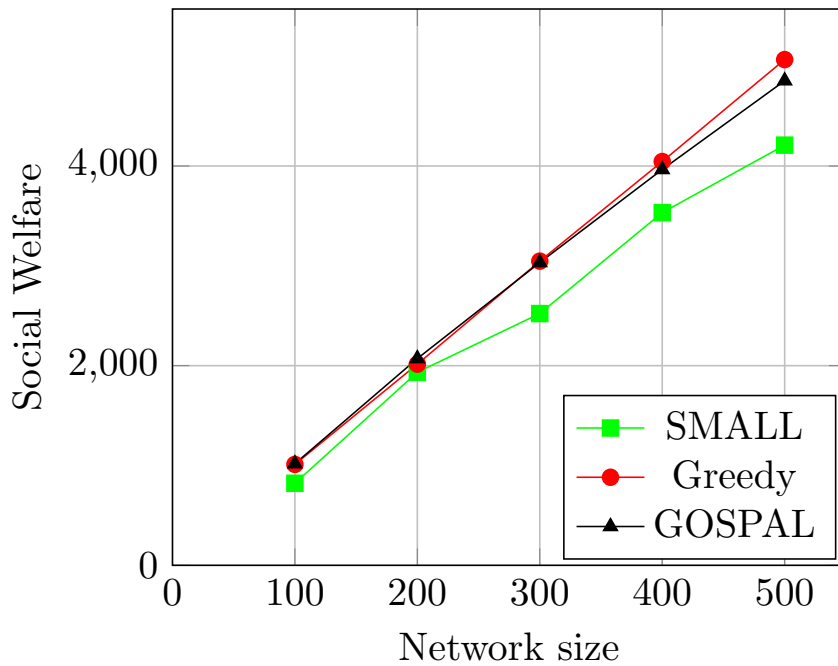
(a) Social Welfare



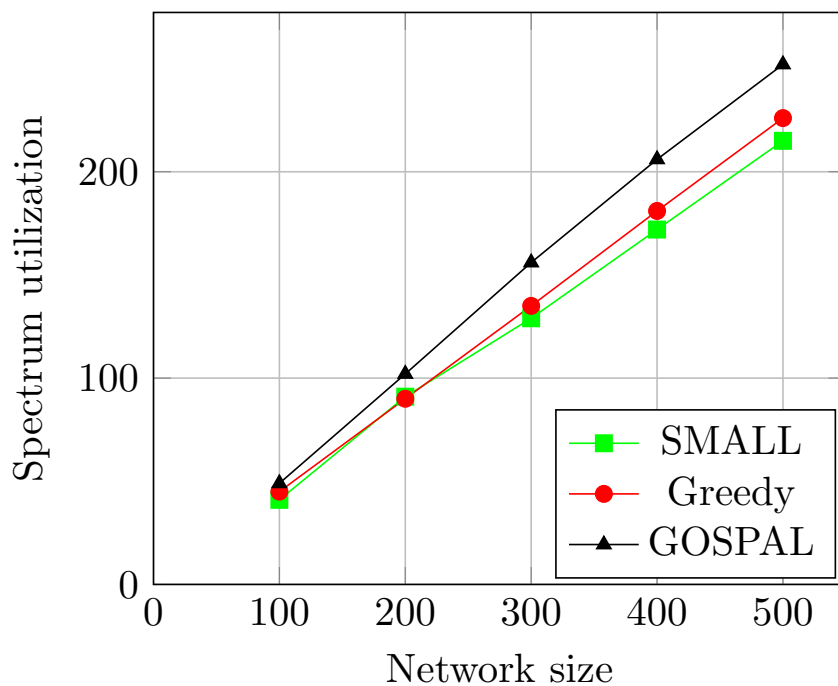
(b) Spectrum utilization

Figure 3.11: Performance comparison for different algorithms with degree distribution $p(x = k) = \frac{k}{10}$ where $k = \{1, 2, 3, 4\}$.

tributed (iid) across base stations, but not across time. The bid distribution across the base stations is generated as follows: for base station i , a value μ_i is sampled uniformly at



(a) Social Welfare



(b) Spectrum utilization

Figure 3.12: Performance comparison for different algorithms with degree distribution $p(x = k) = \frac{5-k}{10}$ where $k = \{1, 2, 3, 4\}$.

random from the interval $[8, 35]$. This value remains unchanged across all the allocations. Now, the bid is generated in k^{th} round of allocation as $\mu_i + q_i(k)$, where $q_i(k)$'s are iid in

the interval $[-2, 1]$. Thus, each base station has a different distribution for the bid value. The fairness index for various schemes is shown in Figure 3.13. In this case, GOSPAL and SMALL significantly outperform the greedy scheme in fairness. Thus, the proposed mechanism and SMALL do not facilitate the undue advantage to the base stations that consistently bid higher than the other base stations. Moreover, preferring the highest bidder most of the time can starve some base stations, potentially leading to a monopoly of one service provider.

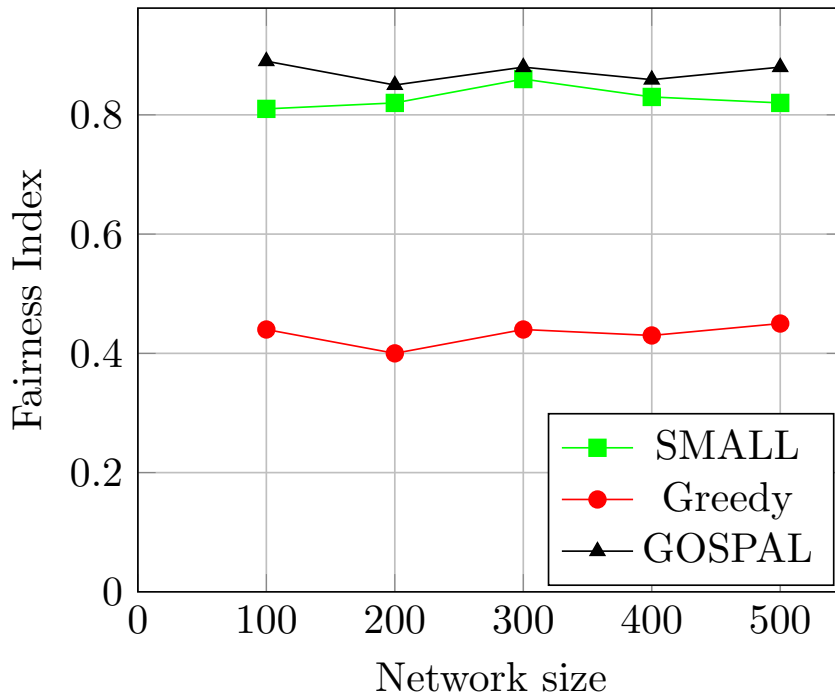


Figure 3.13: Comparison of fairness index for different algorithms in large networks.

3.6 Conclusions

In this chapter, we model a spectrum allocation problem considering the spatial and temporal traffic variations in the wireless access network. We consider a scenario where multiple base stations are allocated static resource to meet the average traffic requirements while additional spectrum to meet the peak traffic requirements are allocated through dynamic spectrum auctions. VCG is a well-known auction-based framework that provides optimal solution along with the strategy-proofness property. However, due to the NP-hard nature of the problem, determining the optimal solution is computationally ex-

pensive [28]. The computational inefficiency renders the VCG mechanism infeasible even for the networks of moderate size. Computational efficiency is essential in an auction-based mechanism to handle the dynamic traffic variations in the network. Therefore, we propose a computationally efficient dynamic spectrum allocation mechanism, which exploits the limited-constraint set property of the wireless access networks. We prove that the proposed mechanism (GOSPAL) is strategy-proof, individually rational, and satisfies monotonicity in spectrum allocation.

Using Monte Carlo simulations, we establish that the proposed mechanism outperforms the other mechanisms in spectrum utilization and fairness. We observe that the social welfare of the proposed mechanism is close to that of the greedy mechanism. However, we observe significant improvement in the social welfare of the proposed mechanism compared to SMALL.

Furthermore, we also analyze the effect of degree distribution on the performance of the various mechanisms. Additionally, when the bids are skewed across base stations, the proposed mechanism also ensures fairness. Thus, the proposed mechanism achieves social welfare, spectrum utilization, and fairness simultaneously in various scenarios in comparison to the other mechanisms.

Chapter 4

Dynamic Spectrum Allocation across Operators

While traditional exclusive licensing of spectrum across mobile operators or service providers continues to be a preferred option, the new concept of Licensed Shared Access (LSA) is receiving growing interest in the research, regulation, and standardization communities. Furthermore, the LSA method allows a wireless operator to share licensed spectrum with predetermined rules. Although the traditional exclusive licensing of spectrum across wireless operators is easier to implement as the spectrum is auctioned by the authorities for a considerable duration of time (for instance, one or more years); however, it leads to inefficient utilization of the spectrum [3].

We model the dynamic spectrum allocation problem across operators using sealed-bid auctions. We consider that multiple base stations are associated with an operator. Operators estimate the resource requirements and the corresponding bid at each base station as per the traffic in the network. Since multiple base stations are associated with an operator, the operator has bids and demands corresponding to its base stations. Unfortunately, devising a computationally efficient strategy-proof spectrum allocation mechanism becomes much more difficult as operators report a vector of bids corresponding to the associated base stations. Thus, an operator may misreport the valuation and demand at a few base stations to increase the overall utility gain. Furthermore, non-co-operative behavior of operators has been considered, which holds as per the practical scenarios.

In this chapter, we design computationally efficient sealed bid auction-based dynamic spectrum allocation algorithms across operators suitable for implementation in short durations to handle the spatio-temporal load variations in the network. The main objective is to maximize the social welfare of the auction. However, achieving optimal social welfare is an NP-Hard problem [28]. Therefore, we focus on devising computationally efficient strategy-proof dynamic spectrum allocation with near-optimal social welfare. First, we study the dynamic spectrum allocation problem across multiple operators in a multi-parameter environment, which has never been focused on in the existing literature. We start the analysis considering only one channel availability in the spectrum database. Moreover, it is assumed that the channel demand at each base station is restricted to 1. We propose Single Channel Strategy-Proof Allocation Mechanism (SC-SPAM), which is also applicable when the channel demand across the base stations of all the operators is uniform (same) and is equal to the number of channels available for auction. We formally prove the desired properties of the auction mechanisms such as strategy-proofness, monotonicity and individual rationality of SC-SPAM.

Further, we extend the analysis for multiple channel availability for auction and propose a generalized spectrum allocation mechanism that is weakly strategy-proof when the spectrum demands across the base stations of an operator are not the same (often arises in practical scenarios). Besides, we also consider the scenario where the channel valuation at a base station may not be linearly increasing with the demand of the channels. For this scenario, we prove that the proposed mechanism follows monotonicity, individual rationality, and also weakly strategy-proof. Weak strategy-proofness is a new notion introduced by us here.

We also perform a comparison of computational complexity between the proposed algorithms against the VCG algorithm and observe that the proposed algorithm is tractable for a large number of base stations. Thus, the proposed algorithms are practically feasible for real-time dynamic spectrum allocation using auctions repeatedly over short periods, considering the traffic variation in the network. We conduct extensive simulations in MATLAB to compare the performances of the proposed algorithms with existing algorithms. Monte Carlo simulations reveal that the proposed algorithms outperform other existing algorithms in various scenarios in terms of social welfare, spectrum utilization,

and execution time.

The rest of the chapter is organized as follows. Section 4.1 describes the system model along with some definitions. In Section 4.2, we propose an algorithm SC-SPAM considering single channel demand at each base station of all the operators along with the detailed discussion on the computational complexity of SC-SPAM. In Section 4.3, SC-SPAM is extended for the scenario when demand across base stations of an operator is non-uniform. We also present a weakly strategy-proof algorithm NUD-SPAM for multiple channel allocation across operators in Section 4.4. We briefly summarize the proposed algorithms in Section 4.5. Simulation results have been discussed in Section 4.6. Finally, we draw the conclusion of the chapter in Section 4.7.

4.1 System Model

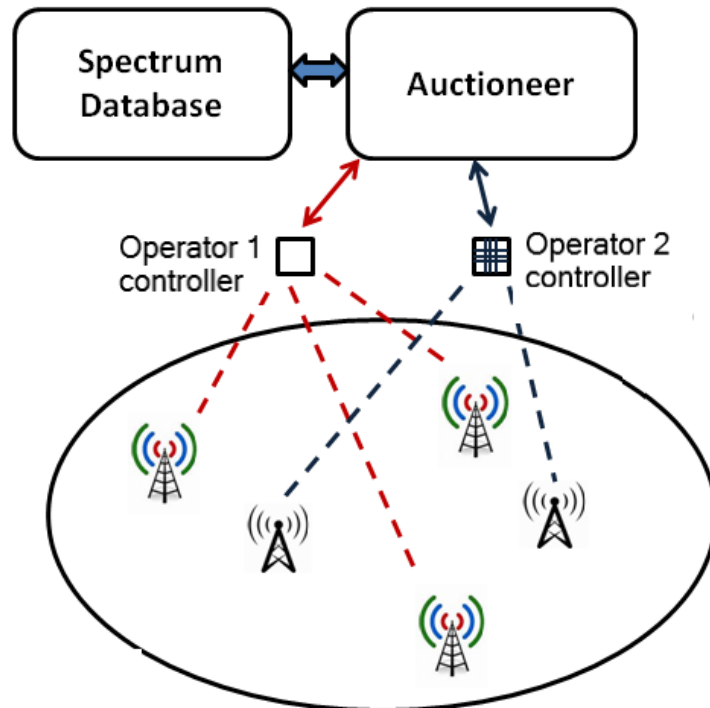


Figure 4.1: Illustration of system model.

We consider a geographical region where multiple operators provide services to the end users. Multiple base stations are associated with each operator in the given region. The system model (Figure 4.1) comprises a controller for each operator, set of base stations

associated with the operators, auctioneer, and spectrum database. There are two decision making devices, controllers, and auctioneer in the system. Each operator has a controller which determines the number of channels (demand) required and the valuation of channels at the base stations associated with the operator. The demand and the valuation may vary over time depending on the traffic conditions of the wireless network. The operators communicate their spectrum demand and valuation at each base station through the controller. The information of the number of channels available for allocation is contained in the spectrum database. We assume that the channels are of equal bandwidth and are orthogonal. Since orthogonal channels do not have overlapping frequency bands, simultaneous operations on orthogonal channels do not cause interference. Auctioneer is another decision making entity, which decides who should get the spectrum (channel) and what should be the appropriate price for providing exclusive ‘right to use’ a channel to an operator.

In our work, unlike the other existing works, operators are bidders (players) instead of individual base stations in the wireless network. Each operator communicates a vector of bids and demands to the auctioneer via the controller for the base stations associated with it.

Other assumptions made in our system model are as follows.

- We assume that an auctioneer has knowledge of the topology in the geographical region. Therefore, the overall conflict graph consisting of all the base stations participating in the auction is available to the auctioneer.
- We assume all channels are homogeneous in characteristics (channels are of same spectrum band) and act as substitutes. Thus, the bid or valuation reported by the operator is channel independent.
- We consider that operators employ Fractional Frequency Reuse (FFR) techniques to cancel interference across its own base stations. Therefore, the same frequency band (channel) can be allocated to the base stations of an operator. Hence, any base station of an operator would experience interference only from the base stations associated with other operators in the given region. We also assume that the channel requirement for each base station is arrived at after including the impact of the interference coordination

technique.

We capture the interference across the base stations of the operators with the help of a graph $\mathcal{G} = (V, \mathcal{E})$, that is obtained from the knowledge of the topology in the geographical region, where V represents the set of vertices (nodes), and \mathcal{E} represents the set of edges in the graph. The set of vertices in the graph correspond to the base stations of various operators in the region. Any two base stations are said to interfere with each other if the geographical distance between them is less than a predetermined value d . In this case, there is an edge between them in the graph. Two interfering base stations (nodes) cannot be assigned the same channel concurrently.

4.1.1 Notations and Definitions

Now, we introduce some notations and definitions considering the multiple operator settings.

- $\mathcal{N} = \{1, 2, \dots, n\}$ represents the set of operators participating in the spectrum auction in a geographical region.
- m_i represents the number of base stations corresponding to operator i .
- $\mathcal{S}_i = \{S_{i1}, S_{i2}, \dots, S_{im_i}\}$ represents the set of base stations of operator i .
- \mathcal{V}_i denotes the true valuation of operator i . $\mathcal{V}_i(\ell, j)$ is true value for ℓ^{th} channel at base station j of operator i if $(\ell - 1)$ channels are already assigned. If $\mathcal{V}_i(\ell, j) = 0$, then base station j does not require ℓ^{th} channel.
- \mathcal{B}_i denotes the bid of operator i . $\mathcal{B}_i(\ell, j)$ is bid for demand ℓ at base station j of operator i if $(\ell - 1)$ channels are already assigned. If $\mathcal{B}_i(\ell, j) = 0$, then base station j does not require channel.
- \mathcal{N}_i represents the set of neighboring base stations which are in conflict with the base stations of operator i (same channel cannot be allocated simultaneously).
- $x_i^f = \sum_{k=1}^K x_i^k$, $k = \{1, \dots, K\}$. K is the total number of channels available in the spectrum database for auction. By x_{ij}^f , we denote the j^{th} component of final allocation vector x_i^f .

- O_i represents operators that are neighbors of i i.e., ($\{\text{operators } y \mid S_y \cap \mathcal{N}_i \neq \phi, y \neq i\}$).
- $d_i = \{d_{i1}, d_{i2}, \dots, d_{im_i}\}$ represents the number of channels required at base stations of operator i .
- $N(\mathcal{G}')$ represents the set of active operators from the conflict graph \mathcal{G}' (operators with non-zero demand).

Definition 5. *An auction is truthful (strategy-proof) if there is no incentive in deviating from the true valuation. Thus, the dominant strategy is to bid at the true valuation no matter what strategy others choose.*

$$\mathcal{U}_i(\mathcal{B}_i, \mathcal{B}_{-i}) \leq \mathcal{U}_i(\mathcal{V}_i, \mathcal{B}_{-i}) \quad \forall \mathcal{B}_i, \forall \mathcal{B}_{-i}. \quad (4.1)$$

where \mathcal{V}_i and \mathcal{U}_i are true valuation and utility of operator i . Moreover, \mathcal{B}_i is the bid of operator i and $\mathcal{B}_{-i} = (\mathcal{B}_1, \dots, \mathcal{B}_{i-1}, \mathcal{B}_{i+1}, \dots, \mathcal{B}_n)$ represents bid of all operators except operator i .

Definition 6. *Spectrum Utilization is defined as the total number of channels assigned to base stations across all the operators.*

$$U^s = \sum_{i=1}^n \sum_{j=1}^{m_i} x_{ij}^f, \quad (4.2)$$

where x_{ij}^f denotes the number of channels allocated at j^{th} base station of operator i .

Definition 7. *Social Welfare is defined as the aggregate true value of the channels assigned to all base stations across all operators.*

$$W^s = \sum_{i=1}^{\mathcal{N}} \sum_{j=1}^{m_i} \sum_{\ell=1}^{x_{ij}^f} \mathcal{V}_i(\ell, j) \quad (4.3)$$

4.2 Strategy-proof auction for Single Channel demand

In this section, we describe the proposed algorithm Single Channel Strategy-proof Auction Mechanism (SC-SPAM) for channel allocation among the base stations of multiple operators. As the name SC-SPAM suggests, we consider only one channel is available

for auction i.e., $K = 1$ where K denotes the number of channels. In auctions, the mechanism design has two steps: channel allocation and price charging strategy. In channel allocation phase, the auctioneer decides who should be given the right to use the channel. What price should be charged is decided in the pricing strategy phase. The price charged enforces the operators to declare their true valuations to ensure a strategy-proof auction.

For single channel scenario, the demand at each base station is restricted to one, i.e., $\ell = 1$ and therefore, for simplicity of notation we denote $\mathcal{V}_i(\ell, j) = v_{ij}$, which represents the true valuation at j^{th} base station associated with operator i (i.e., S_{ij}). Furthermore, \mathcal{V}_i reduces to one dimensional vector, which we denote as $v_i = [v_{i1}, v_{i2}, \dots, v_{im_i}]$. Similarly, $\mathcal{B}_i(\ell, j) = b_{ij}$ denotes bid at j^{th} base station associated with operator i and $\mathcal{B}_i \simeq b_i = [b_{i1}, b_{i2}, \dots, b_{im_i}]$. Next, we define some new terms:

- *True valuation* (σ_i^v): True valuation σ_i^v of any operator i is defined as the sum of the actual valuations (which are private and not known to the auctioneer) of all the base stations corresponding to operator i .

$$\sigma_i^v = \sum_{j=1}^{m_i} v_{ij}. \quad (4.4)$$

- *Bidding valuation* (σ_i^b): Bidding valuation σ_i^b of operator i is defined as the sum of the bids (which may or may not be same as the actual valuation) of all the base stations corresponding to operator i .

$$\sigma_i^b = \sum_{j=1}^{m_i} b_{ij}. \quad (4.5)$$

- *Price* (p_i): It is defined as the price that an operator i has to pay, in case operator i wins the resources (channels), else it is zero.
- *Operator Utility* (\mathcal{U}_i): Utility of an operator i is the difference between the operator valuation (unknown to the auctioneer) and the price charged when a channel is allocated across the base stations of an operator. If an operator does not get a channel, the utility is zero. In other words, it represents the overall gain of an operator i if it is allocated a channel.

$$\mathcal{U}_i(\mathcal{B}_i, \mathcal{B}_{-i}) = \begin{cases} \sigma_i^v - p_i, & \text{if the channel is allocated} \\ 0, & \text{otherwise.} \end{cases}. \quad (4.6)$$

where \mathcal{B}_i is the bid of operator i and \mathcal{B}_{-i} represents the bids of all operators except operator i .

Now, we define critical operator which is used later in the price charging strategy by the auctioneer.

Definition 8. A critical operator $C(i)$ of an operator i is defined as the operator in O_i whose sum of the bids of base stations is maximum among all the operators in O_i . The critical operator $C(i)$ is given as any $y \in O_i$ such that

$$\sum_{k \in \{\mathcal{N}_i \cap S_y\}} b_{yk} \geq \sum_{k \in \{\mathcal{N}_i \cap S_{y'}\}} b_{y'k}, \quad \forall y' \neq y, \quad i \text{ and } y' \in O_i. \quad (4.7)$$

Let us define a set $\mathcal{L}_y^i = \mathcal{N}_i \cap S_y$, which contains the base stations of operator y in conflict with the base stations of operator i . Let Λ_y^i be the valuation of set \mathcal{L}_y^i which is given as, $\Lambda_y^i = \sum b_{yk} \mathbb{1}_{\{S_{yk} \in \mathcal{L}_y^i\}}$. The critical operator of an operator i can be obtained as $C(i) = \arg \max_{y \in O_i} \Lambda_y^i$, $y \in O_i$ and the critical operator valuation σ_i^c is given as, $\sigma_i^c = \max_{y \neq i} \Lambda_y^i, y \in O_i$.

The strategy-proof dynamic spectrum allocation algorithm proposed is described in Algorithm 4. The algorithm takes conflict graph \mathcal{G} and bid vector corresponding to each operator $\{b_i\}_{i \in \mathcal{N}}$ as input. Binary channel allocation vector $\{x_i\}_{i \in \mathcal{N}}$ and payment vector $\{p_i\}_{i \in \mathcal{N}}$ for all the operators are initialized to zero. Initially, we determine the maximum bidding operator and its critical neighbor $C(i^*) = \arg \max_{y \neq i} \Lambda_y^{i^*}, y \in O_{i^*}$ (line 8). Channel allocation vector, x_i for the maximum bidding operator (winner) is updated to 1 and the payment for the winning operator is updated to the price of the critical neighbor valuation, $\sigma_{i^*}^c$. The conflict graph \mathcal{G}' is updated with the remaining base stations (nodes) after the removal of the base stations corresponding to the winning operator i^* and its neighboring nodes \mathcal{N}_{i^*} . Repeat the process until \mathcal{G}' is NULL (line 13), i.e., no other base stations is present in \mathcal{G}' . For single channel auction, final allocation vector $x_i^f = x_i$, which is a binary vector. By x_{ij}^f and x_{ij} , we denote j^{th} element (allocation at j^{th} base station of operator i) in vectors x_i^f and x_i , respectively. However, when multiple channels are available for auction, $x_{ij}^f \in \mathbb{R}_+$. Hence, the final allocation vector $x_i^f \neq x_i$. Next, we illustrate Algorithm 4 through an example.

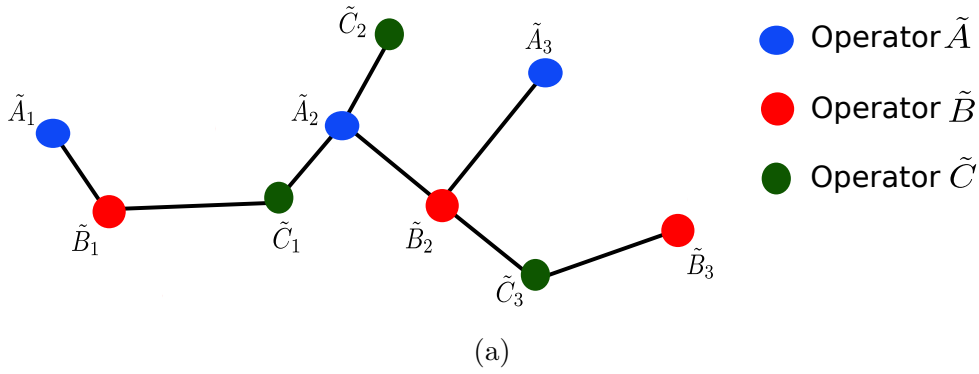
Algorithm 4 Single Channel Strategy-proof Auction Mechanism

-
- 1: **Input:** Conflict Graph \mathcal{G} , bid vector, $\{b_i\}_{i \in \mathcal{N}}$.
 - 2: **Output:** Binary channel allocation vector $\{x_i\}_{i \in \mathcal{N}}$, price $\{p_i\}_{i \in \mathcal{N}}$.
 - 3: Initialize $x_i \leftarrow 0$, $N(\mathcal{G}) = \{1, 2, \dots, n\}$
 - 4: Initialize $p_i \leftarrow 0$, $\mathcal{G}' \leftarrow \mathcal{G}$, $N(\mathcal{G}') \leftarrow N(\mathcal{G})$, $FLAG \leftarrow True$.
 - 5: **while** ($FLAG = True$) **do**
 - 6: Make $i^* \leftarrow \arg \max_{i \in N(\mathcal{G}')} \sigma_i^b$.
 - 7: Find \mathcal{N}_{i^*} .
 - 8: Set $C(i^*) \leftarrow \arg \max_{y \neq i^*} \Lambda_y^{i^*}$, $y \in O_{i^*}$ and $\sigma_{i^*}^c \leftarrow \max_{y \neq i^*} \Lambda_y^{i^*}$, $y \in O_{i^*}$.
 - 9: Make $p_{i^*} \leftarrow \sigma_{i^*}^c$ and $x_{i^*} \leftarrow 1$.
 - 10: **if** ($\mathcal{G}' \cap (S_{i^*} \cup \mathcal{N}_{i^*}) = \mathcal{G}'$) **then**
 - 11: $FLAG \leftarrow False$.
 - 12: **else**
 - 13: $\mathcal{G}' \leftarrow \mathcal{G}' \setminus \{S_{i^*} \cup \mathcal{N}_{i^*}\}$.
 - 14: **end if**
 - 15: **end while**
-

Example: Consider a network of 3 operators $\tilde{A}, \tilde{B}, \tilde{C}$, where each operator has 3 base stations deployed in the region to provide services to their subscribers. The base stations $\{\tilde{A}_1, \tilde{A}_2, \tilde{A}_3\}$, $\{\tilde{B}_1, \tilde{B}_2, \tilde{B}_3\}$ and $\{\tilde{C}_1, \tilde{C}_2, \tilde{C}_3\}$ correspond to operators \tilde{A} , \tilde{B} and \tilde{C} , respectively. The conflict graph is illustrated in Fig. 4.2a based on the interference criteria discussed in Section 4.1.

In Fig. 4.2b, the bid vector reported by each operator is shown. In the first iteration, Operator \tilde{A} has the highest bid among all the operators with a value of $\sigma_{\tilde{A}}^b = 25$. Therefore, Operator \tilde{A} is allocated channel across base stations, and it has to pay the price of its critical operator. As per Definition 8, critical operator for winning operator \tilde{A} is operator \tilde{C} and $p_{\tilde{A}} = \sigma_{\tilde{A}}^c = 18$. Thus, the utility of operator $\tilde{A} = \mathcal{U}_{\tilde{A}} = 7$. We update the conflict graph with the base stations of operators \tilde{B} and \tilde{C} which are not in conflict with the base stations of operator \tilde{A} . In second iteration, the updated \mathcal{G} comprises base stations \tilde{B}_3 and \tilde{C}_3 . Operator \tilde{B} wins the channel and pays the price, $\sigma_{\tilde{B}}^c = 3$. The utility of operator \tilde{B} is 2. Operator \tilde{C} does not get the channel.

Now, if operator \tilde{B} tries to increase its utility by deviating from its true valuation



(a)

	1	2	3	Total
operator \tilde{A}	8	10	7	25
operator \tilde{B}	9	8	5	22
operator \tilde{C}	9	9	3	21

(b)

Figure 4.2: Network of 3 operators (a) Conflict Graph (b) Bid vector table corresponding to operator \tilde{A} , \tilde{B} and \tilde{C} .

$\sigma_{\tilde{B}}^v = 22$ to $\sigma_{\tilde{B}}^b = 28$ by increasing the bid of its base stations, operator \tilde{B} will get channel being the highest bidder among the operators. But, it has to pay the price of its critical operator which is operator \tilde{A} and therefore, pays $\sigma_{\tilde{B}}^c = 25$. This leads to a negative utility -3 for operator \tilde{B} . Thus, bidding at the true valuation is the best strategy for an operator in the auction.

Next, we prove that the proposed algorithm follows monotonicity, individual rationality and strategy-proofness.

Lemma 6. *If operator i is allocated a channel by bidding at σ_i^b , it will also be allocated a channel if it bids $\sigma_i^{b'}$, where $\sigma_i^{b'} \geq \sigma_i^b$ provided all the other operators' bids remain unchanged.*

Proof. As stated in Algorithm 4, all operators are arranged in non-increasing order of their bids $\sigma_i^b, \forall i \in \mathcal{N}$. Let us assume in the sorted list (S , say) operator i lies at position k . Now, keeping all the other operator bids unchanged, increase the bid of operator i to $\sigma_i^{b'}$, and again arrange all the operator bids in non-increasing order in another sorted list S' . Let us say, the position of operator i in S' is l , where $l \leq k$. Thus, the operator

moves higher in the position which ensures that it still gets the channel. This completes the proof. \square

Lemma 7. *Algorithm 4 is individually rational.*

Proof. As stated in the pricing scheme of Algorithm 4, winning operator i is charged price $p_i = \sigma_i^c$. Moreover, we know that the valuation of winning operator i is the highest among all operators.

$$\therefore \sigma_i^b > \sigma_y^b, \quad \forall y \neq i. \quad (4.8)$$

Using Definition 8, $\sigma_i^c = \max_{y \neq i, y \in O_i} \Lambda_y^i$. This implies that

$$\sigma_i^c \leq \max_{y \neq i} \sigma_y^b. \quad (4.9)$$

From Equations (4.8) and (4.9), we get $\sigma_i^c < \sigma_i^b$. Hence, $p_i \leq \sigma_i^b$. This proves individual rationality of the algorithm. \square

Theorem 2. *Algorithm 4 is strategy-proof.*

Proof. To show the strategy-proofness of the algorithm, possible scenarios can be divided into two categories:

Scenario 1: A operator i tries to deviate from truthfulness by bidding greater than the true valuation, i.e., $\sigma_i^b > \sigma_i^v$.

Case (i): Operator i does not win the channel even after bidding untruthfully at σ_i^b , greater than σ_i^v . Hence, it will have utility, $\mathcal{U}_i = 0$.

Case (ii): Operator i wins the channel at its bidding valuation σ_i^b (which is greater than the true valuation) as well as its true valuation σ_i^v . It will have positive utility, $\mathcal{U}_i = \sigma_i^v - p_i$, which is same as in the case operator bids at the true valuation. Thus, bidding at higher valuation does not lead to any extra incentive.

Case (iii): Operator i wins channel at σ_i^b , but loses at σ_i^v . Here, Operator i gets channel on higher bid (by misreporting) which is greater than its critical operator bid (Algorithm 4). But, it has to pay higher price which results in negative utility.

$$\begin{aligned} \mathcal{U}_i &= \sigma_i^v - p_i, \\ &= \sigma_i^v - \sigma_i^c \quad \text{where } p_i = \sigma_i^c, \\ &\leq 0. \quad (\because \sigma_i^v < \sigma_i^c). \end{aligned}$$

Scenario 2 : Operator i tries to deviate from truthfulness by bidding less than the true valuation, i.e., $\sigma_i^b < \sigma_i^v$.

Case (i): Operator i loses the channel at σ_i^b as well as its true valuation, σ_i^v . Thus, it will have $\mathcal{U}_i = 0$.

Case (ii): Operator i wins the channel at σ_i^b as well as its true valuation, σ_i^v which follows from monotonicity (Lemma 6). Thus, it will have $\mathcal{U}_i = \sigma_i^v - p_i$.

Case (iii) : Operator i loses at σ_i^b , but wins bidding at σ_i^v . Thus, the operator suffers loss by deviating to untruthful value with zero utility. However, bidding at σ_i^v results in channel allocation to operator i with non-negative utility $\mathcal{U}_i = \sigma_i^v - p_i$.

From the above scenarios, it can be seen that bidding at $\sigma_i^b \neq \sigma_i^v$, does not improve the utility of an operator. Thus, $\sigma_i^b = \sigma_i^v$ is the *weakly dominant strategy* for operator i . This completes the proof. \square

4.2.1 Complexity Analysis

In this section, we study the computational complexity of the proposed algorithm (SC-SPAM). Computational complexity analysis of the proposed algorithm in case of n operators and the single channel availability in the spectrum database for allocation across the base stations of the operators in the region with the given conflict graph $\mathcal{G} = (V, \mathcal{E})$ is as follows.

The overall complexity of SC-SPAM algorithm is split into two steps, channel allocation strategy and price charging strategy for the winning operator. The algorithm takes $\mathcal{O}(n)$ time to obtain the maximum bidding operator and allocates the channel across its base stations.

To calculate the price charged by the winning operator, algorithm needs to examine the conflicting neighbors corresponding to the base stations of the winning operator. In any graph $\mathcal{G} = (V, \mathcal{E})$, complexity of determining the conflicting nodes is given by $\mathcal{O}(|V| + |\mathcal{E}|)$, where V is the number of vertices (nodes) and \mathcal{E} corresponds to number of edges in the graph. The edges in a graph with V nodes is bounded as $\mathcal{E} \leq \frac{V(V-1)}{2}$. Let us assume i^{th} operator has m_i base stations and the total number of base stations are aggregate of the base stations across all the operators, i.e., $m = \sum_{i \in N} m_i$. Since, the base stations associated with an operator does not conflict with each other, the winning operator i

can conflict with maximum of remaining $m - m_i$ base stations in the given conflict graph. Therefore, the complexity of determining critical neighbor is $\mathcal{O}\left(m_i + \frac{(m-m_i)(m-m_i-1)}{2}\right)$. The term $(m - m_i)$ (in the evaluation of critical neighbor complexity) will keep on decreasing over the iterations, as the number of base stations allocated channel would increase. Thus, the computational complexity of critical neighbor becomes $\mathcal{O}(m_i + (m - m_i)^2)$. On simplification, this approximately reduces to $\mathcal{O}(m^2)$. The complexity of algorithm for an iteration (channel allocation and price charging) is $\mathcal{O}(n + m^2)$. Therefore, the overall complexity of the algorithm is $\mathcal{O}(n(n + m^2))$, where n is the number of operators and m is the total number of base stations in the given region. As the number of base stations are much larger than the number of operators, the overall complexity of the algorithm can be approximated as $\mathcal{O}(nm^2)$.

4.3 Non-uniform demand across Operators

In this section, we extend SC-SPAM for the multiple channel availability in the spectrum database. Moreover, we consider that the demand of channels across the base stations of an operator is not uniform (or same). Instead, the base stations of an operator may have different number of channel requirements depending on the traffic conditions experiences at a particular base station. Let us define the demand of operator i as $d_i = \{d_{i1}, \dots, d_{im_i}\}$, where d_{ij} represents the channel demand at j^{th} base station associated with operator i . It is assumed that the operators do not have strict demand, i.e., they are willing to accept any number of channels between 0 to d_{ij} at base station j .

Let \mathcal{B}_i and \mathcal{V}_i denote the bid and the true value of operator i across its base stations. Here, it is assumed that the valuation of the channel increases linearly with the demand at any base station. This implies that the per channel valuation at a base station is same for every assigned channel. In case, the demand of the channel at any base station is d_{ij} , then the total valuation at the particular base station gets multiplied by the demand, i.e., $d_{ij} \cdot v_{ij}$. The bid vector, $b_i = \mathcal{B}_i(1, :)$ reflects per channel bid for base stations of an operator.

Let us define,

$$\sigma_i^b(k) = \sum_{j=1}^{m_i} b_{ij} \mathbb{1}_{\{d_{ij} > 0\}}, \quad k = \{1, \dots, K\}$$

Algorithm 5 Non-uniform Demand Auction Mechanism (NUD-AM)

Input: Conflict Graph \mathcal{G} , K channels, bid vector $\{\mathcal{B}_i\}_{i \in \mathcal{N}}$; demand vector $\{d_i\}_{i \in \mathcal{N}}$.

Output: Allocation vector $\{x_i^f\}_{i \in \mathcal{N}}$, price $\{p_i\}_{i \in \mathcal{N}}$.

- 1: Initialize demand vector $d'_i \leftarrow d_i$ for every i , $k = K$, $b_i = \mathcal{B}_i(1, :) \forall i \in \mathcal{N}$, $x_i^f \leftarrow \text{Null}$, $\mathcal{G}' \leftarrow \mathcal{G}$
- 2: **while** ($k > 0$) **do**
- 3: Compute $\sigma_i^b(k) = \sum_{j=1}^{m_i} b_{ij} \mathbb{1}_{\{d_{ij} > 0\}}$.
- 4: Allocate channel and compute price (Algorithm 4).
- 5: Update $d'_i \leftarrow d'_i - x_i$ for every i
- 6: Update $x_i^f \leftarrow x_i^f + x_i$
- 7: **procedure** CONFLICT–GRAPH–UPDATION
- 8: If ($d_{ij} = 0$) update $\mathcal{G}' \leftarrow \mathcal{G}' \setminus \{S_{ij}\}$
- 9: Else $\mathcal{G}' \leftarrow \mathcal{G}'$
- 10: **end procedure**
- 11: $k \leftarrow k - 1$.
- 12: **end while**

for every operator i , where b_{ij} is per channel bid corresponding to j^{th} base station of operator i . $\sigma_i^b(k)$ computes the valuation of each operator corresponding to demand of channel at its base stations for a channel. As stated above, at least one channel is required at all the base stations participating in the auction for any operator, therefore, $\sigma_i^b(1) = \sigma_i^b$ (Equation (4.5)).

We propose Non-uniform Demand Auction Mechanism (NUD-AM) in Algorithm 5 which takes the demand vector $\{d_i\}_{i \in \mathcal{N}}$ as input along with the number of channels for auction. Channel allocation and price computation are performed iteratively for each channel available in the spectrum database. For each channel allocation, we compute $\sigma_i^b(k)$, which determines the operator valuation as per the demand at its base stations (line 3). Based on the operator valuation, we determine the channel allocation and the price charged from the operators using SC-SPAM. Then, the demand across base stations is updated based on the allocation vector for every operator (line 5). Next, we update the conflict graph before the next channel allocation. Channels are allocated corresponding to $\sigma_i^b(k)$, to ensure the maximization of the social welfare. The process continues until

all the channels are allocated. Now, we describe the operations of NUD-AM with an example.

4.3.1 Example

We consider a wireless network of 3 operators A , B , and C . Each operator has multiple base stations to provide services to the users in a geographical region. As illustrated in Fig.4.3, operator A , B and C have base stations $\{A_1, A_2, A_3, A_4\}$, $\{B_1, B_2, B_3, B_4\}$ and $\{C_1, C_2\}$, respectively. Note that the channel demand across the base stations of an operator is not the same, and the valuation at any base station increases linearly with the demand. We consider 2 channels are available for auction. An operator can bid for at most the number of channels available for auction at any of its base stations. Each operator submits a bid vector. As stated above bids are linearly increasing with demand, the bid vector contains bid per channel at each base station.

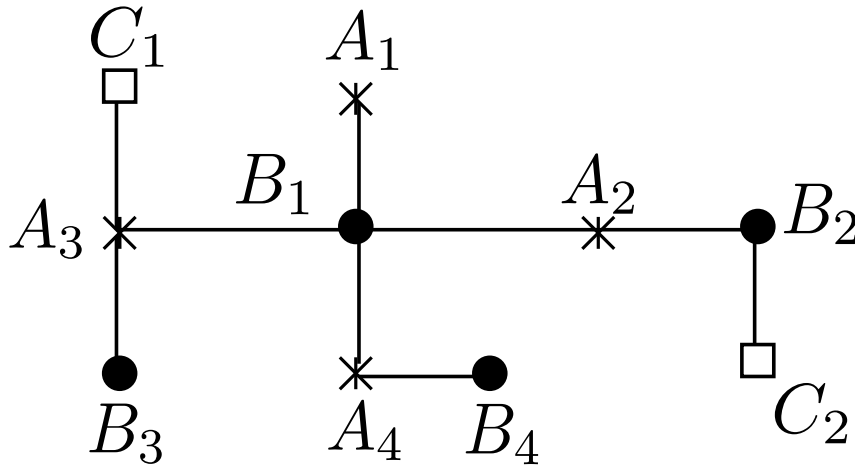


Figure 4.3: Conflict graph of the 3 operators.

We consider the demand vectors for the operators A , B and C are given as $d_A = [2 \ 1 \ 2 \ 2]$, $d_B = [2 \ 1 \ 1 \ 2]$ and $d_C = [2 \ 1]$, respectively. The bids at the base stations of operators A , B and C are represented as $b_A = [8 \ 10 \ 7 \ 6]$, $b_B = [8 \ 9 \ 9 \ 10]$ and $b_C = [10 \ 9]$, respectively. Channel allocation procedure is performed in two iterations.

Case 1 : All operators bid at true value across base stations.

- Iteration 1: First we determine $\sigma_i^b(1)$, $\forall i = \{A, B, C\}$. $\sigma_A^b(1) = 31$, $\sigma_B^b(1) = 36$ and $\sigma_C^b(1) = 19$. Similar to the calculations shown in Section 4, Operators B and C get

channel at base stations $\{B_1, B_2, B_3, B_4\}$ and $\{C_1\}$. Now, we obtain the price charged from the winners of the auction using critical operator (Definition 8). The price charged from operator $p_B = 31$ and $p_C = 0$. Next, we update the conflict graph for second channel allocation with non-zero demand across base stations as illustrated in Fig. 4.4.

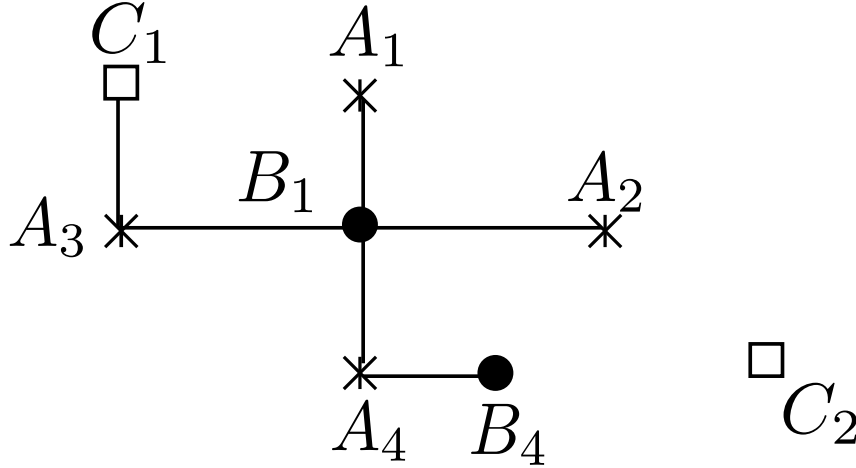


Figure 4.4: Updated conflict graph after the first iteration.

- Iteration 2: Again we perform same procedure as described in Iteration 1 on updated operator bids $\sigma_A^b(2) = 31$, $\sigma_B^b(2) = 18$ and $\sigma_A^C(2) = 19$. Now, base stations $\{A_1, A_2, A_3, A_4\}$ and $\{C_2\}$ get channel corresponding to operators A and C . The price charged from operators A and C are $p_A = 18$ and $p_C = 0$, respectively.

Case 2 : Except operator B all operators bid at their true value.

Let Operator B deviates from the true valuation and submits $b_B = (8, 6, 6, 9)$ to the auctioneer.

- Iteration 1: As Operator B deviates from the true value, $\sigma_B^b(1)$ reduces to 29. Channels are allocated at $\{A_1, A_2, A_3, A_4\}$ and $\{C_2\}$ base stations of operators A and C , respectively. The price charged are $p_A = 29$ and $p_C = 0$. Next, update the conflict graph.

- Iteration 2: Channels are allocated on the updated graph shown in Fig. 4.5 at $\{B_1, B_2, B_3, B_4\}$ and $\{C_1\}$ base stations of operators B and C , respectively. We observe that the demand at base station A_2 is zero, so it is no longer the part of the conflict graph. Therefore, the price charged from the operator B and C are 21 and 0, respectively.

It is observed that operator B gets the same number of channels in both the cases (true valuation and misreporting to lower bid value). However, the price charged at the

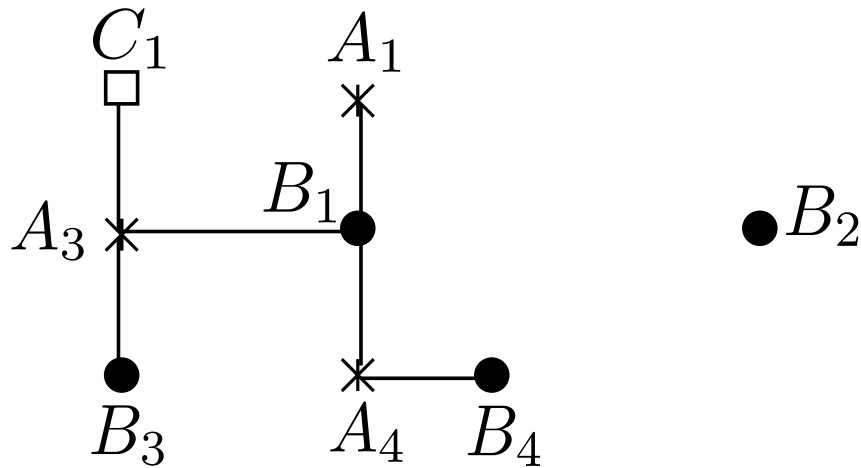


Figure 4.5: Updated conflict graph after the first iteration.

true value and the deviated bid value are 31 and 21, respectively for operator B . This clearly shows that the utility gain of operator B is 10. Hence, NUD-AM is not always strategy-proof.

As channel allocation procedure for a channel in NUD-AM is the same as SC-SPAM, therefore, NUD-AM is strategy-proof individually for every iteration. But it may not be strategy-proof as a whole. The reason behind NUD-AM not being strategy-proof is the updation of the conflict graph after each allocation. This results in the removal of base stations where demand is satisfied. This shows that addressing non-uniform demand across the base stations is a challenging problem. Next, we present another algorithm for this purpose.

4.4 Weakly Strategy-proof Algorithm for Non-uniform Demand

Algorithm NUD-AM proposed in Section 4.3 considers non-uniform demand across the base stations of an operator where the channel valuation increases linearly with the demand at the base stations. This implies that per channel bid at each base station remains the same with the demand. As NUD-AM charges price sequentially from the base stations in each step (iteration), it fails to be strategy-proof in certain cases, e.g. if an operator chooses to bid lower than its true valuation. In this section, we propose a Non-uniform Demand Weakly Strategy-proof Auction Mechanism (NUD-WSPAM) which ensures that

the operators have no incentive to deviate from the true valuation even if the demand across base stations is non-uniform and per channel bid may differ with the demand at a base station.

We consider that the bids are non-increasing with the demand which means each subsequent channel is valued less than the previous channel - this is akin to the assumption of decreasing marginal utility made commonly in economics. Hence, the operators are required to report the bid corresponding to multiple channel demand at each base station to the auctioneer. We assume that the demand at any base station across the network cannot be greater than the total number of channels available in the spectrum database. Now, each operator reports a bid vector for each base station associated with it. Let \mathcal{B}_i denotes the bid for operator i . Here, $\mathcal{B}_i(\ell, j)$ is bid for demand ℓ at base station j of operator i , if $(\ell - 1)$ channels are already assigned. We enforce that the bids submitted by operators are non-increasing i.e.,

$$\mathcal{B}_i(\ell, j) \geq \mathcal{B}_i(\ell + 1, j), \text{ for all } i, j, \ell.$$

The non-increasing marginal true value per channel with the demand is also considered by the authors in [47]. The authors referred the pattern of non-increasing marginal bid with the demand as *flexible bidding*. Furthermore, authors in [77], have studied the saturated throughput variation with the bandwidth at the base stations. It is observed that the saturated throughput may not increase linearly with the bandwidth.

In Algorithm 6, we present a generalized algorithm NUD-WSPAM. Unlike previous mechanisms, NUD-WSPAM first determines allocation for all the channels present in the spectrum database and then computes the price to be charged. At each iteration, a channel is allocated using Algorithm 4 for every channel available in the spectrum database as mentioned in line 4. To compute the price, we update the conflict graph which comprises the base stations where channel requirement is not satisfied after the allocation is complete. The price is charged based on the critical operator in the final updated graph (line 19).

As described in Algorithm 6, allocation is performed iteratively for each channel and then the bids are updated after each allocation for all the operators. The bid of operator i is \mathcal{B}_i , where base station j has multiple bids given as $\{\mathcal{B}_i(\ell, j) | 0 < \ell \leq d_{ij}\}$. Let b_i^r denotes the active bids (maximum of bid for the demand that is not satisfied) at the base stations

Algorithm 6 Non-uniform Demand Weakly Strategy-proof Auction Mechanism (NUD-WSPAM)

Input: Conflict Graph \mathcal{G} , K channels, non-increasing bid vector, $\mathcal{B}_{i\{i\in\mathcal{N}\}}$, demand vector $\{d_i\}_{i\in\mathcal{N}}$.

Output: Final allocation vector $\{x_i^f\}_{i\in\mathcal{N}}$, price $\{p_i\}_{i\in\mathcal{N}}$

1: Initialize final allocation vector $x_i^f \leftarrow 0$, $\mathcal{G}' \leftarrow \mathcal{G}$

2: Initialize $p_i \leftarrow 0$, $b_i = \mathcal{B}_i(1, \cdot) \quad \forall i \in \mathcal{N}$

3: **while** ($K > 0$) **do**

4: Find x_1, \dots, x_n using Algorithm 4

5: Update $x_i^f \leftarrow x_i^f + x_i, \forall i$

6: Update $d_i^f \leftarrow d_i^f - x_i^f, \forall i$

7: **procedure** BID-UPDATION

8: for $i = 1 : n$

9: for $j = 1 : m_i$

10: $b_{ij}^f = \mathcal{B}_i(x_{ij}^f + 1, j)$

11: end

12: end

13: **end procedure**

14: **procedure** CONFLICT-GRAPH-UPDATION

15: see Algorithm 5

16: **end procedure**

17: $K \leftarrow K - 1$

18: **end while**

19: Charge price using Equation (4.12).

of operator i in r^{th} iteration. The bid updation process is described in the Algorithm 6. By b_i^f , we denote the updated bid vector after all the K channels are allocated. Thus, bid vector b_i^f projects the bids at the base stations of operator i for $(K + 1)^{\text{th}}$ iteration, where K is the number of channels available. The bid at base station j of operator i in vector b_i^f is given as $b_{ij}^f = \mathcal{B}_i(x_{ij}^f + 1, j)$, where x_{ij}^f is final allocation of operator i at base station j or j^{th} component of x_i^f . The vector b_i^f has the highest bid values corresponding

to unsatisfied demand (non-increasing bid assumption) for operator i .

Let d_i^f , $i \in O$ denotes the final demand vector of operator i after the allocation process is complete. Here, $d_{ij}^f = 0$ signifies that the demand is satisfied at j^{th} base station of operator i . Furthermore, the set of base stations where demand is unsatisfied is indicated as S_i^f i.e., $S_i^f = \{j | d_{ij}^f > 0\}$. Based on S_i^f , final conflict graph \mathcal{G}^f is obtained. \mathcal{G}^f has base stations where demand is not satisfied.

Let, $\Gamma_y^i = \mathcal{N}_i \cap S_y^f$ denotes the base stations of operator y in \mathcal{G}^f which are in neighborhood (in conflict) of base stations of operator i in initial conflict graph \mathcal{G} . We define the critical operator $C(i)$ any $y \in O_i$ such that

$$\sum_{k \in \Gamma_y^i} b_{yk}^f \geq \sum_{k \in \Gamma_{y'}^i} b_{y'k}^f, \quad \forall y' \neq y, y' \in O_i. \quad (4.10)$$

For single channel auction, Equation (4.10) reduces to Definition 8. The only difference is that the base stations where the demand is zero after the allocation process is no longer part of the conflict graph \mathcal{G}^f . We compute the valuation of operator y which is not allocated channel denoted as χ_y^i . Critical operator valuation σ_i^c is obtained using Equation (4.12).

$$\chi_y^i = \sum_{k \in \Gamma_y^i} b_{yk}^f. \quad (4.11)$$

$$\sigma_i^c = \chi_{C(i)}^i. \quad (4.12)$$

The price charged from operator i is $p_i = \sigma_i^c$. This price reduces to the earlier critical operator valuation mentioned in Section 4.2 for the single-channel scenario.

Let us introduce a new concept of *weak strategy-proofness*:

Definition 9. Let \mathcal{V}_i denotes the true valuation of operator i . An auction is said to be weakly strategy-proof if an operator does not gain by deviating to $\tilde{\mathcal{B}}_i$ from \mathcal{V}_i , where $\tilde{\mathcal{B}}_i$ satisfies either (1) $\exists j$ such that $\tilde{\mathcal{B}}_i(\ell, j) > \mathcal{V}_i(\ell, j)$, $\forall \ell$ or (2) $\exists j$ such that $\tilde{\mathcal{B}}_i(\ell, j) < \mathcal{V}_i(\ell, j)$, $\forall \ell$. i.e.,

$$\mathcal{U}_i(\tilde{\mathcal{B}}_i, \mathcal{V}_{-i}) \leq \mathcal{U}_i(\mathcal{V}_i, \mathcal{V}_{-i}) \quad \forall \tilde{\mathcal{B}}_i \& \mathcal{V}_{-i}. \quad (4.13)$$

where, $\tilde{\mathcal{B}}_i$ satisfy conditions (1) or (2) and $\mathcal{V}_{-i} = \{\mathcal{V}_1, \dots, \mathcal{V}_{i-1}, \mathcal{V}_{i+1}, \dots, \mathcal{V}_n\}$ is tuple with bid of all other operators except operator i .

4.4.1 Example

We revisit the Example 4.3.1 in the context of NUD-WSPAM. The wireless network is illustrated in Fig.4.3 is same except the channel valuation at a base station is no longer linearly increasing with the demand. As stated earlier, per channel valuation is non-increasing function of demand at any base station. An operator can bid for at most the number of channels available for auction at any base station. We consider demand vectors to be the same as mentioned in the example previously. Let q_{ij} represents the bid vector at base station j of operator i corresponding to its demand. The bid at base stations of operator A are given as $\mathcal{B}_A = [q_{A1}^T \ q_{A2}^T \ q_{A3}^T \ q_{A4}^T]$, where $q_{A1} = [8 \ 5]$, $q_{A2} = [10 \ 0]$ and $q_{A3} = [7 \ 3]$ and $q_{A4} = [6 \ 3]$. Here, a^T indicates the transpose of a . The bid for operator B is $\mathcal{B}_B = [q_{B1}^T \ q_{B2}^T \ q_{B3}^T \ q_{B4}^T]$, where $q_{B1} = [8 \ 4]$, $q_{B2} = [9 \ 0]$, $q_{B3} = [9 \ 0]$ and $q_{B4} = [10 \ 3]$. The bid for operator C is $\mathcal{B}_C = [q_{C1}^T \ q_{C2}^T]$, where $q_{C1} = [10 \ 5]$, $q_{C2} = [9 \ 0]$.

Case 1: All operators reveal their true valuations

- Iteration 1: From the given bid vectors, we determine bids of the operators, $\sigma_A = 31$, $\sigma_B = 36$ and $\sigma_C = 19$. The channel is allocated across the base stations of the highest bidding operator. Then channel is allocated to the base stations of the remaining operators in the order of decreasing valuations which do not conflict with the base stations that are already allocated channel. Therefore, the channel is allocated to operator B at $\{B_1, B_2, B_3, B_4\}$ base station and operator C at $\{C_1\}$ base station.

- Iteration 2: For second channel allocation, demand and bid vectors are updated depending on the allocation in previous iteration. The updated demand vectors are $d_A = [2 \ 1 \ 2 \ 2]$, $d_B = [1 \ 0 \ 0 \ 1]$ and $d_C = [1 \ 1]$. The operators valuation for the iteration is determined from the updated bid $\sigma_A = 31$, $\sigma_B = 7$ and $\sigma_C = 19$. Channel is allocated to operator A at $\{A_1, A_2, A_3, A_4\}$ and operator C at $\{C_2\}$ base stations.

This completes the channel allocation phase. Now, the demand at the operators is $d_A = [1 \ 0 \ 1 \ 1]$, $d_B = [1 \ 0 \ 0 \ 1]$ and $d_C = [1 \ 0]$.

Price Charging Step: In Algorithm 6, the price is charged after all the channels are allocated based on the base stations where demand is non-zero. We construct the conflict graph with the base stations having demand greater than zero as illustrated in Fig. 4.6. Each operator is charged as per their critical operator (see Definition 8). The sum of

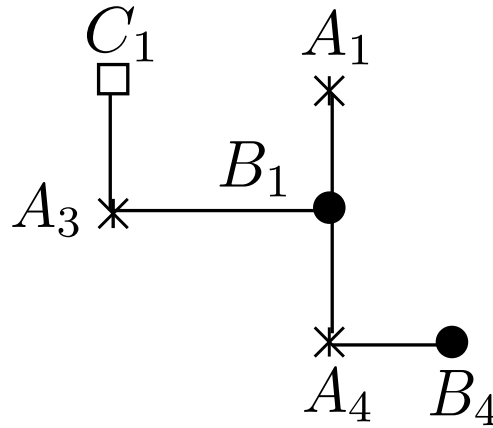


Figure 4.6: Updated conflict graph after channel allocation phase is complete.

the highest bids of the base stations $\{B_1, B_4\}$ of operator B for which demand is not satisfied comprise the critical operator of operator A . Similarly, the bids of base stations $\{A_1, A_3, A_4\}$ constitute the critical operator for operator B and the bid at the base station $\{A_3\}$ is critical operator bid for operator C . Thus, the price charged from operators A , B and C is given by $p_A = 7$, $p_B = 11$ and $p_C = 3$.

Case 2: Operator B deviates from true valuation and bids at a lower value

Now, we revisit the wireless network mentioned in Fig. 4.3, considering that except operator B others submit bid equal to their true value for the associated base stations. The demand vector of all the operators remain unchanged as in the first case. Let the operator B deviates to bid $\mathcal{B}'_B = [q'_{B1}{}^T, q'_{B2}{}^T, q'_{B3}{}^T, q'_{B4}{}^T]$, where $q'_{B1} = (8, 4)$, $q'_{B2} = (6, 0)$, $q'_{B3} = (6, 0)$ and $q'_{B4} = (9, 3)$. As described in Case 1, channel is allocated to the operators.

- Iteration 1: Here, the operator bids for channel allocation are $\sigma_A = 31$, $\sigma_B = 29$ and $\sigma_C = 19$. Operators A and C are allocated channel at base stations $\{A_1, A_2, A_3, A_4\}$ and $\{C_2\}$, respectively.
- Iteration 2: Second channel is allocated to base stations $\{B_1, B_2, B_3, B_4\}$ and $\{C_1\}$.

We can see that operator B gets channel at their base stations in iteration 2. Channel allocation remains the same even after deviating from the true valuation. Now, we determine the price charged by the operators.

Price Charging Step: We update the conflict graph based on the remaining channel demand across the base stations of every operator as illustrated in Fig. 4.6. Then, we

determine the price charged from every operator based on the critical operator. The price charged remains the same as it is obtained for Case 1 (operators reveal their true valuations).

From the above example, it is seen that the deviation from true valuation does not provide utility gain. Thus, operators have no incentive in misreporting the true valuation. This implies that Algorithm 6 is strategy-proof.

As we defined earlier, $\sigma_i^b(k) = \sum_j b_{ij}^k$, where $b_i^k = [b_{i1}^k \dots b_{im_i}^k]$ has the bids at which operator i demands channel at its base stations in k^{th} iteration of allocation.

Lemma 8. *Algorithm 6 is individually rational.*

Proof. As per the assumption, marginal bid per channel decreases with the demand ℓ at any base station i.e., $\mathcal{B}_i(\ell, j) \geq \mathcal{B}_i(\ell', j)$ for $\ell < \ell'$ for all operator i , base station j . Therefore, each operator bid is non-increasing sequentially in the allocation process i.e., $\sigma_i^b(k) \geq \sigma_i^b(k')$ for $k < k'$, where k denotes channel allocation iteration.

Operator i with maximum bid gets channel in each iteration. As stated in Algorithm 6, updated graph \mathcal{G}^f comprises base stations $\{s | s \in S_y^f, \forall y\}$. Operator i is charged as $\sigma_i^c = \max_{y \neq i} \chi_y^i$. As proved in Lemma (7), $\sigma_i^c(k) \leq \sigma_i^b(k)$, for all k . But, in Algorithm 6, σ_i^c is determined from \mathcal{G}^f . Therefore, $\sigma_i^c \leq \sigma_i^c(k), \forall k$.

Let x_i^f denotes the final allocation vector for operator i . We denote the sum of the channel bids corresponding to allocation vector x_i^f is α_i^b . Thus, $\alpha_i^b = \sum_{j=1}^{m_i} \sum_{\ell=1}^{x_{ij}^f} \mathcal{B}_i(\ell, j)$. Moreover, $\alpha_i^b \geq \sigma_i^b(1)$, where $\sigma_i^b(1)$ is operator i bid for first channel. As we know $\sigma_i^c < \sigma_i^b$, therefore $\sigma_i^c < \alpha_i^b$. Now, the price charged is given by

$$\begin{aligned} p_i &= \alpha_i^b - \sigma_i^c, \\ &\leq \alpha_i^b. \quad (\because 0 \leq \sigma_i^c \leq \alpha_i^b). \end{aligned}$$

Thus, $0 \leq p_i \leq \alpha_i^b$. This proves that Algorithm 6 is individually rational. \square

Lemma 9. *In Algorithm 6, suppose final allocation vectors of operator i are x_i^f and \tilde{x}_i^f at bids $(\mathcal{B}_i, \mathcal{B}_{-i})$ and $(\tilde{\mathcal{B}}_i, \mathcal{B}_{-i})$, respectively. If there exists some base station j such that $\tilde{\mathcal{B}}_i(\ell, j) > \mathcal{B}_i(\ell, j) \quad \forall \ell$, then $\tilde{x}_i^f - x_i^f \geq 0$. This implies that the number of channels allocated across the base stations of operator i at $\tilde{\mathcal{B}}_i$ are atleast equal to the number of channels allocated at \mathcal{B}_i .*

Proof. As per the assumption in Section 4.4, $\tilde{\mathcal{B}}_i(\ell, j) \geq \tilde{\mathcal{B}}_i(\ell', j)$ such that $\ell < \ell'$ for all base stations j . Let operator i be allocated channels in k iterations in the allocation process at \mathcal{B}_i . As channel allocation is performed greedily based on the bid, with a bid $\tilde{\mathcal{B}}_i \geq \mathcal{B}_i$, it must be allocated at least k iterations. Since \mathcal{B}_{-i} is unchanged, operator i may get a channel in more than k iterations, if increase in bid results in $\sigma_i^b > \sigma_y^b$, for $y \neq i$ in more iterations in the allocation process. \square

Theorem 3. *Algorithm 6 is weakly strategy-proof.*

Proof. To prove the strategy-proofness, we are required to show that the deviation from the true valuation for any operator can never increase the utility. We consider two scenarios: (1) if an operator bids at a value higher than the true value, and (2) if an operator bids at a value less than the true valuation.

Let σ_i^t denote the sum of the true valuations at the base stations of operator i for the allocated channels.

Let β_i^t denote the sum of the bids of the channels allocated across the base stations of operator i .

Critical valuation, utility and final conflict graph at β_i^t are denoted as $\tilde{\sigma}_i^c$, \tilde{U}_i and $\tilde{\mathcal{G}}^f$, respectively. Let x_i^f and \tilde{x}_i^f denote the final allocation vector of operator i with bids σ_i^t and β_i^t , respectively. Further, we define $\tilde{x}_i^f > x_i^f$, if \exists at least a base station ℓ such that $\tilde{x}_i^f(\ell) > x_i^f(\ell)$.

Scenario 1 : The operator bid is more than the true valuation of the channels allocated at its base stations, $\sigma_i^t < \beta_i^t$. Here, again we may have following cases:

Case (i): Final allocation vector for all operators remains unchanged i.e., $\tilde{x}_i^f = x_i^f$, $\forall i$. Therefore, $C(i)$ and σ_i^c for operator i remains the same even at β_i^t . Hence, operator utility \mathcal{U}_i remains the same.

Case (ii): Operator i is allocated more number channels i.e., $\tilde{x}_i^f > x_i^f$. Since supply is limited, number of channels allocated to some operators other than i decreases i.e., $\tilde{x}_y^f < x_y^f$ such that $y \neq i$. Let us say, operator i is allocated extra channels in iteration k . Then, $\sigma_i^b(k) > \sigma_y^b(k) > \sigma_i^v(k)$ for $y \neq i$. However, at true value unsatisfied base stations of operator i are not allocated channel and are present in \mathcal{G}^f . Due to untruthful bidding of operator i , $\tilde{\mathcal{G}}^f$ comprise of the base stations of operator y with higher aggregate true

valuation. Therefore, $\tilde{\sigma}_i^c > \sigma_i^c$, this implies $\tilde{\mathcal{U}}_i < \mathcal{U}_i$. Hence, deviation from true value does not increase utility of operator i .

Case (iii): Operator i is allocated less number channels i.e., $\tilde{x}_i^f < x_i^f$. This is not possible due to monotonicity (Lemma 9).

Scenario 2 : The operator bid is less than the true valuation of the channels allocated at its base stations, i.e., $\sigma_i^t > \beta_i^t$.

Case (i): The number of channels allocated across the base stations and the final allocation vector remains unchanged.

With the similar argument as in Case (a) of Scenario 1. The utility of the operator i does not change.

Case (ii): Operator i is allocated more number channels i.e., $\tilde{x}_i^f > x_i^f$. This is not possible due to monotonicity (see Lemma 9).

Case (iii): Operator i is allocated less number channels i.e., $\tilde{x}_i^f < x_i^f$. As the number of channels allocated decrease on deviation from the σ_i^t , operator i suffers loss.

Thus, we establish that the deviation from true valuation does not lead to utility gain. Therefore, the proposed algorithm is weakly strategy-proof. \square

4.5 Summary of the Proposed Mechanisms

In this section, we summarize the key features (strategy-proofness and computational complexity) of the proposed mechanisms and the various scenarios in Table 4.1.

In Table 4.1, n denotes the number of operators, $m = \sum_{i=1}^n m_i$ is the total number of base stations across all the operators present in the region, and K is the number of channels available for auction. The detailed computation complexity analysis of SC-SPAM is presented in Section 4.2.1. For K channel availability, computational complexity becomes $\mathcal{O}(K \cdot nm^2)$ using similar analysis as given for SC-SPAM.

4.6 Simulation Results

In this section, we evaluate the performance of the proposed algorithms in multi-operator settings in a wireless network. In the simulations, we consider 3 operators providing

Table 4.1: Summary

Algorithms	Scenario	Strategy-proof	Computational Complexity
SC-SPAM	Single channel, Uniform demand	Strong	$\mathcal{O}(nm^2)$
NUD-AM	Multi-channel, Non-uniform demand, linear bid	No	$\mathcal{O}(K \cdot nm^2)$
NUD-WSPAM	Multi-channel, Non-uniform demand, non-linear bid	Weak	$\mathcal{O}(K \cdot nm^2)$
SPECIAL	Multi-channel, Uniform demand, non-linear bid	Strong	$\mathcal{O}(K \cdot m^2)$

services in a region. We model the wireless network by creating conflict graphs $\mathcal{G} = (V, \mathcal{E})$ using the configuration model [74]. To create an overall topology of the wireless network in a given region, we first generate three conflict graphs $\mathcal{G}_{12}, \mathcal{G}_{13}, \mathcal{G}_{23}$. Here, \mathcal{G}_{iy} represents a conflict graph across the base stations of operators i and y . Using the conflict graphs, we obtain corresponding binary interference matrices $\mathcal{I}_{12}, \mathcal{I}_{13}$ and \mathcal{I}_{23} , where \mathcal{I}_{iy} represents the interference among the base stations of operator i and operator y . In an interference matrix, 1 indicates interfering pair of base stations. Further, we obtain interference matrices \mathcal{I}_{yi} from the transpose of the matrix \mathcal{I}_{iy} . The overall interference matrix \mathcal{I} of wireless access network in the region is obtained using $\mathcal{I}_{12}, \mathcal{I}_{13}, \mathcal{I}_{23}, \mathcal{I}_{21}, \mathcal{I}_{31}$, and \mathcal{I}_{32} . We perform Monte Carlo simulations for various scenarios. All the results are obtained by averaging over 50 different topologies. The simulations are performed in MATLAB [75]. We evaluate the performance of the algorithms based on Spectrum Utilization and Social Welfare mentioned in Definitions 6 and 7, respectively.

We compare the proposed algorithms with VCG [27], SMALL [41] and SPECIAL [47] mechanisms. As discussed earlier, VCG mechanism chooses an allocation with the highest social welfare (optimal) from the set of all the feasible allocations. SMALL groups the non-conflicting base stations together and determines the group valuation for each group.

The group valuation is obtained as the number of base stations with the bid greater than the minimum bid of the group times the minimum bid. Channel is allocated to the highest bidding group and all the base stations except the one with minimum bid are charged with the minimum bid in the group. SPECIAL considers that the demand at each base station is equal to the number of channels available for auction along with the flexible bidding at the base stations described in Section 4.4.

4.6.1 Performance evaluation for Single Channel

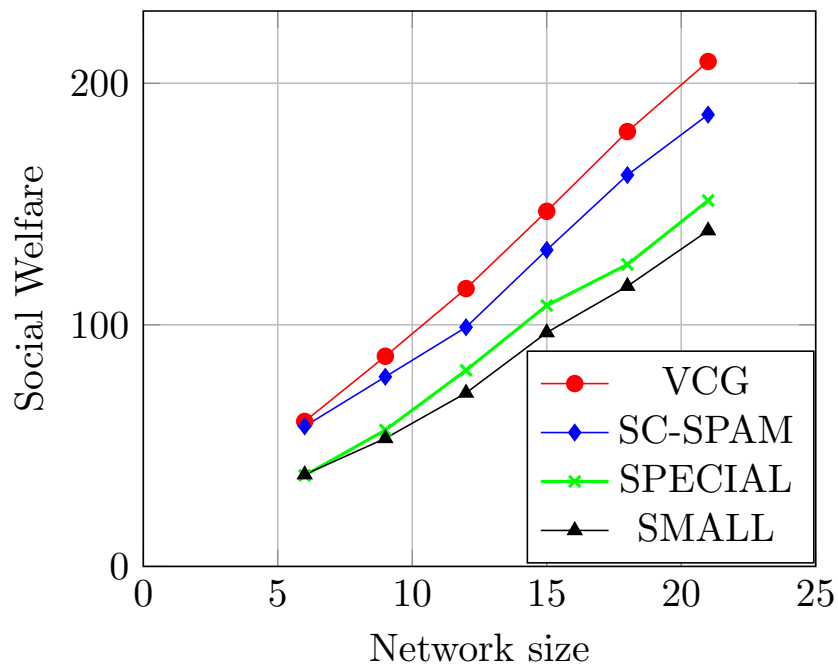
4.6.1.1 Social Welfare and Spectrum Utilization

The bids across the base stations are uniformly distributed in the interval $[15, 25]$ for each operator. As VCG becomes computationally intractable for large networks, we restrict our simulations to small size networks which vary from 6 to 21 base stations. In this case, a single channel is available in the spectrum database. In Fig. 4.7, we observe that the social welfare and the spectrum utilization of SC-SPAM are close to the optimal value obtained from VCG. However, SC-SPAM outperforms SMALL and SPECIAL both in spectrum utilization and social welfare.

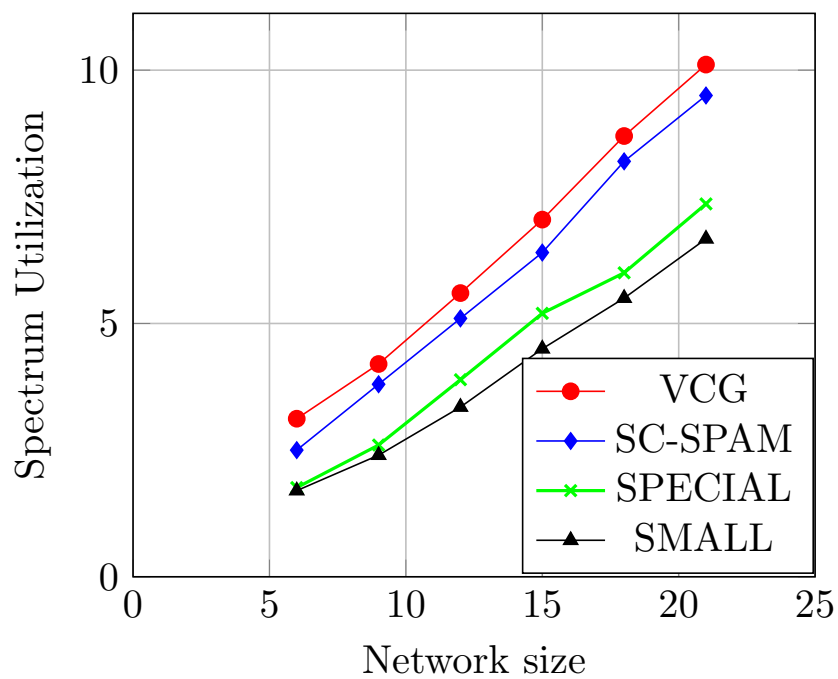
4.6.1.2 Execution time

We evaluate the performance of SC-SPAM against other existing algorithms based on their required execution times for dynamic spectrum allocation illustrated in Fig. 4.8. We observe that the proposed mechanism (SC-SPAM) outperforms significantly. Furthermore, results justify the exponential increase in the execution time of VCG with an increase in the number of base stations. Although VCG provides optimal social welfare, the computational complexity makes it infeasible for dynamic spectrum allocation even in moderately sized (comprising 10 – 15 base stations) network.

Another important observation is that for VCG, SPECIAL and SMALL algorithms execution time varies significantly even with the small increase of base stations in the network. However, the execution time of SC-SPAM does not vary significantly with the increase of base stations in the network. With the least execution time of SC-SPAM among the algorithms, SC-SPAM is the best candidate for resource allocation in real-time implementation.



(a) Social Welfare



(b) Spectrum utilization

Figure 4.7: Performance comparison of the VCG, SC-SPAM, SPECIAL and SMALL in three operator scenario.

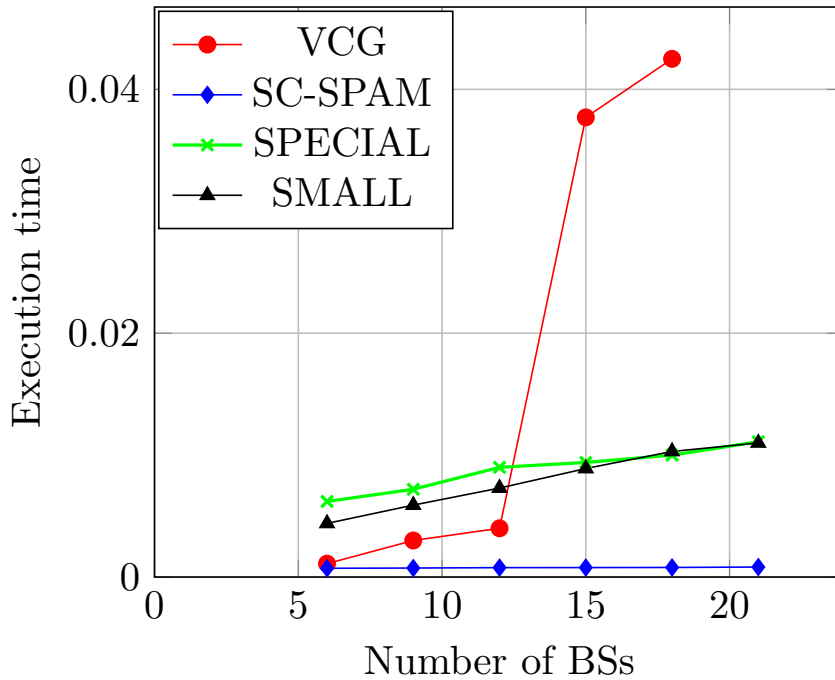
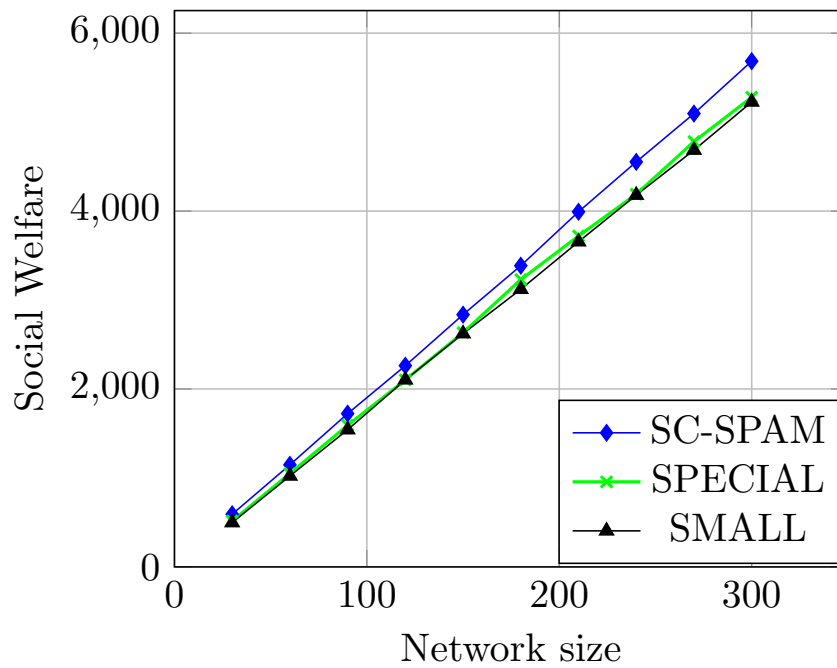


Figure 4.8: Comparison of execution times of various algorithms.

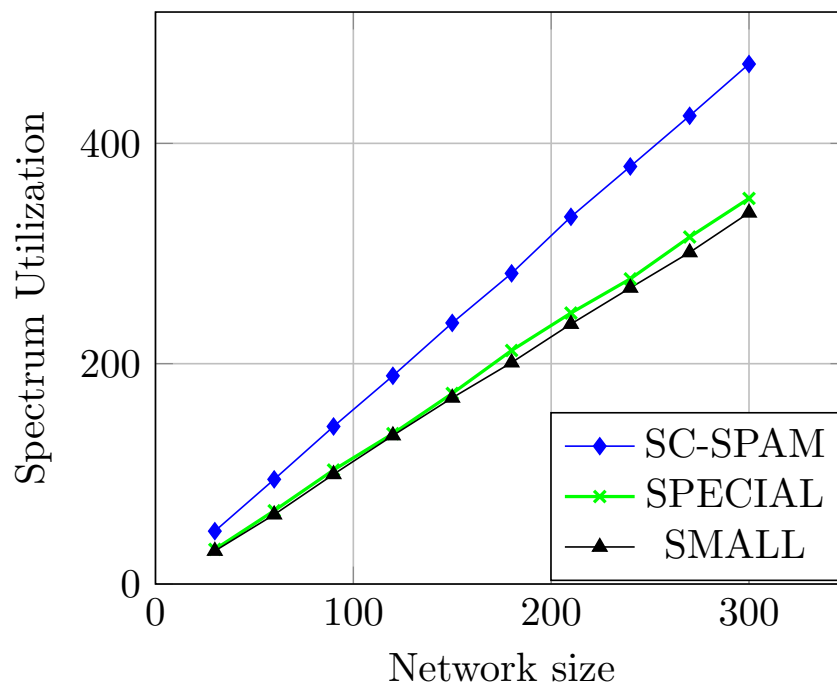
4.6.2 Performance evaluation for Multiple Channels

4.6.2.1 Social Welfare and Spectrum utilization

Next, we compare the performance of the proposed mechanisms with SMALL [41] in large networks with the number of base stations ranging from 30 to 300. We consider that 2 channels are available in the spectrum database. Each base station has a demand of 2 channels for all the operators. Each operator submits a per channel bid vector at every base station. The operators choose bids uniformly between $[10, 25]$. From Fig. 4.9, we observe that the performance of the proposed mechanism for multiple channel allocation is better than that of SMALL and SPECIAL. Here, spectrum utilization is determined as the total number of channels allocated across the base stations of all the operators. The trend observed justifies the following facts: First, SMALL sacrifices the base stations with minimum bid to achieve strategy-proofness, resulting in lower social welfare. Second, base stations only in the winning groups are allocated channel, even though there may be some base stations which do not conflict with the winning base stations and therefore can be allocated channels. Furthermore, it is seen that the performance of SMALL and SPECIAL degrades with an increase in the number of base stations in the region.



(a) Social Welfare



(b) Spectrum utilization

Figure 4.9: Performance comparison for uniform demand $d = 2$ across the base stations of multiple operators, with linearly increasing bid with demand at each base station.

4.6.2.2 Percentage of base stations allocated resource

In Fig.4.10, we compare the performance of various algorithms based on the percentage of base stations allocated at least one channel in resource allocation process. The simulations are performed considering both linearly increasing bid per channel and flexible bidding at the base stations. A variation of SC-SPAM with multiple channel availability and uniform demand across base stations is considered in SC-SPAM(NLB). Furthermore, evaluation of SC-SPAM(NLB) is performed considering the flexible bid at base stations. It is observed that the flexible bidding with non-uniform demand across the base station scenario (NUD-WSPAM) outperforms all the other scenarios of resource allocation. The intuition behind the observation is that in NUD-SPAM, some base stations may drop out in subsequent channel allocations when the demand is satisfied.

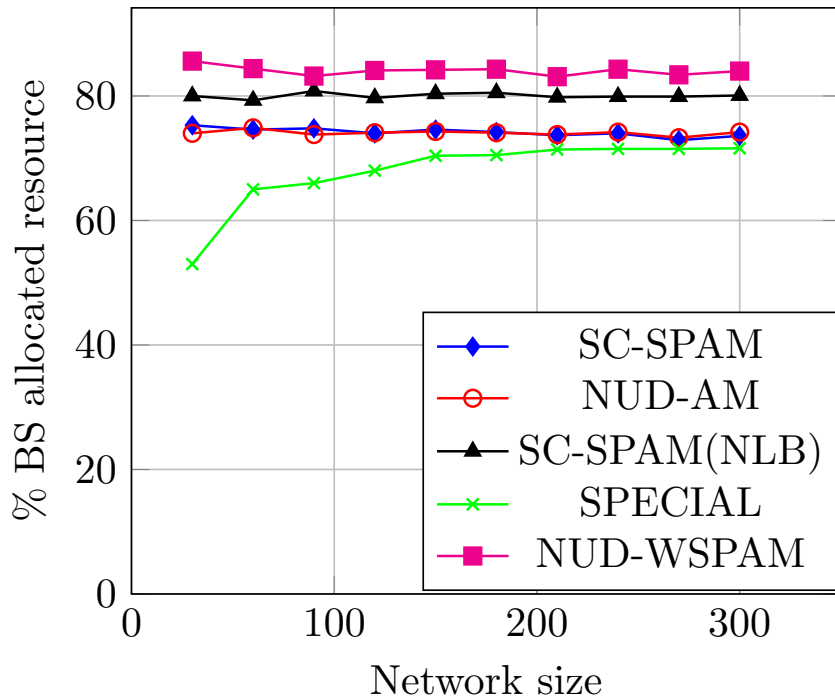


Figure 4.10: Comparison of percentage of base stations allocated channel in wireless networks.

4.6.2.3 Spectrum Utilization vs. Channels in NUD-WSPAM

We consider channel demand at any base station to be a function of the traffic in the cell. The demand at any base station is uniformly distributed in the interval $[0, 3]$. We

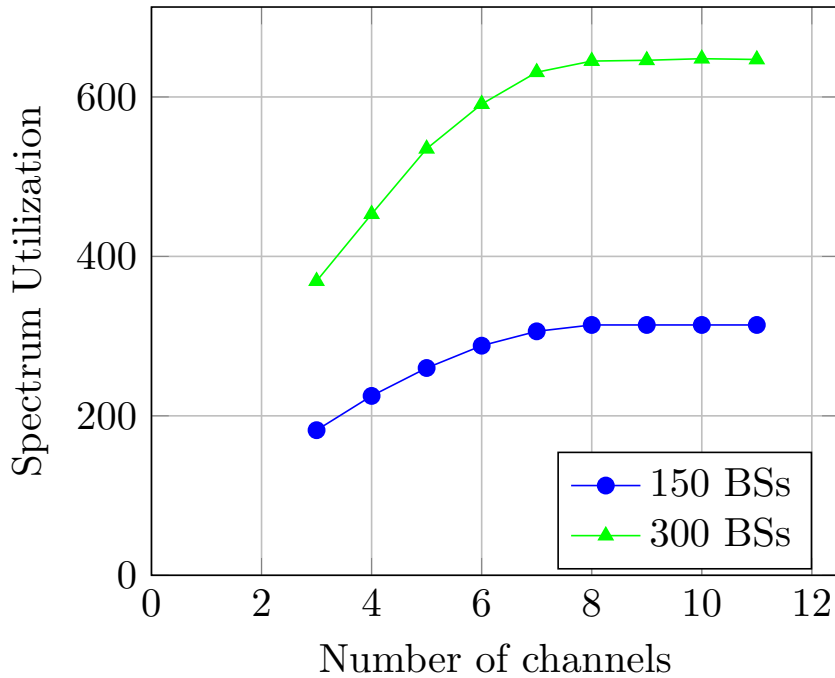


Figure 4.11: Comparison of spectrum utilization and number of channels for NUD-WSPAM in large networks.

perform simulations to evaluate the number of channels required to satisfy the demands across the base stations for all operators in the region. In Fig.4.11, we observe that the number of channels required to fulfill the demand for all the operators shows a similar trend irrespective of the number of base stations. The number of channels required for the wireless network of 150 base stations remains same as that of 300 base stations. The reason for this behavior is that the degree distribution of base stations does not change with the size of the network (number of base stations).

4.7 Conclusions

In this chapter, we have investigated the problem of spectrum allocation at the operator level, for multiple existing operators in a region. We consider multiple base stations to be associated with an operator to provide services to the end-users. Therefore, an operator has demand and valuation corresponding to each base station associated with it. To address the issue of multiple valuations at an operator, we have modeled the spectrum allocation problem among non-cooperative operators in a multi-parameter environment to

maximize the social welfare of the system. First, we propose a strategy-proof mechanism for single-channel demand across base stations of co-existing operators. Then we extend it for multiple channels considering non-uniform demand across the base stations of the operators. We prove that the mechanisms SC-SPAM and NUD-WSPAM are guaranteed to be strategy-proof and weakly strategy-proof, respectively. The performances of the proposed algorithms are evaluated using Monte Carlo simulations and compared with those of the other existing mechanisms. The performances of the proposed mechanisms are near-optimal in terms of spectrum utilization and social welfare. Furthermore, the analysis of computational complexity reveals that the proposed mechanisms are implementable in large networks in real-time scenarios. Thus, the proposed mechanisms solve the issue of intractability arising in VCG mechanism.

Chapter 5

Dynamic Spectrum Allocation for Wireless Backhaul in Heterogeneous Networks

The amount of traffic in cellular networks has been steadily increasing with the advent of technological advancements such as Internet of Things (IoT), smart phones. To support this diverse and burgeoning data traffic, cellular networks have been undergoing significant architectural enhancements. Heterogeneous networks (HetNet) architecture is one of the key advancements in this direction. HetNet comprises a macro cell overlaid with multiple small cells (pico/femto cells) leading to the network densification. HetNet deployment is one way to achieve higher spectral efficiency in regions with high User Equipment (UE) density when the available radio resources are limited. These small cells can be supported with the help of low power base stations. The addition of small cells to an existing macro cell not only improves the network capacity and coverage but also provides better Quality of Service (QoS) to UEs. However, fiber based backhaul connectivity to each small cell is neither cost effective nor practically feasible and wireless backhaul may be a more suitable option for the same. Integrated Access and Backhaul (IAB) [78] has been considered by Third Generation Partnership Project (3GPP) as a cost-efficient solution to address the requirement of connectivity to each small cell in Fifth Generation (5G) cellular network.

3GPP 5G standard has defined IAB feature to enable wireless backhauling (relaying) in 5G New Radio (NR) based Radio Access Network (RAN). The 5G IAB architecture

comprises two different types of network elements (NE), IAB-nodes and IAB-donors. An IAB-node provides last mile connectivity to UEs. It is a gNB-Distributed Unit (gNB-DU) augmented with wireless backhaul capability to connect to an IAB-donor. The IAB-donor, plays the role of a gNB-Centralized Unit (gNB-CU) for IAB-nodes. IAB-donors have additional functionality to support wireless backhaul connectivity to downstream IAB-nodes. An IAB-donor terminates the wireless backhauling towards the CN, it may be connected to CN through fiber or other similar wire-line infrastructure

Multiple IAB-nodes (small cell gNBs) may be connected to a single IAB-donor in a hierarchical tree like structure as shown in Fig. 5.1. Since more than one IAB-node is connected to a single IAB-donor, there is a need to share the backhaul resource (wireless spectrum) among these IAB-nodes. A simple scheme that can be used for resource allocation (spectrum sharing) in wireless backhaul is static allocation, wherein spectrum is allocated to IAB-nodes for a large duration, which is utilized to serve UEs associated with them.

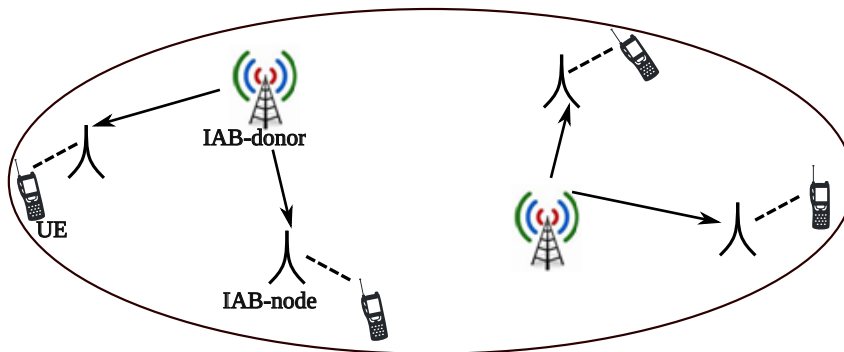


Figure 5.1: Illustration of IAB network

In this chapter, we investigate the problem of resource allocation in IAB enabled HetNet, which are expected to play a vital role in next generation networks. Therefore, we focus on devising the dynamic spectrum allocation (DSA) mechanism for IAB networks, considering the structural arrangement and the behavior of the network entities. Although the static allocation of resources at IAB-nodes is simple and easy to implement, but this renders the spectrum severely under-utilized during the off-peak hours [79]. Moreover, the statistics suggest that the mobile data traffic varies temporally as well as spatially across the network [3]. Hence, static allocation of scarce and expensive spectrum cannot be considered an efficient solution.

We propose an auction-based framework for DSA in IAB networks considering the 3 Tier hierarchical structure across IAB-donor, IAB-nodes, and UEs in the system. The aim of auction mechanism is to maximize the social welfare (sum of the true valuation of the UEs). The proposed mechanism is computationally efficient such that the dynamic variations in the traffic can be taken into account. The proposed strategy-proof mechanism achieves optimal solution, despite restriction of the communication between the IAB-donor and the UEs, imposed by the hierarchical structure. However, using simulations, we establish that the proposed DSA mechanism achieves optimal social welfare. We formally prove the individual rationality, monotonicity, and strategy-proofness of the proposed sub-mechanism.

The chapter has been organized as follows. We briefly describe the system model of IAB enabled 5G HetNet considering hierarchical structure across the IAB-donors, IAB-nodes and UEs and formulate the resource allocation problem in Section 5.1. In Section 5.2, some definitions and preliminaries of the auction-based mechanism pertaining to the hierarchical structure are provided. We propose the auction-based mechanism in Section 5.3, and also demonstrate the desired characteristics, such as, strategy-proofness, individual rationality. We evaluate the performance of the proposed mechanism against the optimal scheme using simulations in Section 5.4. Finally, we conclude the chapter in Section 5.5.

5.1 System Model

We consider a scenario of downlink transmission in IAB enabled 5G HetNet. The system model comprises IAB-donors and IAB-nodes in HetNet settings to provide connectivity (service) to UEs. In a HetNet setting, IAB-nodes are low power BSs, supporting small coverage area cells. A UE associates itself with one of the BSs over wireless channel. We assume that a UE is associated with the BS (IAB-node) with the best channel condition. Typically, multiple UEs are connected to one BS. These small cell BSs (IAB-nodes) are connected to CN through wireless backhaul provided by IAB-donors. Multiple IAB-nodes (BSs) may be connected to a single IAB-donor. IAB-donors allocate radio resources to downstream IAB-nodes just as an IAB-node does for the UEs connected to it.

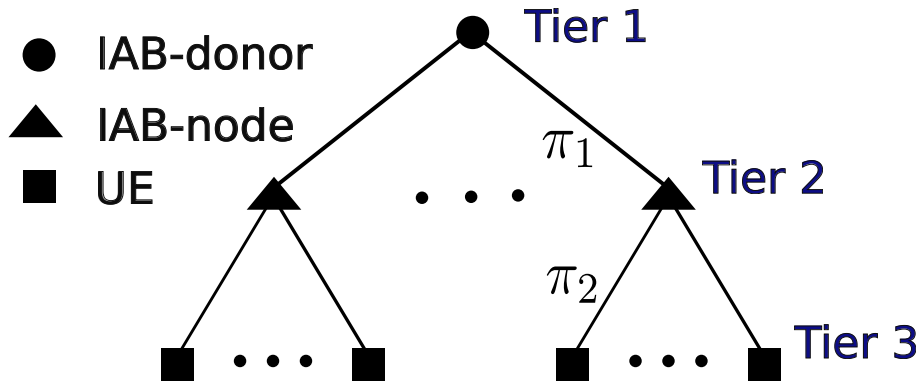


Figure 5.2: Illustration of system model

The entities in HetNet architecture exhibit a hierarchical structure as illustrated in Figure 5.2. We categorize the network entities into 3 levels, namely Tier 1, Tier 2 and Tier 3, which are IAB-donors, IAB-nodes and UEs, respectively.

The UEs requesting a service report their bid to the respective IAB-node. To avoid the excessive control signaling between UEs and IAB-donor, IAB-nodes perform aggregation of bids and report to the IAB-donors. The aggregation of bids also serves the purpose of hiding the UE specific information for privacy concerns. IAB-donor distributes the resources among IAB-nodes based on their reported bids. Subsequently, IAB-nodes allocate the acquired resources across UEs. We assume that IAB-donors and IAB-nodes incur a particular operating cost in the transmission. The operating cost may consist of various facilities such as power consumption, or energy consumed in cooling of apparatus in the network. Therefore, a UE is considered for resource allocation only if the cost of transmission is less than the reported bid. We refer the per RB cost of transmission to a UE incurred by IAB-node as reserve price.

We focus on devising an auction-based dynamic spectrum allocation mechanism in the above settings. Based on the bids and demand reported by IAB-node, Tier 1 entity (IAB-donor) auctions off the resources to Tier 2, then Tier 2 entities (IAB-nodes) distribute acquired resources across Tier 3 entities (UEs) associated with it. Thus, resource allocation in the system is performed at two levels Tier 1 and Tier 2. The entities at any level can only acquire from (allocate to) resources to its immediate higher (lower) level in the hierarchical arrangement.

By $\pi = (\pi_1, \pi_2)$, we denote the resource allocation mechanism, where π_1 and π_2 are sub-mechanisms implemented in Tier 1 and Tier 2 levels, respectively. We assume that

UEs at Tier 3 are non-cooperative, rational, and selfish. Since IAB-nodes are network entities, hence cooperate with the IAB-donors in achieving the goal of resource allocation. For notational clarity, vectors are in bold lower case (e.g. \mathbf{x}); and scalars are in non-bold lower case (e.g. x).

Remarks: Although we have considered only one IAB-node between the IAB-donor and UEs in the system model, however IAB framework supports multiple hop wireless backhauling using IAB-nodes between IAB-donor and UEs [78]. Thus, an IAB network may have multiple Tier hierarchical (tree like) structure similar to the one illustrated in Figure 5.2. The resource allocation approach proposed in this chapter is applicable for generic settings for L hops of hierarchical structure.

5.1.1 Mechanism Design Framework

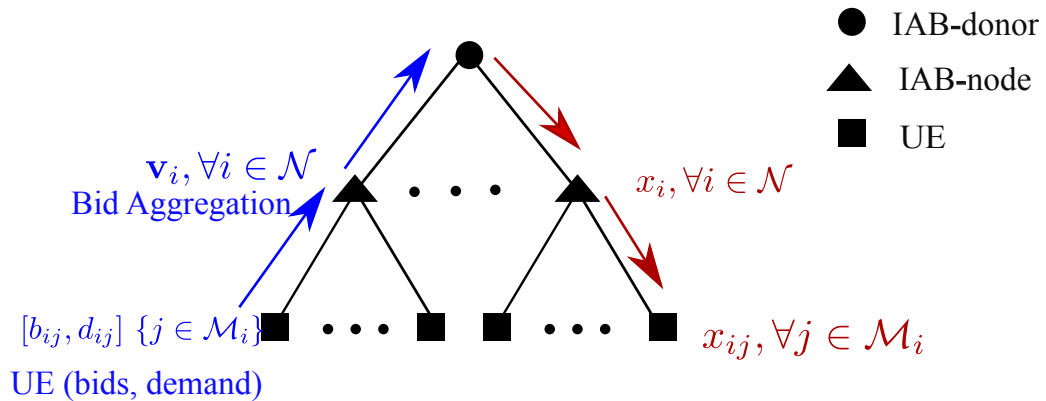


Figure 5.3: Illustration of mechanism design framework

We consider that C is the total number of Resource Blocks (RBs) available at IAB-donor. In general, RB is the smallest unit of radio resource that can be allocated to a UE. Let $\mathcal{N} = \{1, \dots, n\}$ denote the set of IAB-nodes associated with the IAB-donor. Each IAB-node provides services to multiple UEs associated with it. By $\mathcal{M}_i = \{1, \dots, m_i\}$, we denote the set of UEs associated with IAB-node i . Note that a UE can be associated with only one IAB-node at any time instance in the network.

Each UE has a data rate requirement. Based on the required data rate and Channel Quality Indicator (CQI), the number of RBs are evaluated by UE as per the 3GPP standard [80]. Each UE has a resource valuation and demand (required number of RBs) based on the service requested. Let v_{ij} and d_{ij} denote per RB true valuation and the

number of RBs required by UE $j \in \mathcal{M}_i$. Note that true valuation v_{ij} is known in advance to the UE, which is a private information. IAB-nodes, IAB-donor and other UEs in the system do not have any information regarding that. Furthermore, we assume that each UE is selfish and acts rationally. Therefore, if strategically misreporting valuation to the IAB-node has an incentive, UEs may deviate from their true valuation. Let UE $j \in \mathcal{M}_i$ reports bid b_{ij} to IAB-node i , where b_{ij} may or may not be the same as v_{ij} .

Let us denote the allocation vector across the UEs associated with IAB-node i as $\mathbf{x}_i = (x_{i1}, \dots, x_{im_i})$, where $x_{ij} \in \mathbb{Z}_+$ is the number of RBs allocated to UE j associated with IAB-node i . The utility of UE $j \in \mathcal{M}_i$ can be given as:

$$U_{ij}^\pi(x_{ij}) = v_{ij} \cdot \min\{x_{ij}^\pi, d_{ij}\} - p_{ij}^\pi. \quad (5.1)$$

where, p_{ij}^π is the price charged from UE j associated with IAB-node i when RBs are allocated.

As mentioned in Figure 5.3, IAB-nodes act as middlemen between IAB-donor and UEs. Therefore, they do not have any intrinsic valuation for the resource. An IAB-node derives its valuation and demand from the associated UEs. By $d_i = \sum_{j=1}^{m_i} d_{ij}$, we denote the demand at IAB-node i which is aggregate of the demands of the UEs $j \in \mathcal{M}_i$. In addition, IAB-node i reports a vector $\mathbf{v}_i = (v_i(1), \dots, v_i(x_i))$ to IAB-donor, where $v_i(x_i)$ indicates the valuation of IAB-node i when x_i RBs are allocated and $x_i = \{1, \dots, (C+1)\}$. By $\mathbf{x} = (x_1, \dots, x_n)$, we denote allocation vector at Tier 2 entities, where $x_i \in \mathbb{Z}_+$ is the number of RBs acquired by IAB-node i under Tier 1 sub-mechanism (π_1). Furthermore, each IAB-node $i \in \mathcal{N}$ has a reserve price γ_{ij} per RB for the associated UE $j \in \mathcal{M}_i$ based on the cost incurred while providing the service. Using the above notations, we define the social welfare of the system as follows:

Definition 10. *Social welfare of the resource allocation under mechanism π is defined as the aggregate true valuations of the UEs corresponding to the allocation $\mathbf{x}_i = (x_{ij}, \dots, x_{im_i})$ for every UE $j \in \mathcal{M}_i$ across the IAB-nodes $i \in \mathcal{N}$ in the network.*

$$W^\pi(\mathbf{x}_1, \dots, \mathbf{x}_n) = \sum_{i=1}^n \sum_{j=1}^{m_i} v_{ij} \cdot x_{ij}^\pi. \quad (5.2)$$

The term on R.H.S of Equation (5.2) signifies the sum of the true valuations of the UEs, where v_{ij} is a private information of the UEs in the system.

5.1.2 Problem Statement

The resource allocation aims at designing a mechanism π that solves the Social Welfare Optimization (SWO) problem for a given number of RBs (C) at IAB-donor:

$$\begin{aligned}
 \text{SWO : } & \text{maximize}_{\mathbf{x}} \quad W(\mathbf{x}) \\
 & \text{subject to} \quad \sum_{i \in \mathcal{N}} x_i \leq C, \\
 & \quad \quad \quad \sum_{j=1}^{m_i} x_{ij} \leq x_i, \quad \forall i, \\
 & \quad \quad \quad x_i \in \mathbb{Z}_+, x_{ij} \in \mathbb{Z}_+.
 \end{aligned} \tag{5.3}$$

The first constraint states that the aggregate RBs acquired by all the IAB-nodes cannot exceed the total number of RBs available at the IAB-donor. The second constraint states that the total sum of the RBs across all UEs associated with an IAB-node must be less than or equal to the total number of RBs acquired by IAB-node. Here, x_i indicates the number of RBs allocated to IAB-node i under π_1 . The third constraint ensures that the allocation is non-negative at all stages.

As mentioned in Equation (5.3), the goal is to maximize social welfare, which is the sum of true valuations of the UEs. The challenges that arise while solving the above problem are as follows: (i) true valuation is the private information of the UEs, which is not known at the IAB-donors, (ii) lack of direct interaction between IAB-donor and UEs due to the hierarchical structure of the network.

5.2 Hierarchical Allocation Preliminaries

In this section, we present some definitions and preliminaries of the hierarchical resource allocation mechanisms for IAB networks discussed in Section 5.1. First, we define the valuation at the middlemen (IAB-nodes) in the network, which do not have intrinsic valuation. Hence, derive their resource valuation and demand from the associated UEs immediate below in hierarchical structure. The valuation of IAB-nodes are derived as given below:

Definition 11. *The derived-valuation $v_i(x_i) \in \mathbb{R}_+$ at IAB-node $i \in \mathcal{N}$ is the obtained social welfare for the acquired resources under mechanism π_1 , when UEs associated with*

IAB-node i report true valuations. Derived-valuation is given as

$$v_i(x_i) = \max\left\{\sum_{j \in \mathcal{M}_i} v_{ij} \cdot x_{ij} : x_{ij} \leq d_{ij}, \sum_{j \in \mathcal{M}_i} x_{ij} = \min\{x_i, d_i\}\right\}. \quad (5.4)$$

where, $\sum_{j \in \mathcal{M}_i} v_{ij} \cdot x_{ij}$ is the maximum social welfare obtained from UEs $j \in \mathcal{M}_i$ associated with i . $\sum_{j \in \mathcal{M}_i} x_{ij} = \min\{x_i, d_i\}$ indicates that aggregate of the RBs allocated is minimum of aggregate demand $d_i = \sum_{j \in \mathcal{M}_i} d_{ij}$ or RBs available (x_i) at IAB-node i .

The valuation is the maximum amount that a player is willing to pay for the allocated resources in auctions. Next, we define strategy-proof for a single-stage auction and then extend the concept of strategy-proofness in hierarchical settings.

Definition 12. An auction is said to be strategy-proof if the dominant strategy of any player is to reveal true valuation of the object. This implies that there is no incentive or utility gain for a player in deviating from its true valuation, irrespective of other players' strategy, i.e.,

$$U_i(v_i, \mathbf{b}_{-i}) \geq U_i(b_i, \mathbf{b}_{-i}), \quad \forall (b_i, \mathbf{b}_{-i}). \quad (5.5)$$

where, v_i , b_i and $U_i(\cdot)$ are true valuation, bid and utility of player i , respectively. $\mathbf{b}_{-i} = (b_1, \dots, b_{i-1}, b_{i+1}, \dots, b_n)$ represents the bid vector of all players except i .

Definition 13. In hierarchical settings, any mechanism $\pi = (\pi_1, \pi_2)$ is strategy-proof if and only if π_1 , and π_2 enforce strategy-proofness at their level. Moreover, π is strategy-proof if it induces a hierarchical dominant strategy at the IAB-nodes and the UEs such that there is no incentive to deviate from true valuation.

In general, a strategy-proof mechanism is one of the most desirable characteristic in auction-based mechanism as it enforces the players to reveal their true valuations, which is a private information. In other words, if a mechanism is strategy-proof then the dominant strategy of any player is to reveal its true valuation.

5.3 Proposed Mechanism

In this section, we propose a computationally efficient strategy-proof mechanism $\pi = (\pi_1, \pi_2)$ for the hierarchical settings in IAB-enabled HetNet. Each sub-mechanism π_1 and π_2 comprises a resource allocation strategy and pricing scheme. However, the final price to be charged from a UE may be determined by IAB-donor and IAB-nodes simultaneously.

5.3.1 Tier 2 Auction Mechanism (π_2)

The objective of resource allocation is to maximize the social welfare. However, the bids reported by UEs may or may not be the same as true value. We consider that UEs generate elastic traffic and willing to accept any number of RBs in the range of their demand. Since IAB-node is responsible for resource allocation across the associated UEs, IAB-node solves the following optimization problem:

$$\begin{aligned}
 & \max_{x_{i1}, \dots, x_{im_i}} && \sum_{j=1}^{m_i} b_{ij} \cdot x_{ij} \\
 & \text{subject to} && \sum_{j=1}^{m_i} x_{ij} \leq x_i, \\
 & && x_{ij} \leq d_{ij}, \\
 & && x_{ij} \in \mathbb{Z}_+.
 \end{aligned} \tag{5.6}$$

Note that IAB-nodes do not have access to v_{ij} . In Equation (5.6), IAB-node maximizes the aggregate sum of bids reported by UEs subject to the constraint on the number of resources (x_i) assigned by IAB-donor.

We propose sub-mechanism (π_2) in Algorithm 7 which determines the optimal allocation across the set of UEs $j \in \mathcal{M}_i$ based on the reported bids. Note that IAB-nodes distribute the RBs orthogonally across the UEs.

First, arrange the UEs in decreasing order of bids in list L . The resources are allocated across the UEs in greedy fashion, that is the highest bidding UE in L will be allocated the RBs first, then second and so on until all the RBs available at an IAB-node are exhausted. Each UE is charged $p_{ij}^r = \gamma_{ij}$ per RB. Next, we define optimal allocation in Definition 14.

Definition 14. An allocation $\mathbf{x}_i = (x_{i1}, \dots, x_{ij})$ is said to be optimal if it maximizes the aggregate sum of the bids reported by UEs for a given number of RBs x_i , i.e., $\max\{\sum_{j=1}^{m_i} b_{ij} \cdot x_{ij} : x_{ij} \leq d_{ij}, \sum_{j \in \mathcal{M}_i} x_{ij} \leq x_i\}$.

Lemma 10. Algorithm 7 performs optimal allocation.

Proof. The optimality of the allocation can be proved as follows. The algorithm performs the resource allocation greedily based on their bids. Therefore, first UE is selected as

$$\ell = \arg \max_{j \in \mathcal{M}_i} \{b_{ij}\}.$$

Algorithm 7 Sub-mechanism π_2 at IAB-node i

Input: $\mathcal{M}_i, [b_{ij} d_{ij}]$, RBs x_i

Output: allocation x_{ij} , price $p_{ij}^r \forall j \in \mathcal{M}_i$

- 1: Initialize $x_{ij} = 0, \forall j \in \mathcal{M}_i$
- 2: Permute b_{ij} in decreasing order in array L
- 3: Set $\ell \leftarrow 1$
- 4: **while** ($C_i > 0$) **do**
- 5: **if** ($C_i \geq d_{i\ell}$) **then**
- 6: $x_{i\ell} \leftarrow d_{i\ell}$
- 7: **else**
- 8: $x_{i\ell} \leftarrow C_i$
- 9: **end if**
- 10: $C_i \leftarrow C_i - x_{i\ell}$
- 11: $L \leftarrow L \setminus \{L(\ell)\}$
- 12: **end while**
- 13: $p_{ij}^r = \gamma_{ij} \cdot \min\{x_{ij}, d_{ij}\}$

Thus, if we have to select only one UE from \mathcal{M}_i , then optimal allocation is to allocate resources to UE ℓ with the highest bid. Now, update the set of remaining UEs $\mathcal{M}'_i = \mathcal{M}_i \setminus \{\ell\}$. Again determining a single UE with the optimal allocation in \mathcal{M}'_i is the same as in \mathcal{M}_i . Thus, the iterative allocation provides optimal allocation at every reduced set. This leads to the optimal allocation of RBs across the UEs associated with IAB-node i . □

Lemma 11. *If UE j is allocated RBs at bid b_{ij} , then it will also be allocated RBs at $\tilde{b}_{ij} > b_{ij}$, provided bid of other UEs ($\{b_{i\ell} : \ell \neq j, \ell \in \mathcal{M}_i\}$) does not change.*

Proof. As stated in Algorithm 7, RBs are allocated greedily across UEs based on per RB bid b_{ij} for every $j \in \mathcal{M}_i$. Suppose UEs are sorted in decreasing order of their bids in an array, wherein UE j lies at k^{th} position. Assuming UE j increases per RB bid to \tilde{b}_{ij} , while the bids of other UEs ($b_{i\ell} : \ell \neq j$) remain unchanged. Subsequently, UE j shifts at \tilde{k}^{th} position in the sorted array such that $\tilde{k} \leq k$. This implies that if UE is allocated RBs being at k^{th} position in the sorted array, then it is also allocated resource at \tilde{k}^{th} position

after increasing per RB bid. This proves the required. In auction framework, this is called monotonicity property. \square

5.3.2 Tier 1 Auction Mechanism (π_1)

As an IAB-donor can only communicate with the associated IAB-nodes, IAB-donor tries to maximize the valuation reported by the IAB-nodes.

$$\begin{aligned}
 & \max_{\mathbf{x}} \quad \sum_{i \in \mathcal{N}} v_i(x_i) \\
 & \text{subject to} \quad \sum_{i \in \mathcal{N}} x_i \leq C, \\
 & \quad \quad \quad x_i \leq d_i, \\
 & \quad \quad \quad x_i \in \mathbb{Z}_+.
 \end{aligned} \tag{5.7}$$

The first two constraints state the feasibility criteria of resource allocation across IAB-nodes associated with IAB-donor. The third constraint ensures that the allocation to be a non-negative integer value.

The sub-mechanism π_1 distributes the resources across the associated IAB-nodes. Since IAB-nodes are network entities associated with the IAB-donor, IAB-nodes report true valuation (social welfare obtained from UEs) to the IAB-donor. IAB-node i reports a vector \mathbf{v}_i , where $v_i(x_i)$ denotes the social welfare obtained when x_i resources are allocated to IAB-node i . The procedure to compute valuation at IAB-node is given in Algorithm 8.

Based on the valuation at IAB-node i , we propose a sub-mechanism at IAB-donor in Algorithm 9. π_1 computes Γ_i , $\forall i \in \mathcal{N}$ for each RB. Γ_i is aggregate value (social welfare) if the next RB is given to IAB-node i .

$$\Gamma_i(\mathbf{x}) = \sum_{j \neq i} v_j(x_j) + v_i(x_i + 1). \tag{5.8}$$

In each iteration, IAB-node corresponding to the highest Γ_i is allocated a RB. The process is repeated until all RBs are allocated.

Algorithm 8 Valuation at IAB node i

Input: $[b_{ij} \ d_{ij}] \ \forall j \in \mathcal{M}_i$
Output: $v_i(x_i), x_i = \{1, \dots, \min\{\sum_{i=1}^{m_i} d_{ij}, (C + 1)\}\}$

- 1: Initialize $V_i \leftarrow Null$
- 2: **while** ($\mathcal{M}_i \neq Null$) **do**
- 3: $k^* \leftarrow \arg \max_{j \in \mathcal{M}_i} b_{ij}$
- 4: **while** ($d_{ik^*} \geq 1$) **do**
- 5: $V_i = [V_i \ b_{ik^*}]$
- 6: $d_{ik^*} \leftarrow d_{ik^*} - 1$
- 7: **end while**
- 8: $\mathcal{M}_i \leftarrow \mathcal{M}_i \setminus \{k^*\}$
- 9: **end while**
- 10: $v(x_i) = \sum_{\ell=1}^{x_i} V_i(\ell)$

5.3.3 Pricing Scheme for π

The price charged by UEs is given as

$$p_{ij}^\pi = \max\{\gamma_{ij}, p\} \cdot \min\{x_{ij}^\pi, d_{ij}\}. \quad (5.9)$$

where, γ_{ij} is the UE specific reserve price (cost of transmission) set by IAB-node and p is the minimum price per RB to be charged by a UE, if allocated resource. By p , we denote the price set by IAB-donor for each UE which is allocated resources obtained using Algorithm 9. Intuitively, p is the highest bid among the UEs which are not allocated resources.

Lemma 12. *The resource allocation mechanism $\pi = (\pi_1, \pi_2)$ is individually rational.*

Proof. We are required to show that the price charged by UE is less than or equal to $b_{ij} \cdot \min\{d_{ij}, x_{ij}^\pi\}$. UE j is either charged γ_{ij} or p per RB using Equation (5.9). UE j is served by IAB-node i only if $\gamma_{ij} \leq b_{ij}$. Thus, $p_{ij} \leq b_{ij} \cdot \min\{d_{ij}, x_{ij}^\pi\}$. As mechanism π_1 allocates resources greedily based on the valuation reported by IAB-nodes, $\{p \leq b_{ij}, \forall j \in \mathcal{M}_i, i \in \mathcal{N} : x_{ij}^\pi \neq 0\}$. Thus, mechanism π proves to be individually rational. \square

Theorem 4. *The proposed mechanism $\pi = (\pi_1, \pi_2)$ is strategy-proof.*

Algorithm 9 Sub-mechanism π_1 at IAB-donor

Input: \mathcal{N} , $v_i(d_i)$ for $d_i = \min\{C + 1, \sum_{j=1}^{m_i} d_{ij}\}$, RBs C

Output: allocation \tilde{x}_i , $\forall i \in \mathcal{N}$

- 1: Initialize $x_i = 0$, $v_i(0) = 0 \quad \forall i \in \mathcal{N}$, $R \leftarrow C + 1$
- 2: **while** ($R > 0$) **do**
- 3: Set $i^* \leftarrow \arg \max_{i \in \mathcal{N}} \Gamma_i$ (Using Equation 5.8)
- 4: Set $x_{i^*} \leftarrow x_{i^*} + 1$
- 5: **if** ($R = 2$) **then**
- 6: $j^* \leftarrow i^*$
- 7: $\tilde{x}_i \leftarrow x_i$ for every $i \in \mathcal{N}$
- 8: **end if**
- 9: Update $R \leftarrow R - 1$
- 10: **end while**
- 11: $p \leftarrow \Gamma_{i^*}(\mathbf{x}) - \Gamma_{j^*}(\mathbf{x})$

Proof. We are required to show that a UE has no incentive to deviate from its true value. In other words, utility gain is independent of its bid. The utility of UE j is given as

$$\begin{aligned} U_{ij}^\pi &= b_{ij} \cdot \min\{x_{ij}^\pi, d_{ij}\} - p_{ij}^\pi, \\ &= (b_{ij} - \max\{\gamma_{ij}, p\}) \cdot \min\{x_{ij}^\pi, d_{ij}\}. \end{aligned}$$

Case 1: $p = \max\{\gamma_{ij}, p\}$

$$U_{ij} = (b_{ij} - p) \cdot \min\{x_{ij}^\pi, d_{ij}\} \quad (5.10)$$

In Equation (5.10), p is independent of the bids of UEs allocated resource. Thus, to maximize the utility UE must report its true value, i.e., $b_{ij} = v_{ij}$.

Case 2: $\gamma_{ij} = \max\{\gamma_{ij}, p\}$

Again, γ_{ij} is independent of the bid of UE j and computed by the IAB-node based on the cost of transmission (such as power, channel conditions).

From the above described cases, it is seen that the pricing scheme is independent of the bids of the UEs allocated resource(s). Hence, UEs have no incentive to deviate from their true valuation. \square

5.4 Simulation Results

In this section, we compare the performance of the proposed mechanism with that of the optimal resource allocation mechanism. The optimal mechanism achieves the maximum social welfare. In the simulation settings, we consider an IAB network comprising one IAB-donor and multiple IAB-nodes. We evaluate the performance by varying the number of IAB-nodes associated with the IAB-donor. We assume that UEs are uniformly distributed in the region. UEs are served via any one of the IAB-nodes in the system. We consider that 50 units of RBs are available at the IAB-donor. In 3GPP LTE standard [80], 10 MHz channel bandwidth corresponds to 50 RBs. Each UE associated with an IAB-node generates traffic based on the type of service required resulting in a demand for certain RBs. Furthermore, we consider that UEs have elastic traffic. Therefore, UEs accept any number of RBs within their demand. Each UE reports valuation per unit RB requirement uniformly distributed in the interval [5, 20].

Each IAB-node has a reserve price of 5 units per RB. Therefore, UEs only with per unit RB valuation greater than or equal to 5 are considered. The simulation results have been averaged over 100 iterations. MATLAB [75] is used to perform the simulations.

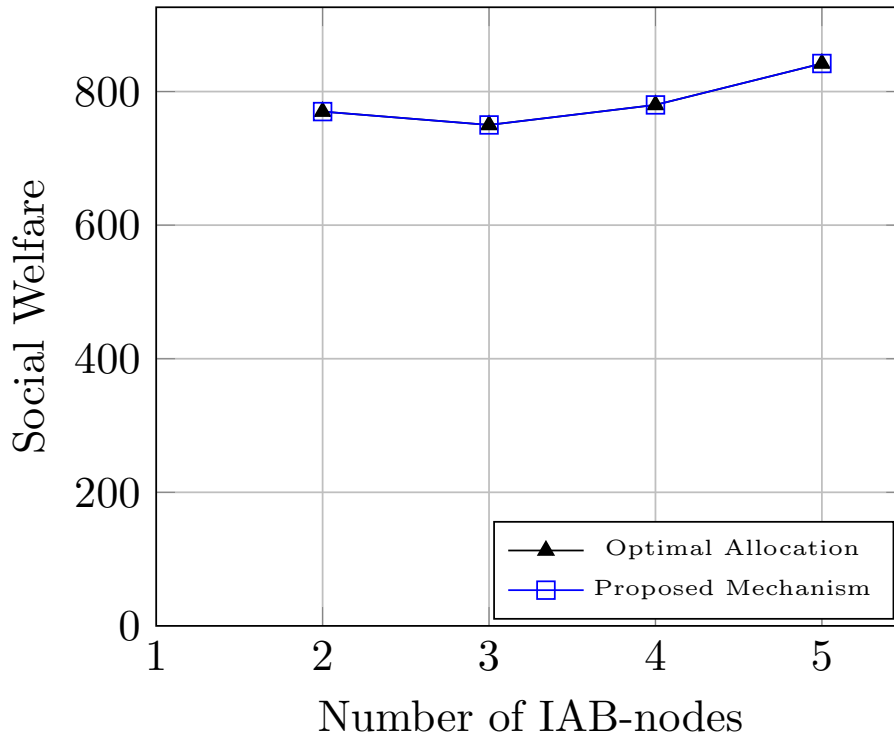


Figure 5.4: Performance comparison of social welfare vs. number of IAB-nodes

We compare the performance based on the social welfare obtained using the proposed mechanism with that of the optimal social welfare for the reported bids and demand. From Fig. 5.4, we observe that the social welfare obtained from the proposed mechanism is same as the optimal solution. The optimal solution is obtained by considering that IAB-nodes are not present in the network. Therefore, resource allocation in such scenario reduces to a single-stage resource allocation problem. Furthermore, we also observe that the increase in the number of IAB-nodes in the system does not affect the performance of the mechanism.

5.5 Conclusions

In this chapter, we study the feasibility of IAB networks to mitigate the requirement of connecting each small cell with the CN using fiber, which frequently arises in ultra dense deployment scenarios in cellular networks. Typically, IAB networks allow wireless backhauling to the UEs using IAB-nodes and IAB-donors, where IAB-donors are connected to the CN via fiber and act as the wireless backhaul providers to the associated IAB-nodes. Thus, leading to a hierarchical (or tree) structure across UEs, IAB-nodes, and IAB-donors. The hierarchical arrangement does not allow direct communication between the IAB-donor and the UEs, thus renders the loss of information (actual bid and demand of UEs) at the IAB-donors. Hence, the problem of wireless backhaul allocation across IAB-nodes becomes challenging. Another drawback is that the radio resource valuation and the requirement at the IAB-nodes dependent on the UEs associated with it. Thus, IAB-nodes do not have their own intrinsic valuation of the resources.

We propose an auction-based framework for DSA considering the hierarchical arrangement across IAB-donor, IAB-nodes, and UEs. We devise a computationally efficient strategy-proof spectrum allocation mechanism such that the social welfare of the auction is maximized. The proposed auction-based mechanism for IAB-network comprises resource allocation sub-mechanisms both at IAB-donors and IAB-nodes, since UEs are served via IAB-nodes using the wireless backhaul received from the IAB-donor. Furthermore, using simulations, we observe that the proposed DSA mechanism achieves optimal social welfare despite the challenges stated above. We also prove the individual rationality,

monotonicity, and strategy-proofness of the mechanism.

Chapter 6

Dynamic Spectrum Allocation in Unicast Multicast Convergence in 5G Network

The main focus of Chapters 3, 4 and 5 has been on devising a computationally efficient mechanism for dynamic spectrum allocation in various scenarios, in the existing cellular network. Although, dynamic spectrum allocation plays a vital role in efficient utilization of resources considering the traffic variation in the network, however it does not consider multicasting when the same content is requested by multiple UEs in the system. Multicast/Broadcast transmission enables a group of User Equipments (UEs) access the same multimedia content over shared radio resources and seems a promising solution to further optimize the radio resource utilization. Furthermore, the traditional cellular networks lack a unified framework, which can support the flexible switching between unicast and multicast mode of transmission for UEs in the system, thus further optimizing the required radio resources to serve UEs in the system. Unlike the previous chapters, here we not only focus on the dynamic resource allocation across the network entities but also propose a unified framework for convergence of unicast multicast services in the network.

One of the early attempts in this direction was Multimedia Broadcast and Multicast Services (MBMS), introduced in 3GPP Release 6. The enhancements in FeMBMS, such as support for dedicated eMBMS carriers (cells), MBMS offload, and larger inter-site distances are likely to play an important role in the future evolution of multicasting/broad-

casting services in 5G and beyond networks [81], [82]. FeMBMS defines three types of cells in wireless networks, i.e., dedicated eMBMS cells (carrier providing only Multicast/Broadcast service), unicast only cells, and mixed-mode cells. In “MBMS Offload”, also called “MBMS operation on Demand” (MOOD) [83], content being delivered as unicast service to UE may be converted into a broadcast/multicast¹ service in order to conserve network resources when the demand for the content increases.

In addition to MBMS features, Dual Connectivity is one of the key features introduced in the standards. Dual Connectivity allows a UE to concurrently connect to two Base Stations (BSs) to receive the services. These BSs may belong to the same Radio Access Technology (RAT) or two different RATs, such as LTE and 5G.

FeMBMS enhancements, along with dual connectivity offer an opportunity for improved resource utilization in networks by dynamically switching data flows from one transmission mode to another. The transmission mode switching may be done based on different factors, e.g., demand for specific content, radio condition experienced by UEs across multicast and unicast carriers (cell), load on different network nodes, etc. For example, in a dense heterogeneous network (HetNet) environment with both unicast and multicast cells, a UE may experience dis-similar radio conditions in different cells. This radio link diversity along with the dual-connectivity capability can be utilized to dynamically arrive at an appropriate transmission mode for individual UEs, enabling improved radio resource utilization in the network. However, the existing 3GPP architecture does not provide any framework to utilize the FeMBMS features together with dual connectivity to improve the network performance.

Figure 6.1 illustrates a high-level MOOD architecture in the 3GPP network. The MOOD architecture enables improved radio resource utilization in the network by sharing radio-resources (via multicast transmission) when the demand for specific content increases. In case multiple UEs concurrently ask for the same content, the Broadcast Multicast Service Center (BM-SC) triggers the flow transition from unicast to multicast mode. Thus, a UE may receive content via eNB/gNB either through Packet Data Network Gateway (PDN-GW) in unicast mode or over Multicast Broadcast Multimedia Service Gateway (MBMS-GW) in multicast mode.

¹ We use broadcast and multicast interchangeably throughout the chapter.

While the MOOD [83] architecture in the 3GPP standards allows for switching between unicast and multicast services, it may solely be based on the demand for specific content. It does not provide any mechanism to utilize factors, such as UE specific radio link quality across different multicast and unicast cells or the load on different network nodes, on eNB/gNB for improved resource utilization and network performance. This becomes all the more limiting when the radio nodes responsible for unicast and multicast transmissions may be separate and the dual connectivity feature is available.

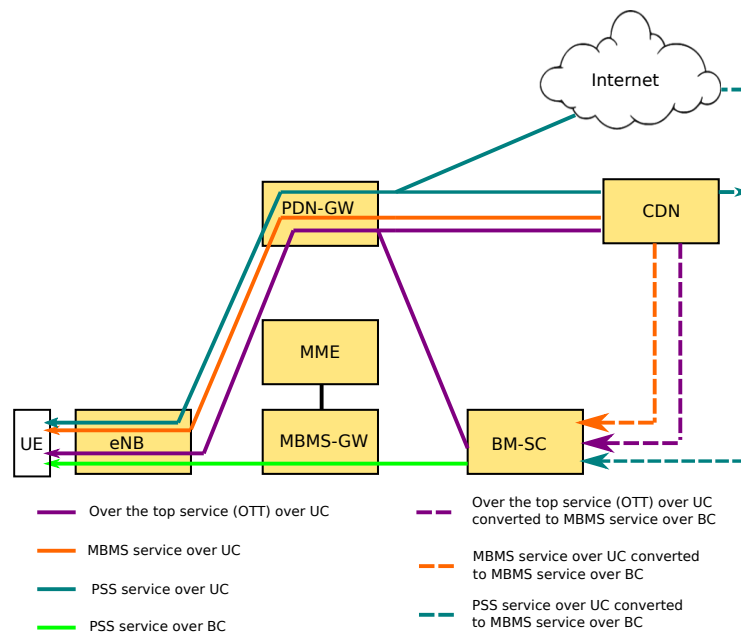


Figure 6.1: Illustration of existing 3GPP architecture for MBMS services (courtesy 3GPP).

This chapter proposes a simple and novel framework to integrate unicast and multicast transmissions in mobile networks and achieve the objectives mentioned above. We have developed a Software Defined Networking (SDN) based architecture for unified management of unicast and multicast services in 4G, 5G & beyond mobile networks. The architecture enables integration of dual connectivity with MBMS services and provides a mechanism to utilize dual connectivity for improved resource utilization and network performance. We also propose resource allocation algorithms aligned with the proposed architecture. While this chapter focuses on the optimal utilization of radio resources, the proposed architectural framework is very generic and can enhance other performance

parameters through the convergence of unicast and multicast transmission. For example, the framework enables switching from unicast to multicast transmission to reduce the load on unicast BSs (eNB/gNB) if they are overloaded. As another example, switching can be done based on the load on the core network elements/functions, such as User Plane Function (UPF) or PDN-GW. However, these scenarios will be explored in future work.

The rest of the chapter is organized as follows: In Section 6.1, we present the proposed SDN based unicast-multicast convergence architecture along with the protocol details. The detailed system model is presented in Section 6.2. In Sections 6.3 and 6.4, we propose network assisted dynamic radio resource allocation schemes across unicast and MBMS cells. Simulations results are discussed in Section 6.5. We conclude the chapter in Section 6.6.

6.1 Proposed System Architecture

In this section, we propose a converged network architecture for the delivery of unicast and multicast services in a cellular mobile network. It is an SDN based architecture enabling efficient utilization of resources in a mobile network by flexibly using unicast or multicast transmission for individual UEs to deliver multimedia content. Even though the focus of this work is on the efficient usage of radio resources, the proposed framework can be used for improved utilization of other network resources as well. Another key strength of the architecture is that, though it has been proposed in the context of FeMBMS, it enables integration of any unicast service delivery framework with any multicast service delivery framework.

The fundamental concept behind SDN is the separation of control and forwarding (data) planes through a standardized protocol interface [84]. SDN provides the flexibility to dynamically handle the resource requirements (e.g. radio resources) in network as per real-time usage patterns and enables efficient utilization of resources in network.

In alignment with the SDN paradigm, various network entities in the proposed architecture can be classified in 2 different planes, i.e., forwarding plane and control plane, as illustrated in Figure 6.2. In standard SDN architecture, an additional application plane is also present. However, for the sake of simplicity, the application plane has been omitted

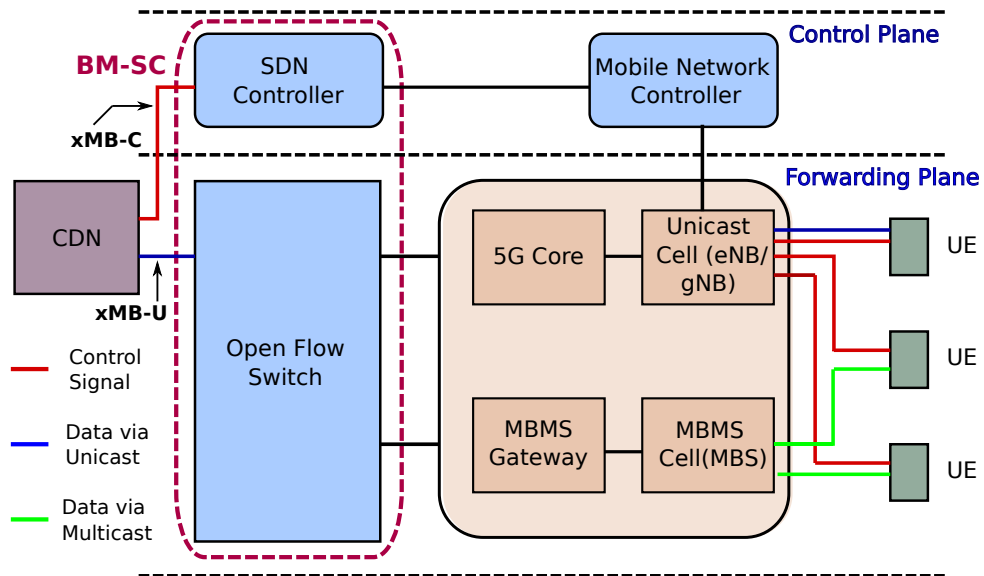


Figure 6.2: SDN based converged mobile network architecture for 5G and beyond.

from the discussion in this work.

4G/5G network elements, i.e., Unicast Core, Multicast Core (MBMS Gateway, etc.), eNB/gNB (unicast cell), and Multicast Base Station (MBS) (managing dedicated MBMS Cell) constitute the forwarding plane in the proposed architecture. An MBS may also be an eNB/gNB capable of MBMS (multicast/broadcast) transmission. Here, Content Delivery Network (CDN) is primarily a part of the data plane though it has a control plane interface “xMB-C” with the BM-SC Control plane (SDN Controller) similar to FeMBMS. These entities are part of the existing 3GPP 4G/5G and MBMS architecture. Additionally, we propose a new network element in the data plane, the OpenFlow switch. The OpenFlow switch is connected to the mobile core (both multicast and unicast core) on one side and the CDN on the other side. It is also responsible for receiving data from the CDN and forwarding it (data) to the mobile core. Furthermore, OpenFlow switch forwards the unicast flows to the unicast core (UPF) for delivery to the UEs via eNB/gNB (unicast transmission) and the multicast core (MBMS Gateway) for delivery to the UEs via a dedicated MBMS cell (multicast transmission).

Though desirable, due to the advantages of potential implementation simplicity with a separate scheduler and hardware platform, a physically separate dedicated MBMS cell is not a necessity in the proposed framework. It can also be seen as a logically separate dedicated MBMS cell wherein the resources on a physical cell can be divided into separate

unicast and multicast resources. Keeping a logically separate MBMS cell (MBS) enables a simple framework for integration of dual connectivity with MBMS services where a user can simultaneously be connected to a unicast and a multicast BS. It also facilitates a flexible convergence of unicast and multicast services, enabling the integration of any multicast technology with any unicast technology.

In the SDN paradigm, the control plane resides above the data plane and has a global view of the network resources. As part of the proposed architecture, we define new network elements in the control plane. For improved scalability and modularity, the control plane contains two separate entities, namely SDN Controller and Mobile Network Controller (MNC). The SDN Controller is responsible for setting up data paths through the underlying OpenFlow switches for individual data flows.

The MNC collects the radio channel quality reports (both for the multicast as well as the unicast cells) from UEs and decide on the policy and further communicates to the SDN controller for transmission (multicast vs. unicast) for each UE. This is done with an aim to achieve efficient radio resource utilization. Moreover, the MNC allocates radio resources for multicast transmission (at dedicated MBMS Cell/MBS). Upon receiving the policy for transmission for individual UEs (unicast or multicast) from the MNC, the SDN Controller establishes the data paths through the underlying switches accordingly, i.e., for UEs expected to receive transmission in the unicast mode, unicast flows are established and for UEs expected to receive transmission in the multicast mode, multicast flows are setup. OpenFlow is proposed to be used as the protocol between the SDN Controller and the underlying switches.

Dual Connectivity allows a UE to receive data from two BSs concurrently. Here, we propose the usage of dual connectivity by UEs to receive data either through an MBS or an eNB/gNB providing unicast service. As shown in Figure 6.2, a UE is always connected to a (unicast) eNB/gNB for control communication. It can also receive data from that eNB/gNB when required. At the same time, UE can also receive data over a multicast channel through an MBS. UE uses its dedicated unicast connectivity to provide relevant information, e.g. the link quality of the available multicast channels in its vicinity or the link quality of its unicast channel. The information provided by the UE may be used by the control plane functions to direct the data to the UE either through the unicast

channel or the multicast channel.

BM-SC is a network entity in the existing 3GPP MBMS architecture, responsible for receiving content from the CDN and delivering them to MBMS UEs via the multicast core [83]. The SDN Controller along with the underlying OpenFlow switches, can be used to support the BM-SC functionality and replace the BM-SC node in the existing network. The proposed architecture simplifies BM-SC node design and enables enhanced forwarding capabilities in BM-SC, allowing dynamic switching of flows across unicast and multicast modes for individual UEs and flexibly delivering them either through the unicast core or the multicast core in order to utilize the radio resources efficiently.

The proposed BM-SC architecture (with a clear separation between the control plane and the data plane functionality) is also better aligned with the 3GPP FeMBMS standard, with the xMB-C (control plane interface between BM-SC and CDN) terminating at the SDN Controller, i.e., at the BM-SC control plane entity and xMB-U (data plane interface between BM-SC and CDN) terminating at the OpenFlow switches, the proposed data plane of BM-SC.

6.1.1 Call Flow Description

Here, we provide details on the working procedure of the proposed architecture. The procedure for a new UE arrival is illustrated in the call flow in Figure 6.3. At first, the UE establishes a unicast connection with eNB/gNB and sends measurement reports, e.g., Channel Quality Indicator (CQI), as measured by it both for the multicast and the unicast channels. CQI is used by a UE to send the information of how good or bad the channel quality is to the network via eNB/gNB. In LTE networks, CQI value ranges between 0 and 15. Higher CQI value corresponds to better channel quality. A set of SNR values are mapped to a certain CQI value in the above mentioned range. In the context of this work, we assume that the measurement report is sent for the best dedicated MBMS cell as perceived by the UE. The measurement report is also sent for the unicast cell; the UE is connected to. eNB/gNB forwards the UE measurement reports to the MNC and then MNC provides the UE related information (UE ID and its IP address, collected from the mobile core network) to the SDN Controller. As indicated below, the shared information is used later when the UE starts downloading the desired content.

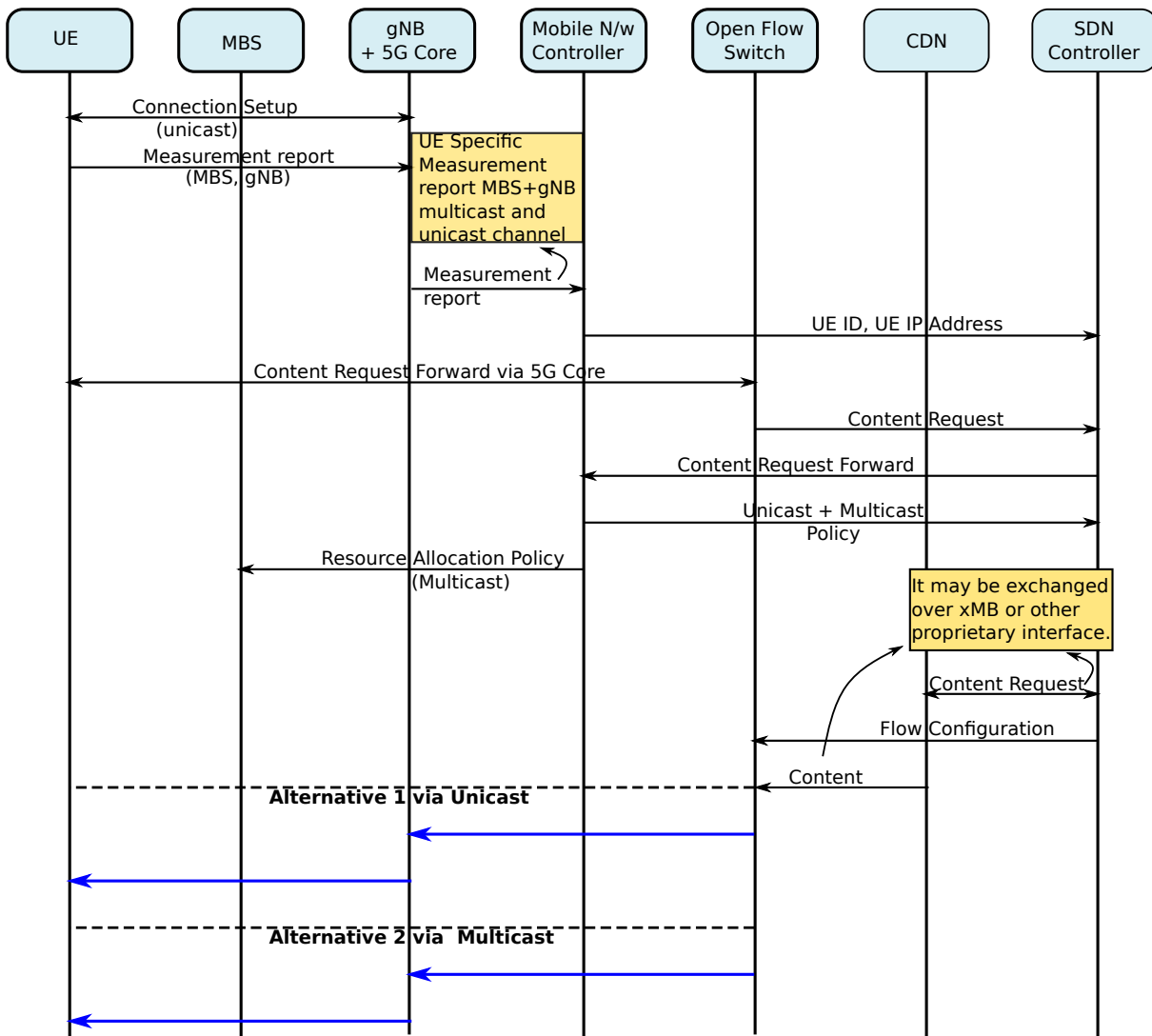


Figure 6.3: Call flow for resource allocation on UE arrival in the network.

Next, the UE sends the request for the desired content to the CDN on its unicast connection. The request first reaches the OpenFlow switch through the unicast core (UPF). Since it is a request from a new UE, the OpenFlow switch forwards it to the SDN Controller to take appropriate action for setting up the data flow on the switch. Upon receiving the content request from a new UE, the SDN Controller forwards the content request to the MNC. The MNC decides the mode of transmission (unicast or multicast) for content delivery to the UE using the channel measurement reports, earlier shared by the UE. The selected transmission mode is conveyed to the SDN Controller. As will become clear in Section IV below, a new UE arrival may also trigger transmission mode switching for existing UEs, receiving the same content. This may be required for the

efficient utilization of radio resources. Hence, MNC provides the updated transmission mode information for existing UEs also to the SDN Controller.

As indicated earlier, the MNC decides which UEs will receive data over multicast mode and which ones over unicast mode based on the channel quality information. Hence, the resource allocation policy (along with the channel quality information for the multicast UEs) is provided to the MBS by the MNC. Based on the policy (essentially the channel quality information and the data rate), the required resources for the multicast transmission are computed by the MBS.

SDN Controller and CDN exchange the content request related information over the 3GPP xMB interface. The SDN Controller is responsible for configuring the flow rules on the OpenFlow switches so that the data received from the CDN can be delivered to UEs either via the unicast core or the multicast core. On receiving the updated transmission mode information from the MNC for individual UEs, the SDN Controller may need to (re)configure the flow rules on the underlying switches for UEs. The flow rules are configured such that for each unicast flow, the switch performs content replication with the individual UE Internet Protocol (IP) address as the destination address and forwards the replicated content to the unicast core to be finally delivered to the UE. For multicast UEs, the switch forwards a single copy of the content with a multicast IP address as the destination via the MBMS Gateway and the MBMS cell.

The messages are shown in the call flow in Figure 6.3 are part of the new protocol defined to support communication between the various network elements of the proposed architecture.

6.2 System Model

We consider a scenario where UEs are interested in multimedia content (typically live streaming type). While the proposed architecture is applicable to both 5G NR and 4G LTE, we consider LTE cells in the system model. The system model considers a dedicated MBMS cell in a region providing multicast service to the UEs inside its coverage area. In addition, one or more LTE cells supporting unicast transmission are also present in that region, overlapping with the coverage area of the multicast cell, as illustrated in Figure

6.4. We assume multicast cells would have a larger coverage area than that of a unicast cells. This is also aligned with the larger inter-site distance for MBMS cells, as proposed under FeMBMS [81].

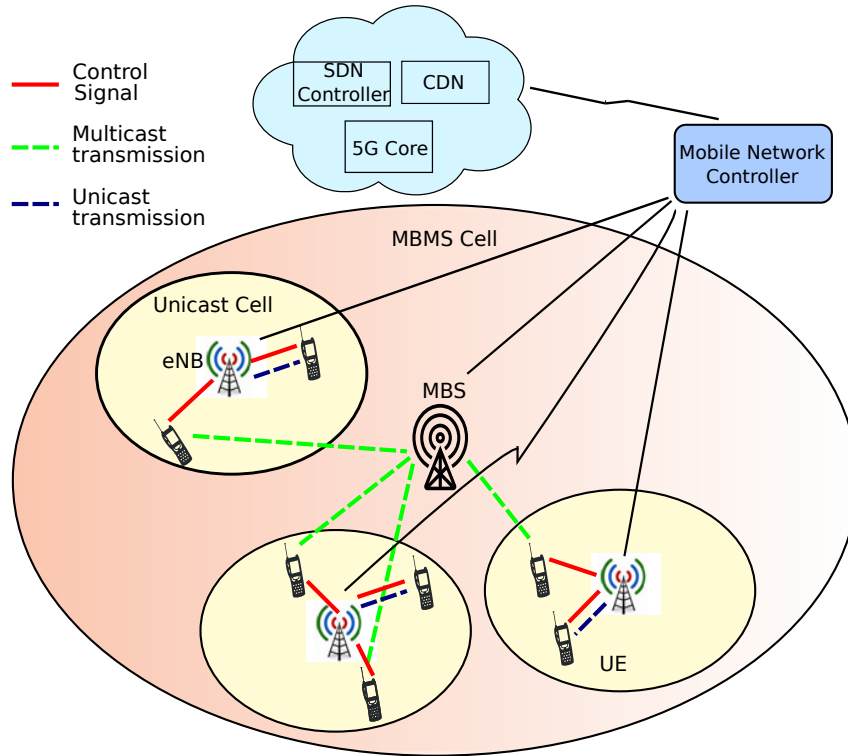


Figure 6.4: System Model.

We assume that each UE is connected to a unicast cell in its vicinity called the anchor cell here. The unicast cell with the best signal strength for a UE is the anchor cell and the eNB controlling the anchor cell is the anchor eNB for that UE. A UE can receive its desired streaming content either via unicast transmission from its anchor cell or via multicast transmission from an MBMS cell. UE also uses the anchor cell for the exchange of control information with the network.

Each UE is capable of dual-connectivity, i.e., it is connected to the anchor cell and at the same time, it can receive data from the MBMS cell, if needed. Further, we assume that a UE requests only one streaming content at a time. This can be generalized to a UE accessing multiple streams simultaneously where individual content streams require orthogonal radio resources for delivery.

The system model considers dynamic UE arrival, which follows a Poisson process. We also assume that UEs are not mobile and hence their channel conditions do not vary.

Although a single dedicated MBMS cell supporting multicast service and multiple LTE cells supporting unicast transmission have been considered in the system model, it can be generalized to include multiple dedicated MBMS cells if we assume that out of all the MBMS cells in the vicinity, UE is served by the one providing the best signal strength. Each UE can be treated as a single point in the considered geographical region, which (the point) can be mapped to one of the MBMS cells (the one with the best signal strength at that point).

We consider that each UE ℓ has a minimum rate requirement R_ℓ to guarantee the required Quality of Service (QoS). When a new UE arrives in the network, it associates itself with an anchor eNB” and reports the Channel Quality Indicator (CQI) as observed by it, both for the best MBMS cell and the anchor (unicast) cell” to the anchor eNB”. The channel reports are forwarded by the eNB to the MNC. Based on the collected CQI reports and the required data rate, MNC computes the number of Resource Blocks (RBs) (W_ℓ^u, W_ℓ^m) needed to serve the UE both via unicast and multicast transmissions as per the 3GPP standards [80].

Depending on the objective function, MNC decides the transmission mode (unicast or multicast) for the new UE and directs the SDN Controller to set up the data flow accordingly. In certain scenarios, MNC may also need to change the transmission modes of some existing UEs and hence it also needs to direct the SDN Controller to modify the data flows for such UEs. Once it decides the transmission modes for individual UEs, the MNC also guides the unicast and the MBMS cells in radio resource allocation, taking into account the CQI values and the rate requirements of individual UEs. After receiving the direction from the MNC, the SDN Controller sets up/modifies the unicast and multicast data flows over the OpenFlow switches, which are finally delivered to the UEs either via the unicast or the MBMS cells.

UE ID ℓ	W_ℓ^u	W_ℓ^m
--------------	------------	------------

Figure 6.5: Illustration of UE structure.

When a new UE arrives in the system, 3 attributes are assigned to the UE: a unique UE ID $\ell \in \mathbb{Z}_+$, W_ℓ^m and W_ℓ^u as shown in Figure 6.5.

In Table I, we present the notations and their significance, which have been used

throughout the chapter.

Notations	Significance
\mathcal{N}	Set of UEs in the system
\mathcal{U}	Set of UEs served via unicast transmission
\mathcal{M}	Set of UEs served via multicast transmission
W_ℓ^u	RBs required to serve UE ℓ via unicast transmission
W_ℓ^m	RBs required to serve UE ℓ via multicast transmission
L	Sorted list of all UEs in the ascending order of W_ℓ^m
$L[\mu]$	UE stored at index μ in list L
$W_{L[\mu]}^u$	RBs required to serve UE at index μ in L via unicast transmission
$W_{L[\mu]}^m$	RBs required to serve UE at index μ in L via multicast transmission
W^u	Total number of RBs required to serve all UEs in set \mathcal{U}
W^m	Total number of RBs required to serve all UEs in set \mathcal{M}
W^s	Total number of RBs required to serve all UEs i.e., $\ell \in \mathcal{U} \cup \mathcal{M}$
R_ℓ	Minimum rate requirement of UE ℓ
W^a	Additional RBs required to include UE ℓ in multicast set
R_ℓ^u	Rate UE ℓ receives via unicast transmission
R_ℓ^m	Rate UE ℓ receives via multicast transmission

Table 6.1: Notations and their significance

When UE $i \in \mathcal{U}$ is served content via unicast transmission, a dedicated set of RBs are allocated to the UE. Thus, the required RBs to serve all UEs in set \mathcal{U} denoted by W^u is the aggregate sum of the RBs required by each UE in \mathcal{U} . Formally, W^u can be defined as follows:

$$W^u = \sum_{\ell \in \mathcal{U}} W_\ell^u. \quad (6.1)$$

Let W^m denote the RBs required for multicast transmission in the system. Unlike UEs in unicast transmission, a common set of RBs are used to serve the UEs in \mathcal{M} for multicast transmission. Therefore, RBs required for multicast transmission in the system is equal to the maximum number of the RBs required by UEs in the set \mathcal{M} . Thus, W^m

is obtained as

$$W^m = \max_{\ell \in \mathcal{M}} W_\ell^m. \quad (6.2)$$

From Equations (6.1) and (6.2), the overall RBs required in the system W^s to serve all the UEs i.e., $\mathcal{U} \cup \mathcal{M}$ can be obtained as follows:

$$W^s = W^u + W^m. \quad (6.3)$$

6.2.1 Problem Formulation

All UEs associated with a specific MBMS cell and receiving a particular multimedia content simultaneously constitute a set (or a group). Along with the MBMS cell, each UE is also associated with a unicast cell (anchor cell). As mentioned earlier, we consider the problem of efficient delivery of content to a set of UEs either through unicast or multicast delivery modes wherein any one of the two modes may be utilized for a particular UE.

The system aims to allocate all UEs in \mathcal{N} to the unicast (\mathcal{U}) and the multicast (\mathcal{M}) sets so that W^s required to serve UEs in \mathcal{N} is minimized provided the individual rate requirement of each UE is satisfied.

$$\begin{aligned} \mathbb{A} : \quad & \min_{\chi} \quad W^s = W^u + W^m \\ & \text{s.t.} \quad \chi_\ell^u + \chi_\ell^m = 1, \quad \forall \ell \in \mathcal{N}, \\ & \quad \quad R_\ell^u \cdot \chi_\ell^u + R_\ell^m \cdot \chi_\ell^m \geq R_\ell, \quad \forall \ell \in \mathcal{N}. \end{aligned} \quad (6.4)$$

The objective is to determine the optimal allocation χ that minimizes the total number of RBs (or resources) required to serve all UEs in the system. The first constraint states that a UE can be served either via unicast or multicast. When a new UE arrives in the system, 3 attributes are assigned to the UE: a unique UE ID $\ell \in \mathbb{Z}_+$, W_ℓ^m and W_ℓ^u as shown above in UE Structure.transmission mode. Here, $\chi_\ell^u \in \{0, 1\}$ denotes UE ℓ is served via unicast cell if $\chi_\ell^u = 1$ otherwise not. Similarly, $\chi_\ell^m \in \{0, 1\}$ denotes UE ℓ is served via MBMS cell if $\chi_\ell^m = 1$. The last constraint reflects that the individual rate requirement of each UE is satisfied.

6.3 Resource Allocation Algorithm

In this section, we propose a resource allocation mechanism for problem \mathbb{A} mentioned in Equation (6.4). As mentioned earlier, we consider the dynamic arrival and departure of UEs in the system.

6.3.1 User (UE) Arrival

Algorithm 10 is designed to achieve the objective in problem \mathbb{A} upon arrival of a new UE in the system. To achieve the optimal radio resource allocation, the algorithm may (re)distribute existing UEs (\mathcal{N}) and the new arrival (UE ID ℓ'), in two disjoint sets, a set of unicast UEs ($\tilde{\mathcal{U}}$) and a set of multicast UEs ($\tilde{\mathcal{M}}$). Algorithm 10 uses a sorted list L of all existing UEs for processing, where UEs are sorted based on their W_ℓ^m values. Upon arrival, the new UE (with ID ℓ') is inserted in list L at the appropriate position (based on $W_{\ell'}^m$). Let μ' be the index of UE ℓ' in list L . Note that UE ID and UE index in list L are independent values in \mathbb{Z}_+ . If $W^m \geq W_{\ell'}^m$ (or $W_{L[\mu']}^m$), i.e., the RBs allocated to existing set \mathcal{M} are greater than that of the RBs required for multicast transmission by new UE. Thus, the UE allocation that achieves optimal RB utilization is $\tilde{\mathcal{U}} \leftarrow \mathcal{U}$ and $\tilde{\mathcal{M}} \leftarrow \mathcal{M} \cup \{\ell'\}$ (or $\tilde{\mathcal{M}} \leftarrow \mathcal{M} \cup \{L[\mu']\}$) (line 6). By $L[\mu']$, we denote the UE stored at index μ' in list L . Therefore, \tilde{W}^s remains unchanged even after the inclusion of new UE ℓ' in the system.

However, if $W^m < W_{L[\mu']}^m$, optimal allocation may require re-assignment of UEs in the unicast \mathcal{U} and the multicast \mathcal{M} sets. First, include new UE $L[\mu']$ (or ℓ') to unicast set \mathcal{U} . Then, set index ν to $|\mathcal{M}| + 1$ in L (which indicates that the set of UEs served via multicast transmission appear before the set of UEs served via unicast transmission mode in list L . This has been discussed in detail in Lemma 1). Next, we check the condition in line 11 iteratively till the last entry in L . If the condition is true then serve UEs via multicast transmission instead of unicast transmission.

We illustrate Algorithm 10 using an example: Consider 6 UEs in the system $\mathcal{N} = \{1, \dots, 6\}$, where $\ell \in \mathcal{N}$ is unique ID assigned to each UE on arrival. As described in Algorithm 10, UEs are sorted in list L in increasing order of W_ℓ^m shown in Table II. As is apparent, the optimal allocation of UEs (in \mathcal{N}) is $\mathcal{U} = \{3, 6, 4\}$, $\mathcal{M} = \{2, 1, 5\}$ with

$W^m = 5$ and $W^u = 5$.

Table II : List L of UEs

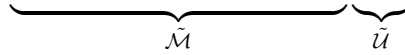
UE Index in $L[\mu]$	1	2	3	4	5	6
UE ID (ℓ)	2	1	5	3	6	4
$W_{L[\mu]}^m$	3	4	5	7	10	14
$W_{L[\mu]}^u$	2	2	2	1	3	1

When a new UE with ID 7 arrives, let the RBs required to serve the new UE via multicast and unicast transmission be 8 and 3, respectively. Next, new UE is inserted in list L (based on the value of W_{ℓ}^m) at index $\mu' = 5$, as shown in Table III. Since $W_{L[5]}^m > W^m$, the UE with ID 7 cannot be served via multicast transmission (i.e., by the MBMS cell) without increasing the required RBs at the MBMS cell. Therefore, it is not added to set \mathcal{M} and instead added to set \mathcal{U} (lines 5 – 8) initially. This leads to an initial value of $W^m = 5$, $W^u = 5 + 3 = 8$ and $W^s = 13$ RBs. However, this may not be the optimal allocation of radio resources, as we will observe shortly. In order to achieve the optimal utilization of resources in the system, the new arrival may require the shifting of the new UE from the set \mathcal{U} to \mathcal{M} along with some existing UEs. This is the key insight into the algorithm. The decision of shifting of UEs is performed using the for loop at line 10 and hence list L is traversed from index $\lambda = \mu'$ till the end.

In iteration 1, the condition (at line 11) happens to be true (i.e., $8 - 5 \leq (1 + 3)$) which implies that RBs required to serve UEs (at $L[4]$ and $L[5]$) can be reduced further if served via MBMS cell. Hence, $L[4]$ and $L[5]$ (i.e., UEs with IDs 3 and 7) are shifted to \mathcal{M} . Now, update W^m , ν and λ to 8, 6, and 6, respectively. Next in iteration 2, condition $W_{L[6]}^m - W^m \leq W_{L[6]}^u$ i.e., $10 - 8 \leq 3$, satisfies. Therefore, $L[6]$ (or UE 6) is also shifted to \mathcal{M} , and $W^m = 10$ and $\nu = 7$ are updated. In last iteration, condition $14 - 10 \leq 1$ false and hence $L[7]$ (or UE 4) continues to remain in set \mathcal{U} , to be served via unicast cell as before the arrival of UE 7. Thus, we get optimal allocation ($\tilde{\mathcal{U}} = \{4\}$, $\tilde{\mathcal{M}} = \{2, 1, 5, 3, 6, 7\}$) on arrival of UE 7 with $W^m = 10$, $W^u = 1$ and $W^s = 11$ (shown in Table III).

TABLE III: Updated list L with new UE

UE Index in $L[\mu]$	1	2	3	4	5	6	7
UE ID (ℓ)	2	1	5	3	7	6	4
$W_{L[\mu]}^m$	3	4	5	7	8	10	14
$W_{L[\mu]}^u$	2	2	2	1	3	3	1



We observe from Tables II and III, that the UE with maximum RB requirement in multicast set (\mathcal{M}) is always less than that of the UE with the minimum RB requirement in unicast set (\mathcal{U}). We give the formal proof of the same in Lemma 13.

Lemma 13. *Suppose allocation $(\mathcal{U}, \mathcal{M})$ is the optimal solution to problem \mathbb{A} , then $\max_{\ell \in \mathcal{M}} W_{\ell}^m < \min_{\ell \in \mathcal{U}} W_{\ell}^m$.*

Proof. Let us consider that UE $\ell^* \in \mathcal{M}$ requires maximum number of RBs for multicast transmission. This implies that $W^m = W_{\ell^*}^m$ using Equation (6.2). Let us assume that there exists a UE $\ell' \in \mathcal{U}$ such that $W_{\ell'}^m \leq W^m$.

As $W_{\ell'}^m \leq W^m$, therefore if we shift UE ℓ from \mathcal{U} to \mathcal{M} the RBs required for unicast transmission in the system W^u are reduced by $W_{\ell'}^u$, with no change in W^m . Thus, the RBs required to serve UEs in the system W^s can be reduced further when UE ℓ' is served via multicast transmission. However, $(\mathcal{U}, \mathcal{M})$ is optimal solution such that $\mathcal{U} \cup \mathcal{M} = \mathcal{N}$, hence W^s cannot be reduced further. This leads to contradiction. Therefore, UE ℓ' cannot have $W_{\ell'}^m \leq W^m$, if the allocation is optimal. Thus, $\max_{\ell \in \mathcal{M}} W_{\ell}^m < \min_{\ell \in \mathcal{U}} W_{\ell}^m$, always hold. \square

Lemma 14. *Suppose the overall system level resource requirement W^s is optimal for UEs $\ell \in \mathcal{U} \cup \mathcal{M}$. Let \tilde{W}^s be the optimal number of RBs after arrival of a new UE ℓ' in the system, i.e., for UEs $\ell \in \mathcal{U} \cup \mathcal{M} \cup \{\ell'\}$. Then, $\tilde{W}^s \geq W^s$.*

Proof. There can be two cases on arrival of a new UE ℓ' in the system: (i) UE ℓ' is served via unicast, or (ii) UE ℓ' is served via multicast.

Case (i): When new UE ℓ' is served via unicast transmission, W^u increases to $\tilde{W}^u =$

Algorithm 10 UE arrival in the network

```

1: Input: New UE ID  $\ell'$ ,  $\mathcal{U}$ ,  $\mathcal{M}$ , List  $L$ 
   Precondition: Disjoint sets  $\mathcal{U}$  and  $\mathcal{M}$  provide optimal RB utilization s.t.  $\mathcal{N} = \mathcal{U} \cup \mathcal{M}$ 
2: Output: Optimal allocation  $\tilde{\mathcal{U}}$ ,  $\tilde{\mathcal{M}}$  with new UE  $\ell'$ 
3: Insert new UE  $\ell'$  in sorted list  $L$ 
4:  $\mu' =$  position of UE  $\ell'$  in  $L$ 
5: if  $W^m \geq W_{L[\mu']}^m$  then
6:    $\tilde{\mathcal{U}} \leftarrow \mathcal{U}$  and  $\tilde{\mathcal{M}} \leftarrow \mathcal{M} \cup \{L[\mu']\}$ 
7: else
8:   Update  $\mathcal{U} \leftarrow \mathcal{U} \cup \{L[\mu']\}$ 
9:    $\nu = |\mathcal{M}| + 1$ 
10:  for  $\lambda = \mu', \dots, \text{length}[L]$  do
11:    if  $W_{L[\lambda]}^m - W^m \leq \sum_{\mu=\nu}^{\lambda} W_{L[\mu]}^u$  then
12:       $\mathcal{U} \leftarrow \mathcal{U} \setminus \{L[\nu], \dots, L[\lambda]\}$ ,
13:       $\mathcal{M} \leftarrow \mathcal{M} \cup \{L[\nu], \dots, L[\lambda]\}$ 
14:       $W^m \leftarrow W_{L[\lambda]}^m$ 
15:       $\nu \leftarrow \lambda + 1$ 
16:    end if
17:  end for
18:   $\tilde{\mathcal{U}} \leftarrow \mathcal{U}$ ,  $\tilde{\mathcal{M}} \leftarrow \mathcal{M}$ 
19:  Update  $W^u$ ,  $W^s$ 
20: end if

```

$W^u + W_{\ell'}^u$. However, W^m does not change, i.e., $\tilde{W}^m = W^m$. Thus, if new UE is delivered content via unicast, system level RB requirement \tilde{W}^s is always greater than the previous system level RB requirement W^s , i.e., $\tilde{W}^s > W^s$.

Case (ii): When new UE ℓ' is served via multicast, then there are two possibilities based on $W_{\ell'}^m$: (a) $W_{\ell'}^m \leq W^m$, then $\tilde{W}^m = W^m$. Therefore, $\tilde{W}^s = W^s$.

(b) $W_{\ell'}^m > W^m$, then W^m must increase at least to $\tilde{W}^m = W_{\ell'}^m$ to include UE ℓ' in multicast set. Let us define the additional RBs required in MBMS cell as $\tilde{W}^a = W_{\ell'}^m - W^m$. With the increase of RBs in MBMS cell from W^m to \tilde{W}^m , all UEs in \mathcal{U} with $W_{\ell}^m \leq \tilde{W}^m$ also shift to multicast transmission mode using Lemma 13. Let set \mathcal{Z} contains all UEs (with

$W_{\ell'}^m \leq W_{\ell'}^m$) which shift to multicast from unicast transmission. Therefore, $\tilde{\mathcal{U}} = \mathcal{U} \setminus \mathcal{Z}$ and $\tilde{\mathcal{M}} = \mathcal{M} \cup \mathcal{Z} \cup \{\ell'\}$, where $\tilde{\mathcal{U}}$ and $\tilde{\mathcal{M}}$ constitute an optimal allocation after arrival of UE ℓ' in the system.

Let $W_{\ell^*}^m = \max_{\ell \in \mathcal{Z}} W_{\ell}^m$. Without UE ℓ' in the system, $(\mathcal{U}, \mathcal{M})$ being the optimal allocation, UEs $j \in \mathcal{Z} \subset \mathcal{U}$ satisfy Equation (6.5).

$$W^a = W_{\ell^*}^m - W^m > \sum_{\ell \in \mathcal{Z}} W_{\ell}^u. \quad (6.5)$$

Here, W^a is the additional RBs required to shift all UEs in \mathcal{Z} from unicast to multicast. Equation (6.5) reflects the fact that shifting UEs from \mathcal{U} to \mathcal{M} will result in higher RB requirement if the allocation is optimal. As $W_{\ell'}^m \geq W_{\ell^*}^m$, therefore $\tilde{W}^a \geq W^a$ (using definitions of \tilde{W}^a and W^a). To serve UEs in $(\mathcal{U} \cup \mathcal{M})$, the RBs required W^s are given as follows:

$$W^s = W^m + W^u = W^m + \sum_{\ell \in \{\mathcal{U} \setminus \mathcal{Z}\}} W_{\ell}^u + \sum_{\ell \in \mathcal{Z}} W_{\ell}^u. \quad (6.6)$$

The overall (unicast + multicast) system level RBs \tilde{W}^s for UEs in $(\mathcal{U} \cup \mathcal{M} \cup \ell)$ are given as

$$\tilde{W}^s = \tilde{W}^m + \tilde{W}^u = W^m + \tilde{W}^a + \sum_{\ell \in \{\mathcal{U} \setminus \mathcal{Z}\}} W_{\ell}^u. \quad (6.7)$$

From Equations (6.6) and (6.7), we obtain $\tilde{W}^s > W^s$ as $\tilde{W}^a > \sum_{\ell \in \mathcal{Z}} W_{\ell}^u$ (using Equation (6.5)). □

Theorem 5. *Algorithm 10 provides optimal solution on UE arrival in the network.*

Proof. Let $(\mathcal{U}, \mathcal{M})$ be the optimal solution, when UE ℓ' is not in the system. The RBs required to serve UEs in sets \mathcal{U} and \mathcal{M} are W^u and W^m , respectively. Thus, the total RBs required in the system are $W^s = W^u + W^m$. The required proof can be split into two cases: Case (i) new UE ℓ' has $W_{\ell'}^m \leq W^m$ and Case (ii) new UE ℓ' has $W_{\ell'}^m > W^m$.

Case (i): From Lemma 14, on arrival of a new UE, the best possibility is that the total RBs required in the system remains unchanged, i.e., $\tilde{W}^s = W^s$, where \tilde{W}^s is the total RBs required in the system on inclusion of new UE ℓ' . As we know that $W^m \geq W_{\ell'}^m$, therefore when UE ℓ' is served via multicast transmission, the total RBs required in the system does not change. Thus, the optimal allocation inclusive of UE ℓ' becomes $\tilde{\mathcal{U}} = \mathcal{U}$ and $\tilde{\mathcal{M}} = \mathcal{M} \cup \{\ell'\}$ with $\tilde{W}^s = W^s$. We can see that Algorithm 10 achieves the same

allocation, as shown by lines 6 and 7.

Case (ii): If UE ℓ' has $W_{\ell'}^m > W^m$, this implies $\tilde{W}^s > W^s$ (using Lemma 14). Let $(\tilde{\mathcal{U}}, \tilde{\mathcal{M}})$ obtained from Algorithm 10 is not optimal. Then there are two possibilities to achieve the optimal allocation.

- Shift UEs from $\tilde{\mathcal{M}}$ to $\tilde{\mathcal{U}}$ to get the optimal allocation: Suppose set of UE in $\mathcal{Z} \subset \tilde{\mathcal{M}}$ are shifted from $\tilde{\mathcal{M}}$ to $\tilde{\mathcal{U}}$. Let $\mathcal{T} = \{L[\tilde{\mu}], \dots, L[\hat{\mu}]\}$, where $\tilde{\mu}, \dots, \hat{\mu}$ are UE indices in L corresponding to UEs in \mathcal{Z} , sorted in increasing order of $W_{L[\mu]}^m$. Suppose $W_{L[\hat{\mu}]}^m = \tilde{W}^m$. Note that if \mathcal{T} does not include UE $L[\hat{\mu}]$, then shifting UEs from multicast to unicast mode does not change W^m , however, W^u would increase. Thus, W^s increases further. Therefore, $L[\hat{\mu}]$ must be included in \mathcal{T} to decrease the RBs required to serve UEs. Let \hat{W}^u and \hat{W}^m are RBs required to serve UEs in $\hat{\mathcal{U}}$ and $\hat{\mathcal{M}}$, respectively obtained after UEs shift. Then $W_{L[\hat{\mu}]}^m - \hat{W}^m > \sum_{j=\tilde{\mu}}^{\hat{\mu}} W_{L[\mu]}^u$ to decrease overall required RBs. However, $W_{L[\hat{\mu}]}^m - \hat{W}^m > \sum_{\mu=\tilde{\mu}}^{\hat{\mu}} W_{L[\mu]}^u$ can never be true as per UE shifting strategy mentioned in line 11 of Algorithm 10. This leads to contradiction. Hence, $\tilde{\mathcal{U}}$ and $\tilde{\mathcal{M}}$ constitute the optimal allocation.

- Shift UEs from $\tilde{\mathcal{U}}$ to $\tilde{\mathcal{M}}$ to achieve optimal allocation: Proof is similar to the previous scenario. Suppose set of UEs $\mathcal{Z} \subset \tilde{\mathcal{U}}$ are shifted from $\tilde{\mathcal{U}}$ to $\tilde{\mathcal{M}}$. After shifting of the UEs, let the allocation becomes $(\hat{\mathcal{U}}, \hat{\mathcal{M}})$. Suppose set $\mathcal{T} = \{L[\mu'], \dots, L[\mu'']\}$ contains UEs sorted in increasing order of $W_{L[\mu]}^m$, for all $L[\mu] \in \mathcal{T}$. The UEs shifted from $\tilde{\mathcal{U}}$ to $\tilde{\mathcal{M}}$ must satisfy $\hat{W}^m - \tilde{W}^m \leq \sum_{\mu=\mu'}^{\mu''} W_{L[\mu]}^u$. However, Algorithm 10 traverses list L till the end to ensure that if shifting of UEs result in reduced RB requirement then UEs are already shifted to achieve $\tilde{\mathcal{U}}$ and $\tilde{\mathcal{M}}$. Thus, $\hat{W}^m - \tilde{W}^m \leq \sum_{\mu=\mu'}^{\mu''} W_{L[\mu]}^u$ condition never holds, hence $(\tilde{\mathcal{U}}, \tilde{\mathcal{M}})$ remains optimal allocation. \square

6.3.2 User (UE) Departure

As the main focus of the system is optimal utilization of the RBs, we are also required to consider the effect of UE departures from the system. Algorithm 11 presents the (re)allocation of UEs across unicast and multicast sets, when a UE departs from the system resulting in optimal RB utilization to the unicast and the MBMS cells.

The first step is to remove the departing UE ℓ' from the list L (UE ℓ' stored at index μ' in list L) mentioned in lines 3 and 4 of the Algorithm. If UE $\ell' \in \mathcal{U}$ leaves the

Algorithm 11 UE departure from the network

- 1: **Input:** \mathcal{U} , \mathcal{M} , UE ℓ' , List L
 - Precondition:* Disjoint sets \mathcal{U} and \mathcal{M} provide optimal RB utilization s.t. $\mathcal{N} = \mathcal{U} \cup \mathcal{M}$
 - 2: **Output:** Optimal allocation $\tilde{\mathcal{U}}$, $\tilde{\mathcal{M}}$ without UE ℓ'
 - 3: $\mu' \leftarrow \text{index}(\ell', L)$
 - 4: Update $L \leftarrow L \setminus \{L[\mu']\}$
 - 5: **if** $\ell' \in \mathcal{U}$ **then**
 - 6: $\tilde{\mathcal{U}} \leftarrow \mathcal{U} \setminus \{L[\mu']\}$ and $\tilde{\mathcal{M}} \leftarrow \mathcal{M}$
 - 7: **else**
 - 8: $\mathcal{M} \leftarrow \mathcal{M} \setminus \{L[\mu']\}$
 - 9: Set $\ell^* \leftarrow \arg \max_{\ell \in \mathcal{M}} W_{\ell}^m$
 - 10: Set $\mu^* \leftarrow \text{index}(\ell^*, L)$, $W^m = W_{L[\mu^*]}^m$
 - 11: **for** $\mu = (\mu^* - 1), \dots, 1$ **do**
 - 12: **if** $W^m - W_{L[\mu]}^m > \sum_{\mu=\mu+1}^{\mu^*} W_{L[\mu]}^u$ **then**
 - 13: $\mathcal{U} \leftarrow \mathcal{U} \cup \{L[\mu + 1], \dots, L[\mu^*]\}$,
 - $\mathcal{M} \leftarrow \mathcal{M} \setminus \{L[\mu + 1], \dots, L[\mu^*]\}$
 - 14: Update $W^m = W_{L[\mu]}^m$
 - 15: $\mu^* \leftarrow \mu$
 - 16: **end if**
 - 17: $\mu \leftarrow \mu - 1$
 - 18: **end for**
 - 19: $\tilde{\mathcal{U}} \leftarrow \mathcal{U}$ and $\tilde{\mathcal{M}} \leftarrow \mathcal{M}$
 - 20: **end if**
-

system (i.e., $W_{\ell'}^m > W^m$), optimal allocation is obtained by removing the UE ℓ' from \mathcal{U} i.e., $\tilde{\mathcal{U}} = \mathcal{U} \setminus \{L[\mu']\}$, while $\tilde{\mathcal{M}} = \mathcal{M}$ remains unchanged (line 6).

If UE $\ell' \in \mathcal{M}$ leaves the system then update multicast set \mathcal{M} by removing UE ℓ' . Then, set index μ^* to UE in list L with maximum RB requirement in \mathcal{M} and hence $W^m = W_{L[\mu^*]}^m$. Next, the difference between the required RBs in multicast transmission for the last UE (UE with maximum RB requirement) in \mathcal{M} (UE index μ^*) and the second last UE (UE index $\mu^* - 1$) in \mathcal{M} is calculated, i.e., $W_{L[\mu^*]}^m$ (or W^m) $- W_{L[\mu^*-1]}^m$. Intuitively, algorithm evaluates whether UE shifting is required or not for optimal utilization of RBs. The calculated difference is compared with the required unicast radio resource of $L[\mu^*]$. If the difference is less than or equal to $W_{L[\mu^*]}^u$, i.e., the unicast resource requirements of the last UE in \mathcal{M} is more than $W^m - W_{L[\mu^*-1]}^m$, no change in \mathcal{U} and \mathcal{M} are required and the existing \mathcal{U} and \mathcal{M} sets remain optimal from the perspective of resource requirement. But if $W^m - W_{L[\mu^*-1]}^m$ is greater than $W_{L[\mu^*]}^u$ then optimal allocation is obtained by moving UE μ^* from \mathcal{M} to \mathcal{U} . This process is repeated in reverse order for all UEs in \mathcal{M} by decreasing the loop index μ iteratively (line 11).

In order to illustrate the departure algorithm, let us take the reverse case of UE with ID 7 departing from the example given earlier. As shown in Table III, the following distribution of UEs across the two sets, $\mathcal{U} = \{4\}$ and $\mathcal{M} = \{2, 1, 5, 3, 7, 6\}$ achieves optimal allocation of RBs in the system. Now, when UE with ID 7 departs from \mathcal{M} (and the system), the distribution of the remaining UEs with IDs $\{1, \dots, 6\}$ across \mathcal{U} and \mathcal{M} changes again and it goes back to the allocation given in Table II, i.e., the one before the arrival of UE 7 in the system. Thus, we get $\mathcal{U} = \{3, 6, 4\}$ and $\tilde{\mathcal{M}} = \{2, 1, 5\}$, which means that after the departure of the UE with ID 7, some UEs from set \mathcal{M} are moved to set \mathcal{U} to achieve the optimal allocation of resources (RBs) in the system. Now, we prove the optimality of Algorithm 11.

Theorem 6. *Algorithm 11 provides optimal solution on UE departure from the network.*

Proof. To prove $(\tilde{\mathcal{U}}, \tilde{\mathcal{M}})$ is optimal allocation after UE departure, we consider two scenarios as mentioned in Algorithm 11:

Scenario 1: UE $\ell' \in \mathcal{U}$ leaves the network

When unicast UE ℓ' leaves the network then the allocation obtained from Algorithm 11 is $\tilde{\mathcal{U}} = \mathcal{U} \setminus \{L[\mu']\}$ (or $\tilde{\mathcal{U}} = \mathcal{U} \setminus \{\ell'\}$) and $\tilde{\mathcal{M}} = \mathcal{M}$. Hence, the RBs required to serve UEs

in $\tilde{\mathcal{U}}$ reduces to $\tilde{W}^u = W^u - W_{\ell'}^u$. However, the RBs required to serve UEs in $\tilde{\mathcal{M}}$ remains unchanged i.e., $\tilde{W}^m = W^m$. Thus, the total RBs required to serve UEs in $\tilde{\mathcal{U}}$ and $\tilde{\mathcal{M}}$ are

$$\tilde{W}^s = \tilde{W}^u + \tilde{W}^m = W^u - W_{\ell'}^u + W^m.$$

Suppose \tilde{W}^s is not minimum, this implies that the allocation $(\tilde{\mathcal{U}}, \tilde{\mathcal{M}})$ is not optimal. The possible options to obtain the optimal allocation are as follows:

- Shift UEs from $\tilde{\mathcal{U}}$ to $\tilde{\mathcal{M}}$ to achieve the optimal allocation: Suppose a set of UEs $\mathcal{Z} \subset \tilde{\mathcal{U}}$ are shifted from $\tilde{\mathcal{U}}$ to $\tilde{\mathcal{M}}$. Let $\mathcal{T} = \{L[\tilde{\mu}], \dots, L[\hat{\mu}]\}$, where $\tilde{\mu}, \dots, \hat{\mu}$ are indices in L corresponding to set of UEs \mathcal{Z} , arranged in increasing order of $W_{L[\mu]}^m$, $\forall L[\mu] \in \mathcal{T}$. Since, allocation $(\mathcal{U}, \mathcal{M})$ is optimal, therefore $W_{L[\hat{\mu}]}^m - W^m > \sum_{\mu=\tilde{\mu}}^{\hat{\mu}} W_{L[\mu]}^u$. However, to further decrease the RB requirement $W_{L[\hat{\mu}]}^m - W^m \leq \sum_{\mu=\tilde{\mu}}^{\hat{\mu}} W_{L[\mu]}^u$ must satisfy. This is a contradiction. Hence, $(\tilde{\mathcal{U}}, \tilde{\mathcal{M}})$ remains optimal allocation.
- Shift UEs from $\tilde{\mathcal{M}}$ to $\tilde{\mathcal{U}}$ to achieve the optimal allocation: When a set of UEs are shifted, optimality of solution can be proved using contradiction, similar to the case of UE shifting from $\tilde{\mathcal{U}}$ to $\tilde{\mathcal{M}}$.

Scenario 2: UE $\ell' \in \mathcal{M}$ leaves the network

The proof is similar to Case (ii) of UE arrival algorithm. □

6.3.3 Optimal Resource Allocation Algorithm

In this section, we present a dynamic resource allocation algorithm for converged architecture described in Section 6.1. When there is either UE arrival (*a*) or UE departure (*d*) in the system, Algorithm 12 is executed. In Algorithm 12, we propose OPTimal resource allocation in Converged Unicast muLticast networks (OPTICUL). As per the given input, OPTICUL provides an optimal UE allocation to unicast and MBMS cells such that the total RBs required to serve all UEs (in set \mathcal{N}) are minimized.

Corollary 6.1. *The computational complexity of the OPTICUL algorithm is $\mathcal{O}(|\mathcal{U}|)$ in case of the arrival of a new UE and $\mathcal{O}(|\mathcal{M}|)$ in case of the departure of a UE, where $|\cdot|$ denotes the cardinality of a set.*

When a new UE arrives in the system, the OPTICUL algorithm achieves the optimal solution by shifting UEs from set \mathcal{U} to \mathcal{M} . Even if the optimal solution requires shifting

Algorithm 12 Resource Allocation Algorithm

-
- 1: **Input:** $\mathcal{I} = \{a, d\}$
 - 2: **Output:** Optimal UE allocation $\tilde{\mathcal{U}}, \tilde{\mathcal{M}}$ with the given action for UE ℓ' .
 - 3: **if** case = a **then**
 - 4: Go to Algorithm 10
 - 5: **else**
 - 6: Go to Algorithm 11
 - 7: **end if**
-

of all UEs from set \mathcal{U} to \mathcal{M} , the maximum number of operations required is equal to $|\mathcal{U}|$. When a UE departs from the system, the OPTICUL algorithm achieves the optimal solution in $\mathcal{O}(|\mathcal{M}|)$ operations. The optimal solution may require shifting of UEs from set \mathcal{M} to \mathcal{U} , which results in shifting of up to $|\mathcal{M}|$ UEs, i.e., at most $|\mathcal{M}|$ operations is required. Thus, the OPTICUL algorithm determines the optimal solution in polynomial time.

6.4 Resource Allocation : Limited Resource Scenario

In this section, we extend the analysis for the scenario when the resources are limited and therefore all UEs cannot be served. Often, in such scenarios it is desirable to maximize the number of UEs that are served. We denote the set of UEs in the system at any instance by $\mathcal{N} = \{1, \dots, n\}$. Let w RBs are available in the system. Mathematically, the problem can be written as \mathbb{B} given below:

$$\begin{aligned} \mathbb{B} : \max_{\ell} \quad & \sum \mathbb{1}_{\{\ell \in \mathcal{U}\}} + \sum \mathbb{1}_{\{\ell \in \mathcal{M}\}} - \sum \mathbb{1}_{\{\ell \in \mathcal{U} \cap \mathcal{M}\}} \\ \text{s. t.} \quad & W^{\mathcal{U}} + W^{\mathcal{M}} \leq w. \end{aligned} \tag{6.8}$$

In optimization problem \mathbb{B} , the objective is to maximize the set of UEs served with the constraint that the aggregate RBs required to serve UEs does not exceed the limit w . $\mathbb{1}_{\{\ell \in \mathcal{U}\}}$, $\mathbb{1}_{\{\ell \in \mathcal{M}\}}$ and $\mathbb{1}_{\{\ell \in \mathcal{U} \cap \mathcal{M}\}}$ are indicator variables. Indicator variables are defined as

$$\mathbb{1}_{\{i \in \mathcal{T}\}} = \begin{cases} 1, & \text{UE } i \in \mathcal{T} \\ 0, & \text{UE } i \notin \mathcal{T} \end{cases}$$

The constraint states that the aggregate RBs (unicast + multicast) allocated to serve UEs is less than that of w . Note that we consider the scenario when RBs are limited and not sufficient to serve all UEs in the system, i.e., $\mathcal{U} \cup \mathcal{M} \subset \mathcal{N}$.

We define cost \mathbf{c} to denote the RBs required to serve a subset of UEs which may belong to unicast or multicast. The cost of a set is equal to the minimum RBs required to satisfy the QoS requirements of the UEs in the set.

As described in system model, each UE can be served either via unicast (through eNB/gNB) or multicast (through MBS) transmission mode. Based on the CQI reports for eNB/gNB and MBS, RB requirement of each UE is evaluated such that their minimum guaranteed rate requirement is satisfied. In unicast mode of transmission, each UE is allocated a unique set of RBs. Thus, for n UEs in the system, there are n unique sets for unicast transmission where each set comprises exactly one UE from \mathcal{N} . We denote x^{th} unicast set by \mathcal{S}_x^{u} . Let the collection of all unicast UE subsets be $\mathcal{S}^{\text{u}} = \bigcup_{x=1}^n \mathcal{S}_x^{\text{u}}$.

In multicast transmission mode, multiple UEs can be served simultaneously over a common set of RBs. We can construct atmost n unique multicast sets in increasing order of RB requirement of UEs in the system, as the RBs required by UEs in a multicast set is obtained using Equation 6.2. We denote multicast sets by \mathcal{S}_y^{m} , where y is the index of the set. By $\mathcal{S}^{\text{m}} = \bigcup_{y=1}^n \mathcal{S}_y^{\text{m}}$, we denote the collection of all possible multicast UE sets.

Let us consider an example with 4 UEs in the system, i.e., $\mathcal{N} = \{1, 2, 3, 4\}$. For unicast transmission, each UE requires orthogonal set of RBs, therefore we get singleton set corresponding to each UE. $\mathcal{S}_1^{\text{u}} = \{1\}$, $\mathcal{S}_2^{\text{u}} = \{2\}$, $\mathcal{S}_3^{\text{u}} = \{3\}$ and $\mathcal{S}_4^{\text{u}} = \{4\}$. Suppose signal strength from MBS received by UEs is as follows: $\zeta_2 > \zeta_1 > \zeta_4 > \zeta_3$, where ζ_ℓ denotes the signal strength of UE ℓ . Hence, n multicast subsets with increasing radio resource requirement (based on the UE with the worst signal strength in the set) are listed as: $\mathcal{S}_1^{\text{m}} = \{2\}$, $\mathcal{S}_2^{\text{m}} = \{2, 1\}$, $\mathcal{S}_3^{\text{m}} = \{2, 1, 4\}$ and $\mathcal{S}_4^{\text{m}} = \{2, 1, 4, 3\}$. In set \mathcal{S}_3^{m} UEs 1, 2 and 4 share a set of RBs which are equal to the RBs required by UE 4. In other words, a content can be delivered to UEs in set \mathcal{S}_3^{m} simultaneously and the number of RBs required are equal to the RBs required by the UE with worst channel conditions (that is UE 4). We define a set Γ comprising all unicast sets in \mathcal{S}^{u} and multicast sets in \mathcal{S}^{m} , i.e., $\Gamma = \mathcal{S}^{\text{u}} \cup \mathcal{S}^{\text{m}}$. In the above example, $\Gamma = \{\mathcal{S}_1^{\text{u}}, \mathcal{S}_2^{\text{u}}, \mathcal{S}_3^{\text{u}}, \mathcal{S}_4^{\text{u}}, \mathcal{S}_1^{\text{m}}, \mathcal{S}_2^{\text{m}}, \mathcal{S}_3^{\text{m}}, \mathcal{S}_4^{\text{m}}\}$, a family of sets. Note that a UE may be served either via unicast or multicast mode. Consider the

following optimization problem:

$$\begin{aligned}
\mathbb{C} : \quad & \max_{\Gamma_k} \quad \left| \bigcup_{\Gamma_k \in \mathbf{\Gamma}} \Gamma_k \cdot z_k \right| \\
\text{s.t.} \quad & \sum_{k=1}^{|\mathbf{\Gamma}|} \mathbf{c}(\Gamma_k) \cdot z_k \leq w, \\
& z_k \in \{0, 1\}.
\end{aligned} \tag{6.9}$$

Here, $|\mathbf{\Gamma}| = 2|\mathcal{N}|$, where $|\mathcal{N}|$ denotes cardinality of \mathcal{N} . Γ_k denotes the k^{th} set in $\mathbf{\Gamma}$. If $z_k = 1$, UEs in set Γ_k are served. $\mathbf{c}(\Gamma_k)$ denotes the cost (RBs required) to serve UEs in k^{th} set in $\mathbf{\Gamma}$.

The objective of the optimization problem \mathbb{C} is to maximize the cardinality of the union of the sets served (total number of UEs served) with the constraints that the aggregate cost to serve the UE sets is less than or equal to the total RBs available (w) in the system.

6.4.1 Proposed Algorithm

We propose Constrained-OPTimal resource allocation for Converged Unicast and multicast (C-OPTICUL) algorithm presented in Algorithm 13. \mathcal{S}^u , \mathcal{S}^m and w are provided as inputs to the algorithm. First, unicast and multicast sets are sorted by their cost in lists L_u and L_m , respectively. Then, an empty set with cost zero is inserted in L_m at the beginning (say, index 0). Initialize optimal allocation, θ^* to zero. Algorithm traverses each set in L_m starting at 0 (line 7). A multicast set is chosen from L_m and UEs from the selected set are stored in \mathbf{t} and the cost of \mathbf{t} is denoted as $\mathbf{c}(\mathbf{t})$ which is same as the cost of the particular multicast set. Now, each set in L_u is considered one by one and the following conditions are evaluated: (i) sufficient RBs are available to serve the selected unicast UE and (ii) UE in the selected unicast set is not a member of \mathbf{t} . If both conditions are satisfied, the UE from the selected unicast set is inserted in \mathbf{t} and the $\mathbf{c}(\mathbf{t})$ is increased by the cost of the selected unicast set. Next, optimal allocation θ^* is updated if cardinality of \mathbf{t} is greater than θ^* . $|\mathbf{t}|$ signifies the number of UEs served in allocation \mathbf{t} . Note that there can be more than one solution (allocation) with the maximum numbers of UEs served.

Algorithm 13 Allocation in the limited resource scenario

```

1: Input:  $\mathcal{S}^u, \mathcal{S}^m, w$ 
2: Output: Optimal allocation  $\theta^*$ 
3: Sort  $\mathcal{S}_x^u$  based on  $\mathbf{c}$  in list  $L_u$ 
4: Sort  $\mathcal{S}_y^m$  based on  $\mathbf{c}$  in list  $L_m$ 
5: Insert an empty set with cost 0 in  $L_m$  (index it 0)
6: Initialize:  $\theta^* \leftarrow 0$ 
7: for  $k = 0 : L_m(\text{end})$  do
8:      $\mathbf{t} \leftarrow L_m(k)$ 
9:      $\mathbf{c}(\mathbf{t}) \leftarrow \mathbf{c}(L_m(k))$ 
10:    for  $j = 1 : L_u(\text{end})$  do
11:        if  $\mathbf{c}(L_u(j)) \leq w - \mathbf{c}(\mathbf{t})$  then
12:            if  $\mathbf{t} \cap L_u(j) = \phi$  then
13:                 $\mathbf{t} \leftarrow \mathbf{t} \cup L_u(j)$ 
14:                 $\mathbf{c}(\mathbf{t}) \leftarrow \mathbf{c}(\mathbf{t}) + \mathbf{c}(L_u(j))$ 
15:            end if
16:        end if
17:    end for
18:    if  $\theta^* < |\mathbf{t}|$  then
19:         $\theta^* \leftarrow |\mathbf{t}|$ 
20:    end if
21: end for
    
```

Lemma 15. *Optimal solution to optimization problem \mathbb{C} can have atmost one subset from the set \mathcal{S}^m .*

Proof. We prove this using contradiction. Let the optimal solution comprises two multicast sets \mathcal{S}_y^m and \mathcal{S}_ℓ^m such that $\mathbf{c}(\mathcal{S}_y^m) < \mathbf{c}(\mathcal{S}_\ell^m)$. As we know that the cost of a multicast set is equal to the radio resources required by the UE with the worst CQI in that multicast set. This implies that UEs with better multicast channel conditions are a member of the multicast set with \mathcal{S}_ℓ^m . Thus \mathcal{S}_y^m is contained in \mathcal{S}_ℓ^m i.e., $\mathcal{S}_y^m \subset \mathcal{S}_\ell^m$. Thus, the total number of UEs being delivered content via multicast is equal to the cardinality of \mathcal{S}_ℓ^m . This implies that only one multicast set (with higher cardinality) needs to be taken into

account in evaluation of the cost. \square

Lemma 16. *For a fix number of RBs, if UEs are served via unicast transmission mode only then optimal solution (which maximizes the number of UEs served) is obtained by allocation of RBs to UEs in the increasing order of their cost until either all RBs are exhausted or the remaining RBs are not sufficient to serve any of the remaining UEs.*

Proof. Let \mathcal{N} be the set of all UEs and w is the total number of RBs available in the system. In order to serve the UEs, we select them in increasing order of their cost (RB requirement). Let us denote the set of UEs selected by the above order as \mathcal{L} such that $|\mathcal{L}| = p$. Assume that \mathcal{L} is not the optimal solution to problem \mathbb{C} . This implies that there exists some other order which serves more UEs in the system. Assume that a different ordering serves $q > p$ UEs denoted by set \mathcal{L}' . Let the aggregate cost of UEs in set \mathcal{L} is $w_p \leq w$ such that UEs in set $U \setminus \mathcal{L}$ cannot be served as their individual cost is greater than the remaining RBs i.e., $> (w - w_p)$. Since, $q > p$ hence $q \geq p + 1$ as $p, q \in \mathbb{Z}_+$. Consider $q = p + 1$. As q UEs are served, this implies that the aggregate cost of q UEs is less than or equal to w , i.e., $w_q \leq w$, where w_q denotes the aggregate cost of UEs in \mathcal{L}' . Now, if the UEs in \mathcal{L}' are re-arranged in increasing order of their cost then \mathcal{L} must contain q UEs. However, this is not possible due to constraint on RB availability. This proves that the selecting UEs in increasing order of cost serves provide optimal solution, provided unicast transmission is the only mode to serve UEs. \square

Theorem 7. *Algorithm 13 provides an optimal solution to optimization problem \mathbb{C} , which maximizes the number of UEs served in the given fixed resources (RBs).*

Proof. The proof follows from Lemma 15 and Lemma 16. \square

Corollary 7.1. *The computational complexity of the C-OPTICUL algorithm is $\mathcal{O}(|\mathcal{N}|)$, where $|\mathcal{N}|$ denotes the total number of UEs in the system.*

The number of feasible outcomes (allocations which satisfy the limited resource constraint condition in C-OPTICUL algorithm) are at most $|\mathcal{N}| + 1$. Thus, determining the optimal solution (the allocation with the maximum number of served UEs) requires to check only $|\mathcal{N}| + 1$ possibilities. Corollary 2 states that the C-OPTICUL algorithm is computationally feasible even for a large number of UEs in the system. Hence, the efficient utilization of limited RBs can be performed.

6.5 Simulation Results

As the primary focus of the chapter is on efficient radio resource utilization, we evaluate the performance of the proposed algorithms through simulations. The simulations are performed in MATLAB [75]. Next, we describe the simulation settings.

6.5.1 Simulation Settings

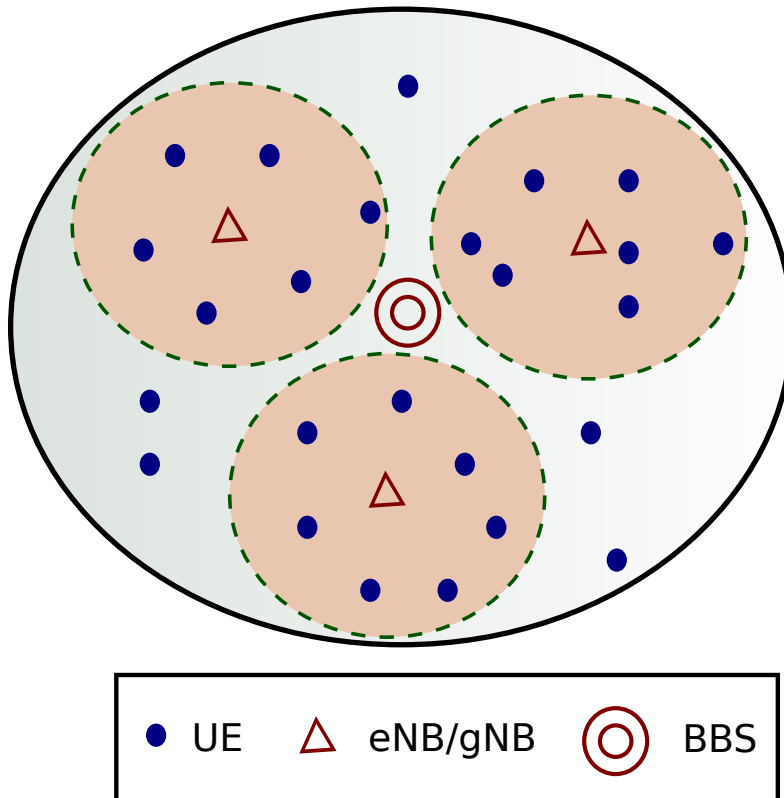


Figure 6.6: Illustration of simulation settings.

We consider a system with a single MBMS cell and 3 unicast cells. The simulation parameters are considered as per 3GPP standards and are listed in Table 6.2 [85]. UEs are distributed uniformly across the region in MBMS cell overlapping with unicast cells. Each UE is capable of dual connectivity, which allows it to receive data from a multicast BS while being connected with one of the unicast eNBs (anchor BS) concurrently. Based on the CQI of UEs, first we map CQI to the modulation coding scheme (MCS). Then, for the given rate requirement of each UE, MCS to transport block size (TBS) mapping is performed as given in Table 7.1.7.1-1 in [23]. The required number of RBs are obtained

based on the TBS index using Table 7.1.7.2.1-1 in [80]. LTE has been used for simulations and not 5G NR. Though similar results may hold for 5G NR.

Table 6.2: Simulation parameters

Parameters	Values
Carrier Frequency	2 GHz
Number of MBMS cell	1
Number of LTE cells	3
Channel Model	3D-UMa
Noise Figure-UE	9dB
Mobility	3km/h
UE Distribution	Uniform
Multicast BS (MBMS) Model	
Coverage radius	250 m
Transmit Power	43 dBm
Antenna Height	25 m
Antenna	Omni-directional
eNB BS (Unicast) Model	
Coverage radius	100 m
Transmit Power	37 dBm
Antenna Height	25 m
Antenna	Omni-directional

In simulations, we consider that each UE has a certain data rate requirement, and UE arrival and departure are dynamic. Moreover, same content is required by UEs in the system. Based on the CQI reported by a UE for both the multicast cell and the best unicast cell (anchor cell), the required number of RBs for both the unicast and the multicast transmission to serve the UE are computed as per the 3GPP standards [80].

6.5.2 Performance Comparison

First, we evaluate the performance of the algorithm proposed in Section 6.3, which achieves efficient utilization, considering that sufficient resources are available to serve all the UEs in the system. Performance of the proposed algorithm is compared against the “multicast only transmission scheme” when all UEs are served via multicast transmission mode. In the multicast scheme, all UEs are served via the MBMS cell. Therefore, the RBs required to serve all UEs are equal to the RBs required by the UE with the worst CQI in the MBMS cell.

- *UE Arrival Only*

We consider a scenario where a content is streaming for a duration of 45 minutes. UE arrival process follows poisson distribution with average arrival rate $\lambda_a = 3$ UEs per minute. Each UE has a data rate requirement of $R = 3.5$ Mbps. We compare the performance of Algorithm 10 with the multicast scheme, assuming that once a UE arrives in the system, it stays for the remaining duration of the content streaming. In Figure 6.7, we observe that Algorithm 10 outperforms the multicast scheme in terms of RBs. The reason behind poor performance in multicast scheme is due to the fact that in multicast transmission, the required number of RBs depends on the channel condition experienced by the worst UE in the system. However, Algorithm 10 provides optimal resource utilization by splitting the UEs across unicast and multicast cells based on the channel conditions of each UE in the system. Thus, UEs with poor channel conditions for multicast transmission are served via unicast cell.

Next, we analyze the performance when UE arrival process does not have uniform uniform distribution. Typically, we observe a large number of UEs arrive at the beginning (say for initial 10 minutes, bursty traffic) and after that UE arrival rate decreases considerably. We simulate the scenario by considering that for initial 10 minutes, the UE arrival follows poisson process with average arrival rate $\lambda_b = 5$ UEs per minute and thereafter the UE arrival rate goes down to $\lambda_a = 1$ UEs per minute. The data rate requirement of each UE is 3.5 Mbps. In Figure 6.8, the trend observed is similar to that of the previous case, except the fact that the number of RBs required to serve UEs increases sharply due

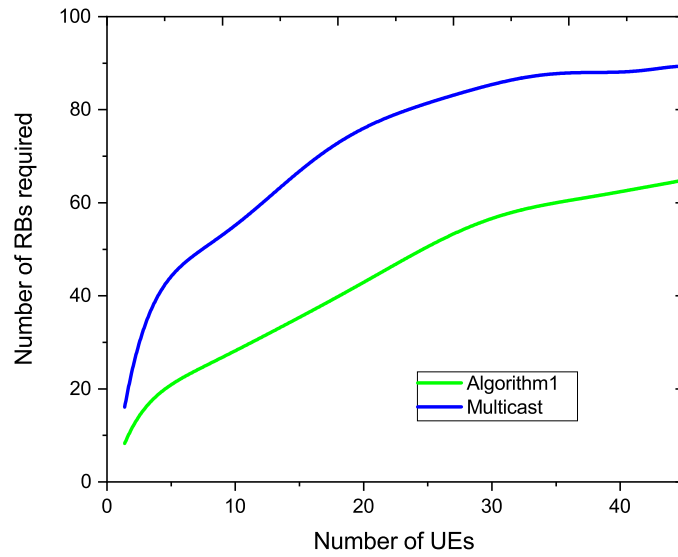


Figure 6.7: Resource Utilization (RBs required) vs. number of UEs [$R = 3.5$ Mbps].

to bursty traffic.

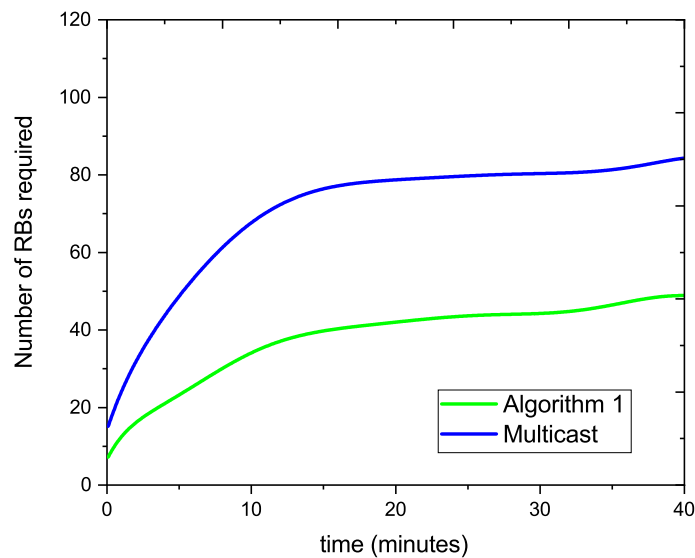


Figure 6.8: Resource Utilization (RBs required) vs. number of UEs [For $t = [0 10]$: $\lambda_b = 5$; and $t = [10 40]$: $\lambda_a = 1$, $R = 3.5$ Mbps].

We also analyze the effect of required data rate (of UEs) on the performance of the proposed mechanism against the multicast scheme. Again, we consider UE arrival as a

poisson process with average arrival rate $\lambda_a = 3$ UEs per minute for the duration of content streaming. We compare the number of RBs saved (difference between RBs required in multicast and Algorithm 10) in Figure 6.9, while varying the data rate requirement of each UE as 2.0 Mbps, 2.5 Mbps and 3.0 Mbps. We observe that the number of RBs saved by the proposed algorithm over the multicast scheme increases as the number of UEs increases in the system. To satisfy the higher data rate requirements for a given channel condition, UE requires more number of RBs. Therefore, as the data rate requirement of UE requesting the same content increases a significant improvement (in terms of the number of RBs saved) is observed in the performance of Algorithm 10.

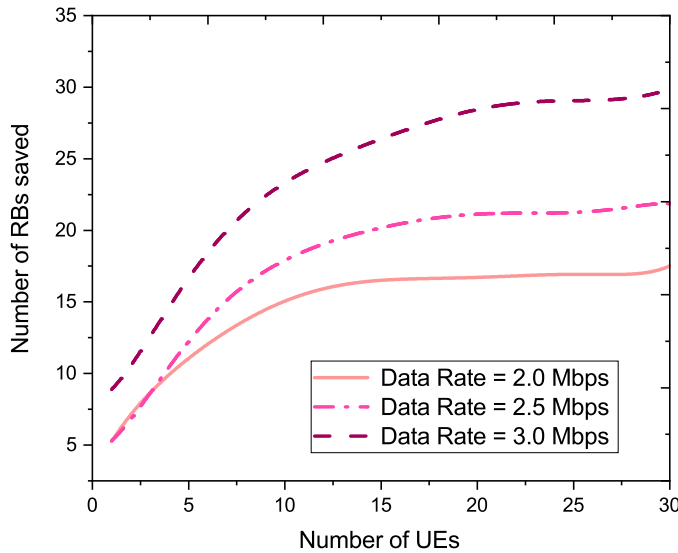


Figure 6.9: Comparison of the number of RBs saved in Algorithm 10 against multicast scheme at different UE data rates [Data rates $R = \{2.0, 2.5, 3.0\}$ Mbps].

- *UE Arrival and Departure*

Next, we consider a scenario where UEs arrive as well as depart from the system. The total duration of content streaming is 40 minutes. In this scenario, UEs arrive at an average arrival rate $\lambda_a = 4$ UEs per minute for initial 10 minutes. After that we consider only UE departures in the system. The departure time between UEs in the system is exponentially distributed with parameter μ_d . We choose $\mu_d = 1/10$. From

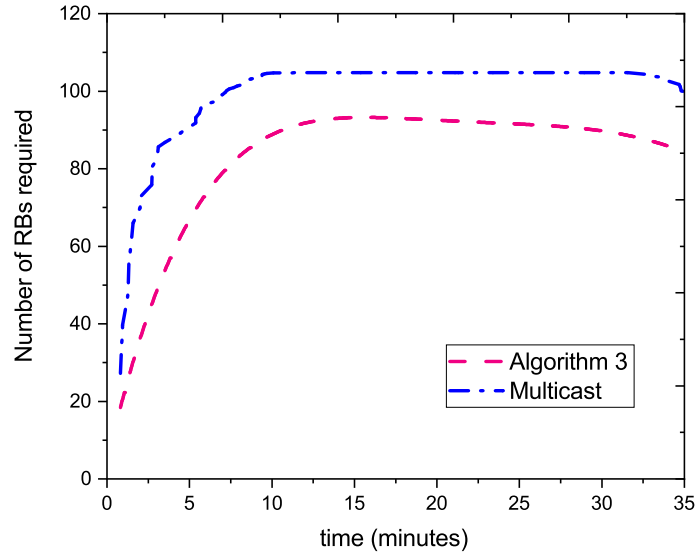


Figure 6.10: Resource Utilization (RBs required) vs. time [For $t = [0, 10]: \lambda_a = 4$ and $t = [10, 45]: \mu_d = 1/10, R = 3.5$ Mbps].

the simulations, it is observed that the resource requirement to satisfy all the UEs in the system increases in the beginning, then remains constant and later decreases as the UEs depart using Algorithm 12 (OPTICUL) (Figure 6.10). However, in the multicast transmission scheme, RB requirement in the system is effected only if UE experiencing the worst channel condition departs. As Algorithm 12 allows switching of UEs from unicast to multicast transmission, we achieve optimal RB utilization.

6.5.3 Limited Resource Scenario

Next, we consider the limited resources (or RBs) scenario discussed in Section 6.4. We perform simulations by varying the number of RBs in the system and compare the performance of Algorithm 13 with the multicast transmission scheme. In Figure 6.11, it is observed that Algorithm 13 outperforms the multicast transmission scheme and shows significant improvement in terms of the number of UEs served in the limited amount of RBs available.

We also compare the system throughput obtained through various algorithms. System throughput is defined as the sum of the product of the UE data rate and the number

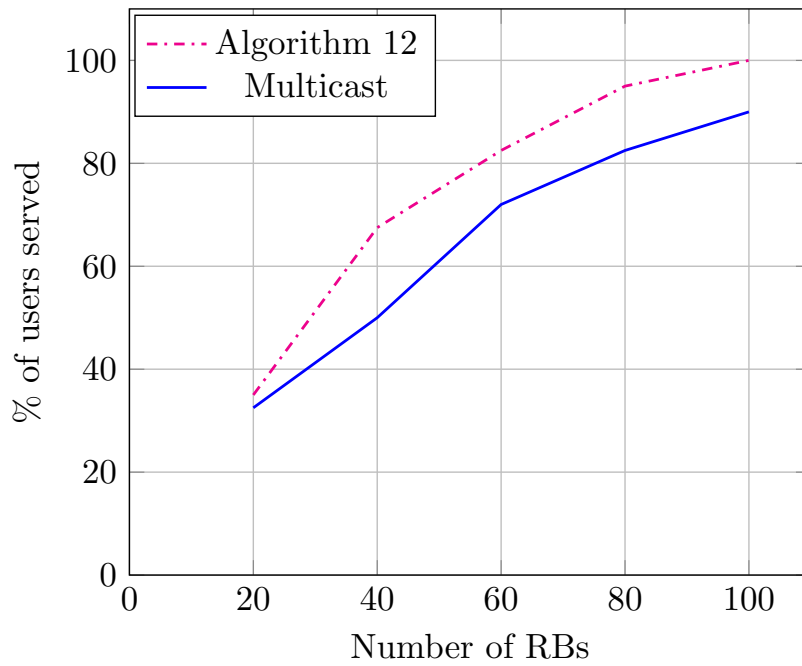


Figure 6.11: Percentage of UEs served vs. RBs in limited resource scenario.

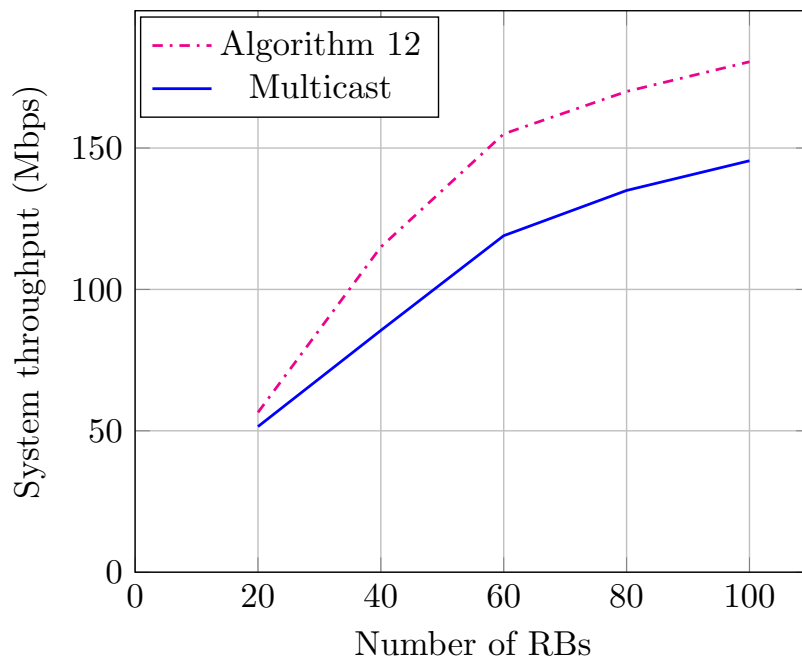


Figure 6.12: System throughput vs RBs in limited resource scenario.

of UEs served in the system. We have considered UEs with rate requirements of 3.5 Mbps, 4 Mbps, and 4.5 Mbps in simulations. From Figure 6.12, we observe that Algorithm 13 outperforms the multicast transmission scheme .

6.6 Conclusions

In this chapter, we have proposed a novel SDN based architecture which enables the convergence of unicast and multicast services in the next-generation mobile network. The architecture enables integration of dual connectivity with the MBMS services and provides a mechanism to utilize dual connectivity for improved radio resource utilization and network performance. Thus, the architecture provides flexible switching of the traffic between unicast and multicast transmission mode for efficient utilization of resources in the wireless network. Moreover, we identify new protocols and specify enhanced forwarding functions for existing BM-SC in the proposed architecture. In addition, the proposed architecture also enables the sharing of radio link quality information of UE to the SDN controller. For the unified architecture, we propose an efficient radio resource allocation algorithm for unicast and multicast transmission for guaranteed minimum QoS to every user in the system. Our scheme considers dynamic traffic variation in the network. We formally prove the optimality of the proposed algorithm.

Chapter 7

Summary of the Contributions and Future Research Directions

The research work in this thesis is focused on the efficient utilization of spectrum (radio resources) in cellular networks. Efficient utilization of spectrum has always been an area of research irrespective of the technology in use. Although the simulations are performed on an LTE network, the results and mechanisms are applicable in 5G and beyond networks. In this chapter, we summarize the main contributions of the thesis and also discuss possible extensions to this work.

7.1 Summary of the Contributions

In practice, auctions are used for spectrum allocation. Therefore, we use an auction-based mechanism for dynamic spectrum allocation in various scenarios appropriate to the existing and the next-generation networks. We aim at maximizing the social welfare of the auction. Chapter 3 considers the dynamic spectrum allocation problem across base stations subject to the interference constraints. We exploit the fact that each base station receives interference from a limited set of neighboring base stations in the network. Due to interference constraints, the problem is provably NP-hard, and hence achieving the optimal solution in polynomial time is not possible. Contrary, in dynamic spectrum allocation, the mechanism must be computationally efficient such that the spatio-temporal traffic variations can be taken into account. We propose a strategy-proof dynamic spec-

trum allocation mechanism GOSPAL, which achieves a near-optimal solution. GOSPAL involves the grouping of non-conflicting base stations. The number of groups is restricted by the degree of the base station with maximum conflicting base stations in the network. Moreover, the randomized grouping of base stations ensures fairness while allocating resources. Using Monte Carlo simulations, we observe that the proposed mechanism achieves near-optimal social welfare, spectrum utilization, and fairness.

In Chapter 4, we investigate the problem of dynamic spectrum allocation among the co-existing operators in a geographical region. Typically, multiple base stations are associated with an operator. Therefore an operator reports a vector of bids corresponding to each associated base station. Now, by reporting a bid vector, an operator has more choices to deviate from the true value. We start by analyzing the problem for a single channel scenario; that is, only one channel is available in the database, and the demand at each base station is restricted to 1. We propose SC-SPAM mechanism (Algorithm 4), which is computationally efficient and achieves near-optimal social welfare. We also prove SC-SPAM to be strategy-proof, individually rational, and follows monotonicity. Using simulations, we observe that the execution time of SC-SPAM does not change with the increase in the number of base stations in the network. The observation reflects the fact that SC-SPAM does not consider the individual bid of the base station while allocating resources but the aggregate bid from the base stations of an operator.

Next, we also analyze the problem when multiple channels are available in the spectrum database. Here, we consider not only non-uniform demand across the base stations but also allow flexible bidding. Flexible bidding (decreasing bids with demand) means that each next channel is valued less than the previous - this is akin to the assumption of decreasing marginal utility made commonly in economics. When the operator deviates from the true value with such bids, the deviated bid also decreases with the demand. We propose NUD-WSPAM, a variation of SC-SPAM. We introduce the notion of weak strategy-proofness (Definition 9). Using simulations, we observe that NUD-WSPAM outperforms the other existing algorithms.

In Chapter 5, we investigate the dynamic spectrum allocation in IAB-enabled HetNet settings. Due to multi-hop transmission between IAB-donor and users via IAB-nodes, the dynamic spectrum allocation problem no longer remains the same as in Chapters 3 and 4.

With the presence of IAB-nodes, the resource allocation happens to follow a hierarchical structure. Although IAB-donor does not have direct access to the user bids and demand, we aim to maximize social welfare. IAB-nodes derive the bids and demand from the associated users and report to the respective IAB-donor. We propose a polynomial-time strategy-proof algorithm, which achieves optimal social welfare.

In Chapter 6, our contributions are two folds: first, we propose an SDN-based unified architecture for the convergence of unicast and multicast services in the next-generation mobile network. Second, we develop algorithms to efficiently utilize the resources by optimal splitting (available resources) between unicast and MBMS cells. The proposed architecture enables the integration of dual connectivity with the MBMS services and provides a mechanism to utilize dual connectivity for improved radio resource utilization and network performance. The architecture ensures flexible switching of the traffic between unicast and multicast transmission modes. Moreover, we identify new protocols and specify enhanced forwarding functions for existing BM-SC in the proposed architecture. In addition, the proposed architecture also enables the sharing of radio link quality information of users to the SDN controller.

For the unicast multicast convergence architecture, we develop algorithms in two scenarios: First, we optimize the radio resources required in the system by dynamically splitting across unicast and MBMS cells for a set of users (receiving the same multimedia content) in the system, provided the individual rate requirement of each user is satisfied. As per the practical scenarios, we consider the dynamic arrival and departure of users in the system. We propose OPTICUL (Algorithm 12), which guarantees minimum QoS to each user in the system. The algorithm triggers whenever a new user arrives, or an existing user departs. Thus, the traffic variations in the network are taken into account in our algorithm. Moreover, OPTICUL has polynomial time complexity, which makes it feasible for real applications. We also prove the optimality of the algorithm.

In the second scenario, we propose C-OPTICUL, which aims at maximizing the number of users served with the constraint on the number of resources available in the system. C-OPTICUL is a low complexity algorithm and computes the optimal solution. Formally, we prove the optimality of the solution.

The main objective of this thesis has been on the development of computationally ef-

efficient dynamic spectrum allocation mechanisms. While we have investigated the dynamic spectrum allocation problem for various scenarios, further extensions of the proposed algorithms are possible. In the next section, we have a discussion on the possible extensions for future work.

7.2 Future Research Directions

In Chapters 3 and 4, we propose strategy-proof dynamic spectrum allocation mechanisms assuming the channels to be homogeneous, and therefore the valuation/bid remains the same for any channel available in the database. However, this can be further extended for heterogeneous channels, where the bid value may also depend on the specific characteristics of the channel. This aspect directly translates into the generalization of the mechanisms in practical scenarios.

In Chapter 5, we propose a strategy-proof mechanism for IAB-enabled HetNet settings. In our framework, we consider the 3-Tier arrangement, where the aggregation of bids reported by users is performed by the IAB-nodes to reduce the signaling overhead and hide the user-specific information. The proposed mechanism can be generalized for any number of hops in the network. In our work, we do not impose any constraint on the capacity of IAB-nodes. Hence, it transparently allocates the resources acquired from IAB-donor among the users. This can be further investigated by enforcing some constraints on the IAB-nodes. Another possible extension could be where IAB-nodes (middle-men) may have their own interests in resource allocation, thus may not be transparent while reporting the bids to the IAB-donor. This scenario can be investigated in hierarchical settings.

In Chapter 6, we propose a unified architecture for unicast multicast convergence. This architecture can be further evaluated with respect to other existing architectures such as MOOD. We also propose a dynamic spectrum allocation mechanism to distribute the spectrum between unicast and multicast cells considering the arrival and departure of users in the system. However, we assume that the channel conditions do not vary significantly for a user. The problem can be further investigated by relaxing the assumption on channel conditions. The aspect may not be straightforward due to the NP-hard

nature of the problem. While this work is focused on the optimization of radio resources, the proposed architectural framework can easily be extended to optimize other network parameters. For example, the load on different network nodes (eNB/gNB/UPF) can be distributed evenly by flexibly using multicast/unicast transmission modes in the system. Currently, 5G does not have any standard on the convergence of unicast multicast services; therefore, the framework can be further explored in terms of architecture and protocol for standardization in 5G and beyond networks. The architecture can also be enhanced to incorporate the non-3GPP broadcast technologies, such as ATSC, DVB, which may have considerable practical significance. Moreover, we can also study the architectural enhancements needed for integration with satellite communication as part of beyond 5G network.

As discussed in Chapter 1, dynamic spectrum allocation is expected to play a vital role in addressing the diverse requirements of the next-generation mobile networks. We believe that the algorithms and the architectural enhancements proposed in this thesis hold great promises towards practical implementation purposes since they address the issues related to various scenarios in the existing as well as the future mobile networks.

Bibliography

- [1] W. S. H. M. W. Ahmad, N. A. M. Radzi, F. Samidi, A. Ismail, F. Abdullah, M. Z. Jamaludin, and M. Zakaria, “5G technology: Towards Dynamic Spectrum Sharing using Cognitive Radio Networks,” *IEEE Access*, vol. 8, pp. 14460–14488, 2020.
- [2] “Ericsson mobility report,” 2020. [Online]. Available: <https://www.ericsson.com/en/mobility-report/reports/november-2020>.
- [3] U. Paul, A. P. Subramanian, M. M. Buddhikot, and S. R. Das, “Understanding Traffic Dynamics Cellular Data Networks,” in *IEEE INFOCOM*, pp. 882–890, 2011.
- [4] H. Wang, J. Ding, Y. Li, P. Hui, J. Yuan, and D. Jin, “Characterizing the Spatio-Temporal Inhomogeneity of Mobile Traffic in Large-scale Cellular Data Networks,” in *ACM HOTSPOT*, pp. 19–24, 2015.
- [5] “FCC, ET Docket No 03-222 Notice of proposed rule making and order,” 2003.
- [6] T. Johnny, “Adaptive Protocol suite for Next Generation Wireless Internet,” in *International Conference on Personal Wireless Communications*, pp. 509–513, IEEE, 2005.
- [7] S. D. J. H. S. D. M. E. Haleplidis, K. Pentikousis and O. Koufopavlou, “RFC 7426 - Software-Defined Networking (SDN): Layers and Architecture Terminology,” 2015.
- [8] N. M. Akshatha, P. Jha, and A. Karandikar, “A centralized sdn architecture for the 5g cellular network,” in *5G World Forum*, pp. 147–152, IEEE, 2018.
- [9] V. G. Nguyen, T. X. Do, and Y. Kim, “SDN and Virtualization-based LTE Mobile Network Architectures: A Comprehensive Survey,” *Wireless Personal Communications*, vol. 86, no. 3, pp. 1401–1438, 2016.

-
- [10] 3GPP TS 23.501, “System Architecture for the 5G System,” 2017. [Online]. Available: <https://portal.3gpp.org/desktopmodules/Specifications/SpecificationDetails.aspx?specificationId=3144>.
- [11] 3GPP TS 38.401, “Next Generation Radio Access Network (NG-RAN) Architecture Description,” 2017. [Online]. Available: <https://portal.3gpp.org/desktopmodules/Specifications/SpecificationDetails.aspx?specificationId=3219>.
- [12] M. Nekovee, “Opportunities and Enabling Technologies for 5G and Beyond-5G Spectrum sharing,” *Handbook of Cognitive Radio*, pp. 1–15, 2018.
- [13] F. Ahmed, A. Kliks, L. Goratti, and S. N. Khan, “Towards Spectrum Sharing in Virtualized Networks: A Survey and an Outlook,” in *Cognitive Radio, Mobile Communications and Wireless Networks*, pp. 1–28, Springer, 2019.
- [14] S. Mishra, S. Singh, and B. S. P. Mishra, “A Comparative Analysis of Centralized and Distributed Spectrum Sharing Techniques in Cognitive Radio,” in *Computational Intelligence in Sensor Networks*, pp. 455–472, Springer, 2019.
- [15] V. Brik, E. Rozner, S. Banerjee, and P. Bahl, “DSAP: A Protocol for Coordinated Spectrum Access,” in *International Symposium on New Frontiers in Dynamic Spectrum Access Networks*, pp. 611–614, IEEE, 2005.
- [16] S. A. Zekavat and X. Li, “User-central wireless system: Ultimate dynamic channel allocation,” in *International Symposium on New Frontiers in Dynamic Spectrum Access Networks*, pp. 82–87, IEEE, 2005.
- [17] C. Peng, H. Zheng, and B. Y. Zhao, “Utilization and fairness in spectrum assignment for opportunistic spectrum access,” *Mobile Networks and Applications*, vol. 11, no. 4, pp. 555–576, 2006.
- [18] G. Dlodla, L. Mfupe, and F. Mekuria, “Overview of Spectrum Sharing Models: A Path towards 5G Spectrum Toolboxes,” in *International Conference on Information and Communication Technology for Development for Africa*, pp. 308–319, Springer, 2017.

- [19] S. Sankaranarayanan, P. Papadimitratos, A. Mishra, and S. Hershey, “A Bandwidth Sharing Approach to improve Licensed Spectrum Utilization,” in *International Symposium on New Frontiers in Dynamic Spectrum Access Networks*, pp. 279–288, IEEE, 2005.
- [20] Q. Zhao, L. Tong, and A. Swami, “Decentralized cognitive MAC for dynamic spectrum access,” in *International Symposium on New Frontiers in Dynamic Spectrum Access Networks*, pp. 224–232, IEEE, 2005.
- [21] H. Zheng and L. Cao, “Device-centric Spectrum Management,” in *Symposium on New Frontiers in Dynamic Spectrum Access Networks*, pp. 56–65, IEEE, 2005.
- [22] J. Huang, R. A. Berry, and M. L. Honig, “Spectrum Sharing with Distributed Interference Compensation,” in *International Symposium on New Frontiers in Dynamic Spectrum Access Networks*, pp. 88–93, IEEE, 2005.
- [23] L. Cao and H. Zheng, “Distributed spectrum allocation via local bargaining,” in *SECON*, pp. 475–486, 2005.
- [24] , “Third generation partnership project,” 2007. [Online]. Available: <https://portal.3gpp.org/desktopmodules/Specifications/>.
- [25] M. R. Garey and D. S. Johnson, *Computers and Intractability : A Guide to the Theory of NP-Completeness*, vol. 29. WH Freeman New York, 2002.
- [26] V. Krishna, *Auction Theory*. Academic press, 2009.
- [27] T. Roughgarden, *Twenty Lectures on Algorithmic Game Theory*. Cambridge University Press, 2016.
- [28] X. Zhou, S. Gandhi, S. Suri, and H. Zheng, “eBay in the Sky: Strategy-proof Wireless Spectrum Auctions,” in *ACM ICMCN*, pp. 2–13, 2008.
- [29] W. Vickrey, “Counterspeculation, Auctions, and Competitive Sealed Tenders,” *The Journal of finance*, vol. 16, no. 1, pp. 8–37, 1961.
- [30] E. H. Clarke, “Multipart Pricing of Public Goods,” *Public choice*, vol. 11, no. 1, pp. 17–33, 1971.

-
- [31] T. Groves, “Incentives in Teams,” *Econometrica: Journal of the Econometric Society*, vol. 41, no. 4, pp. 617–631, 1973.
- [32] S. Gandhi, C. Buragohain, L. Cao, H. Zheng, and S. Suri, “Towards Real-time Dynamic Spectrum Auctions,” *Computer Networks*, vol. 52, no. 4, pp. 879–897, 2008.
- [33] Z. Ji and K. R. Liu, “Cognitive Radios for Dynamic Spectrum Access-Dynamic Spectrum Sharing: A Game Theoretical Overview,” *IEEE Communications Magazine*, vol. 45, no. 5, 2007.
- [34] N. Clemens and C. Rose, “Intelligent Power Allocation Strategies in an Unlicensed Spectrum,” in *IEEE Symposium DySPAN*, pp. 37–42, 2005.
- [35] R. Etkin, A. Parekh, and D. Tse, “Spectrum Sharing for Unlicensed Bands,” *IEEE Journal on Selected Areas in Communications*, vol. 25, no. 3, pp. 517–528, 2007.
- [36] J. Qiu, Q. Wu, Y. Xu, Y. Sun, and D. Wu, “Demand-Aware Resource Allocation for Ultra-dense Small Cell Networks: An Interference-separation Clustering-based Solution,” *Transactions on Emerging Telecommunications Technologies*, vol. 27, no. 8, pp. 1071–1086, 2016.
- [37] A. P. Subramanian, M. Al-Ayyoub, H. Gupta, S. R. Das, and M. M. Buddhikot, “Near-Optimal Dynamic Spectrum Allocation in Cellular Networks,” in *IEEE Symposium DySPAN*, pp. 1–11, 2008.
- [38] A. Gopinathan, Z. Li, and C. Wu, “Strategyproof Auctions for Balancing Social Welfare and Fairness in Secondary Spectrum Markets,” in *IEEE INFOCOM*, pp. 3020–3028, 2011.
- [39] J. Jia, Q. Zhang, Q. Zhang, and M. Liu, “Revenue Generation for Truthful Spectrum Auction in Dynamic Spectrum Access,” in *ACM Symposium MOBIHOC*, pp. 3–12, 2009.
- [40] R. B. Myerson, “Optimal Auction Design,” *Mathematics of Operations Research*, vol. 6, no. 1, pp. 58–73, 1981.
- [41] F. Wu and N. Vaidya, “SMALL: A Strategy-proof Mechanism for Radio Spectrum Allocation,” in *IEEE INFOCOM*, pp. 81–85, 2011.

-
- [42] X. Zhou and H. Zheng, “TRUST: A General Framework for Truthful Double Spectrum Auctions,” in *IEEE INFOCOM*, pp. 999–1007, 2009.
- [43] D. Yang, X. Zhang, and G. Xue, “PROMISE: A Framework for Truthful and Profit Maximizing Spectrum Double Auctions,” in *IEEE INFOCOM*, pp. 109–117, 2014.
- [44] Y. Chen, J. Zhang, K. Wu, and Q. Zhang, “TAMES: A Truthful Double Auction for Multi-demand Heterogeneous Spectrums,” *IEEE Transactions on Parallel and Distributed Systems*, vol. 25, no. 11, pp. 3012–3024, 2014.
- [45] G. S. Kasbekar and S. Sarkar, “Spectrum Auction Framework for Access Allocation in Cognitive Radio Networks,” *IEEE/ACM Transactions on Networking*, vol. 18, no. 6, pp. 1841–1854, 2010.
- [46] C. Yi and J. Cai, “Multi-item Spectrum Auction for Recall-based Cognitive Radio Networks with Multiple Heterogeneous Secondary Users,” *IEEE transactions on Vehicular Technology*, vol. 64, no. 2, pp. 781–792, 2015.
- [47] F. Wu, T. Zhang, C. Qiao, and G. Chen, “A Strategy-Proof Auction Mechanism for Adaptive-Width Channel Allocation in Wireless Networks,” *IEEE Journal on Selected Areas in Communications*, vol. 34, no. 10, pp. 2678–2689, 2016.
- [48] I. A. Kash, R. Murty, and D. C. Parkes, “Enabling Spectrum Sharing in Secondary Market Auctions,” *IEEE Transactions on Mobile Computing*, vol. 13, no. 3, pp. 556–568, 2014.
- [49] W. Tang and R. Jain, “Hierarchical Auction Mechanisms for Network Resource Allocation,” *IEEE Journal on Selected Areas in Communications*, vol. 30, no. 11, pp. 2117–2125, 2012.
- [50] R. Jain and P. Varaiya, “A design for an asymptotically efficient combinatorial bayesian market: Generalizing the satterthwaite-williams mechanism,” in *International Conf. on Game Theory, Stony Brook (July 2007)*, 2007.
- [51] S. Shakkottai and R. Srikant, “Economics of network pricing with multiple isps,” *IEEE/ACM Transactions On Networking*, vol. 14, no. 6, pp. 1233–1245, 2006.

-
- [52] M. Yang, Y. Li, D. Jin, J. Yuan, L. Su, and L. Zeng, "Opportunistic Spectrum Sharing Based Resource Allocation for Wireless Virtualization," in *IEEE Innovative Mobile and Internet Services in Ubiquitous Computing*, pp. 51–58, 2013.
- [53] B. Liu and H. Tian, "A Bankruptcy Game-Based Resource Allocation Approach among Virtual Mobile Operators," *IEEE Communications Letters*, vol. 17, no. 7, pp. 1420–1423, 2013.
- [54] K. Zhu and E. Hossain, "Virtualization of 5G Cellular Networks as a Hierarchical Combinatorial Auction," *IEEE Transactions on Mobile Computing*, vol. 15, no. 10, pp. 2640–2654, 2015.
- [55] P. Lin, X. Feng, Q. Zhang, and M. Hamdi, "Groupon in the Air: A three-stage auction framework for Spectrum Group-buying," in *IEEE INFOCOM*, 2013.
- [56] P. Lin, X. Feng, and Q. Zhang, "Flexauc: Serving Dynamic Demands in Spectrum Trading Markets with Flexible Auction," in *IEEE INFOCOM*, pp. 2265–2273, 2014.
- [57] D. Gomez-Barquero, D. Navratil, S. Appleby, and M. Stagg, "Point-to-Multipoint Communication Enablers for the Fifth Generation of Wireless Systems," *IEEE Communications Standards Magazine*, vol. 2, no. 1, pp. 53–59, 2018.
- [58] W. Guo, M. Fuentes, L. Christodoulou, and B. Mouhouche, "Roads to Multimedia Broadcast Multicast Services in 5G New Radio," in *IEEE BMSB*, pp. 1–5, 2018.
- [59] 3GPP TS 38.214 v16.3.0, "NR; Physical layer procedures for data," 2020. [Online]. Available: <https://portal.3gpp.org/desktopmodules/Specifications/SpecificationDetails.aspx?specificationId=3216>.
- [60] T. Tran, D. Navrátil, P. Sanders, J. Hart, R. Odarchenko, C. Barjau, B. Altman, C. Burdinat, and D. Gomez-Barquero, "Enabling Multicast and Broadcast in the 5G Core for Converged Fixed and Mobile Networks," *IEEE Transactions on Broadcasting*, 2020.
- [61] J. Liu, W. Chen, Z. Cao, and K. B. Letaief, "Dynamic Power and Sub-carrier Allocation for OFDMA-based Wireless Multicast Systems," in *IEEE ICC*, pp. 2607–2611, 2008.

- [62] R. O. Afolabi, A. Dadlani, and K. Kim, “Multicast Scheduling and Resource Allocation Algorithms for OFDMA-based Systems: A Survey,” *IEEE Communications Surveys & Tutorials*, vol. 15, no. 1, pp. 240–254, 2012.
- [63] S. Pizzi, M. Condoluci, G. Araniti, A. Molinaro, A. Iera, and G.-M. Muntean, “A Unified Approach for Efficient Delivery of Unicast and Multicast Wireless Video Services,” *IEEE Transactions on Wireless Communications*, vol. 15, no. 12, pp. 8063–8076, 2016.
- [64] P. Scopelliti, G. Araniti, G.-M. Muntean, A. Molinaro, and A. Iera, “A Hybrid Unicast-Multicast Utility-based Network Selection Algorithm,” in *IEEE BMSB*, pp. 1–6, 2017.
- [65] R. Kaliski, C.-C. Chou, H.-Y. Meng, and H.-Y. Wei, “Dynamic Resource Allocation Framework for MooD (MBMS Operation on-demand),” *IEEE Transactions on Broadcasting*, vol. 62, no. 4, pp. 903–917, 2016.
- [66] R. Kaliski, C.-C. Chou, and H.-Y. Wei, “Further Enhanced Multimedia Broadcast/-Multicast Service in LTE-Advanced Pro,” *IEEE Communications Standards Magazine*, vol. 3, no. 3, pp. 44–51, 2019.
- [67] L. Militano, M. Condoluci, G. Araniti, and A. Iera, “Multicast Service Delivery Solutions in LTE-Advanced Systems,” in *IEEE ICC*, pp. 5954–5958, 2013.
- [68] J. F. Monserrat, J. Calabuig, A. Fernandez-Aguilella, and D. Gomez-Barquero, “Joint Delivery of Unicast and E-MBMS Services in LTE Networks,” *IEEE Transactions on Broadcasting*, vol. 58, no. 2, pp. 157–167, 2012.
- [69] D. Lee, J. So, and S. R. Lee, “Power Allocation and Subcarrier Assignment for Joint Delivery of Unicast and Broadcast Transmissions in OFDM Systems,” *IEEE Journal of Communications and Networks*, vol. 18, no. 3, pp. 375–386, 2016.
- [70] G. Araniti, V. Scordamaglia, A. Molinaro, A. Iera, G. Interdonato, and F. Spano, “Optimizing Point-to-Multipoint Transmissions in High Speed Packet Access networks,” in *IEEE BMSB*, pp. 1–5, 2011.

- [71] G. Araniti, M. Condoluci, L. Militano, and A. Iera, "Adaptive Resource Allocation to Multicast Services in LTE Systems," *IEEE Transactions on Broadcasting*, vol. 59, no. 4, pp. 658–664, 2013.
- [72] S. ul Zuhra, P. Chaporkar, and A. Karandikar, "Toward Optimal Grouping and Resource Allocation for Multicast Streaming in LTE," *IEEE Transactions on Vehicular Technology*, vol. 68, no. 12, pp. 12239–12255, 2019.
- [73] J. Chen, M. Chiang, J. Erman, G. Li, K. Ramakrishnan, and R. K. Sinha, "Fair and Optimal Resource Allocation for LTE Multicast (eMBMS): Group Partitioning and Dynamics," in *IEEE INFOCOM*, pp. 1266–1274, 2015.
- [74] F. Chung and L. Lu, "Connected Components in Random Graphs with given Expected Degree Sequences," *Annals of combinatorics*, vol. 6, no. 2, pp. 125–145, 2002.
- [75] "MATLAB Toolbox." <https://in.mathworks.com>.
- [76] R. K. Jain, D.-M. W. Chiu, and W. R. Hawe, "A Quantitative Measure of Fairness and Discrimination," *Eastern Research Laboratory, Digital Equipment Corporation, Hudson, MA*, 1984.
- [77] R. Chandra, R. Mahajan, T. Moscibroda, R. Raghavendra, and P. Bahl, "A Case for Adapting Channel Width in Wireless Networks," in *ACM SIGCOMM computer communication review*, vol. 38, pp. 135–146, 2008.
- [78] 3GPP TR 38.874 v16.0.0, "NR; Study on Integrated Access and Backhaul," 2009. [Online]. Available: <https://portal.3gpp.org/desktopmodules/Specifications/SpecificationDetails.aspx?specificationId=3232>.
- [79] R. Murthy, R. Chandra, T. Moscibroda, and P. Bahl, "Senseless: A Database-Driven White Spaces Network," *IEEE Transactions on Mobile Computing*, vol. 11, no. 2, pp. 189–203, 2012.
- [80] 3GPP TS 36.213 v15.2.0, "LTE; Evolved Universal Terrestrial Radio Access (E-UTRA); Physical layer procedures," 2018. [Online]. Available: <https://portal.3gpp.org/desktopmodules/Specifications/SpecificationDetails.aspx?specificationId=2427>.

-
- [81] 3GPP TS 23.246 v16.1.0, “Multimedia Broadcast/Multicast Service; Architecture and Functional Description,” 2019. [Online]. Available: <https://portal.3gpp.org/desktopmodules/Specifications/SpecificationDetails.aspx?specificationId=829>.
- [82] 3GPP TS 26.346 v16.6.0, “Multimedia Broadcast/Multicast Service improvements; Protocols and codecs,” 2020. [Online]. Available: <https://portal.3gpp.org/desktopmodules/Specifications/SpecificationDetails.aspx?specificationId=1452>.
- [83] 3GPP TR 26.849 v12.1.0, “Multimedia Broadcast/Multicast Service (MBMS) improvements; MBMS operation on demand,” 2015. [Online]. Available: <https://portal.3gpp.org/desktopmodules/Specifications/SpecificationDetails.aspx?specificationId=1476>.
- [84] S. D. J. H. S. D. M. E. Haleplidis, K. Pentikousis and O. Koufopavlou, “RFC 7426 - Software-Defined Networking (SDN): Layers and Architecture Terminology,” 2015.
- [85] 3GPP TR 36.931 v.15.0.0, “Evolved Universal Terrestrial Radio Access (E-UTRA); Radio Frequency (RF) requirements for LTE Pico Node B,” 2020. [Online]. Available: <https://portal.3gpp.org/desktopmodules/Specifications/SpecificationDetails.aspx?specificationId=2589>.

List of Publications

Part of Ph.D. Thesis

Journal Publications

- J1** I. Yadav, A. A. Kulkarni, and A. Karandikar, “Strategy-Proof Spectrum Allocation among Multiple Operators in Wireless Networks”, accepted in IEEE Transactions on Vehicular Technology, 2020.

Conference Publications

- C1** I. Yadav, A. A. Kulkarni, and A. Karandikar, “Strategy-Proof Spectrum Allocation among Multiple Operators,”, in proc. of WCNC, pp. 1-6, 2019.
- C2** I. Yadav, P. Chaporkar, and A. Karandikar, “GOSPAL: An Efficient Strategy-Proof Mechanism for Constrained Resource Allocation”, in proc. of VALUETOOLS, pp. 187-188, 2019.

Preprints/Submitted/Under Preparation

- J2** I. Yadav, P. Chaporkar, and A. Karandikar, “Dynamic Spectrum Allocation in Wireless Networks: An Auction-Based Approach”, In Preparation (Journal).
- J3** I. Yadav, P. Jha, and A. Karandikar, “Unicast Multicast Convergence in 5G & beyond: Supplementing FeMBMS with SDN and Dual Connectivity”, Under review (Journal).
- C3** I. Yadav, P. Chaporkar, A. Karandikar and P. Jha, “Spectrum Allocation in IAB Networks: A Hierarchical Auction-based Approach”, Under review (Conference).

Other Publications

Patents

- P1 I. Yadav, P. Jha, and A. Karandikar, “An Architecture for Content Delivery over Wireless Networks”, Patent filed, June 2019 (India)(201921022025).